DOT/FAA/RD-94-25
DOT-VNTSC-FAA-94-12

Office of Research and
Development Service
Washington, D.C. 20591

Aircraft Wake Vortex Takeoff Tests at O'Hare International Airport

J. Yarmus
D. Burnham
A. Wright
T. Talbot

U.S. Department of Transportation
Research and Special Programs Administration
John A. Volpe
National Transportation Systems Center
Cambridge, MA 02142

Final Report
August 1994

U.S. Department of Transportation
Federal Aviation Administration

REPORT DOCUMENTATION PAGE

Form Approved
OMB No. 0704-0188

1. AGENCY USE ONLY (Leave blank)	2. REPORT DATE	3. REPORT TYPE AND DATES COVERED
	August 1994	Final Report February - May 1992

4. TITLE AND SUBTITLE

Aircraft Wake Vortex Takeoff Tests at O'Hare International Airport

5. FUNDING NUMBERS

FA427/A4072

6. AUTHOR(S)

J. Yarmus, D. Burnham, A. Wright, T. Talbot

7. PERFORMING ORGANIZATION NAME(S) AND ADDRESS(ES)

U.S. Department of Transportation
Research and Special Programs Administration
Volpe National Transportation Systems Center
Cambridge, MA 02142

8. PERFORMING ORGANIZATION REPORT NUMBER

DOT-VNTSC-FAA-94-12

9. SPONSORING/MONITORING AGENCY NAME(S) AND ADDRESS(ES)

U.S. Department of Transportation
Federal Aviation Administration
Research and Development Service
Washington, DC 20591

10. SPONSORING/MONITORING AGENCY REPORT NUMBER

DOT/FAA/RD-94-25

11. SUPPLEMENTARY NOTES

12a. DISTRIBUTION/AVAILABILITY STATEMENT

This document is available to the public through the National Technical Information Service, Springfield, VA 22161

12b. DISTRIBUTION CODE

13. ABSTRACT (Maximum 200 words)

Three wake vortex measurement systems (anemometer, acoustic doppler, and laser doppler) were used to collect wake vortex data from aircraft departing Runway 22L at Chicago's O'Hare airport for nine months in 1980. The data were analyzed to determine vortex decay and vortex transport probabilities. The results support the classification of all B-707 and DC-8 aircraft in the large wake vortex class. The acoustic doppler system was found to be significantly more sensitive than the ground anemometer system to vortices transported long distances laterally by a crosswind. The most efficient lateral transport was noted for crosswinds greater than seven knots. The horizontal and vertical ground wind signatures of a wake vortex are compared.

14. SUBJECT TERMS

Wake Vortex, Vortex Decay, Vortex Lateral Transport

15. NUMBER OF PAGES

96

16. PRICE CODE

17. SECURITY CLASSIFICATION OF REPORT	18. SECURITY CLASSIFICATION OF THIS PAGE	19. SECURITY CLASSIFICATION OF ABSTRACT	20. LIMITATION OF ABSTRACT
Unclassified	Unclassified	Unclassified	

PREFACE

The present method of preventing hazardous wake-vortex encounters is to increase aircraft separations on arrival and departure behind the aircraft generating the strongest wake vortices. These increased separations result in a loss in airport capacity. Previous studies on the duration of the wake-vortex hazard have shown that the present separation standards are overly conservative most of the time. The possibility of regaining lost airport capacity has thus been one driving force behind the extensive effort of the U.S. Department of Transportation to understand the behavior of wake vortices. Data on the decay of wake vortices have also been used to justify increased separation standards and to examine possible reclassification of aircraft according to their measured wake-vortex properties. Data on wake vortices from landing aircraft have been collected at Kennedy, Denver, Heathrow, and O'Hare airports. Data from departing aircraft were collected at the Toronto airport and at O'Hare airport. The O'Hare takeoff study is presented in this report.

Two wake-vortex sensors, the Ground-Wind Vortex Sensing System (GWVSS) and the Monostatic Acoustic Vortex Sensing System (MAVSS) were used to collect most of the available wake-vortex data. The GWVSS was used more extensively, but the MAVSS had the advantage of measuring vortex strength. Before the present work, the Volpe Center had completed a study [unpublished] of vortex lateral transport using GWVSS data alone. In this report, that study will be extended by analyzing the MAVSS data collected concurrently. The overall goals, to which this work contributes, are twofold: evaluation of parallel runway separation standards, and definition of the parameters and potential benefits of a Parallel-Runway Vortex Advisory System (PVAS).

The work described in this report was carried out in two time segments with a hiatus of two years (December 1981 to December 1983) during which the Volpe Center Wake-Vortex Program went unfunded and the associated personnel were assigned to other programs. Because of this break in continuity, some details of the test program activities, data collection and reduction procedures have been lost. The publication of this report was further delayed by subsequent breaks in the wake-vortex program.

English units, with the metric equivalent in parentheses, are used to describe the layout of equipment in this report. Calculated quantities such as vortex strength are presented in metric units.

The following people and institutions made significant contributions to the work reported here. Tom Sullivan was the Volpe Center manager of the data collection. The test site was staffed by the Illinois Institute of Technology Research Institute. Berl Winston was the Volpe Center manager of data reduction. The data reduction and data analysis were carried out by the Systems Development Corporation (SDC). Jim Hallock was deeply involved in the early data analysis and interpretation and, in addition, gave helpful comments on this report.

METRIC/ENGLISH CONVERSION FACTORS

ENGLISH TO METRIC

LENGTH (APPROXIMATE)

1 inch (in.) = 2.5 centimeters (cm)
1 foot (ft) = 30 centimeters (cm)
1 yard (yd) = 0.9 meter (m)
1 mile (mi) = 1.6 kilometers (km)

AREA (APPROXIMATE)

1 square inch (sq in, in^2) = 6.5 square centimeters (cm^2)
1 square foot (sq ft, ft^2) = 0.09 square meter (m^2)
1 square yard (sq yd, yd^2) = 0.8 square meter (m^2)
1 square mile (sq mi, mi^2) = 2.6 square kilometers (km^2)
1 acre = 0.4 hectares (he) = 4,000 square meters (m^2)

MASS - WEIGHT (APPROXIMATE)

1 ounce (oz) = 28 grams (gr)
1 pound (lb) = .45 kilogram (kg)
1 short ton = 2,000 pounds (lb) = 0.9 tonne (t)

VOLUME (APPROXIMATE)

1 teaspoon (tsp) = 5 milliliters (ml)
1 tablespoon (tbsp) = 15 milliliters (ml)
1 fluid ounce (fl oz) = 30 milliliters (ml)
1 cup (c) = 0.24 liter (l)
1 pint (pt) = 0.47 liter (l)
1 quart (qt) = 0.96 liter (l)
1 gallon (gal) = 3.8 liters (l)
1 cubic foot (cu ft, ft^3) = 0.03 cubic meter (m^3)
1 cubic yard (cu yd, yd^3) = 0.76 cubic meter (m^3)

TEMPERATURE (EXACT)

[(x - 32) (5/9)] °F = y°C

METRIC TO ENGLISH

LENGTH (APPROXIMATE)

1 millimeter (mm) = 0.04 inch (in)
1 centimeter (cm) = 0.4 inch (in)
1 meter (m) = 3.3 feet (ft)
1 meter (m) = 1.1 yards (yd)
1 kilometer (km) = 0.6 mile (mi)

AREA (APPROXIMATE)

1 square centimeter (cm^2) = 0.16 square inch (sq in, in^2)
1 square meter (m^2) = 1.2 square yards (sq yd, yd^2)
1 square kilometer (kn^2) = 0.4 square mile (sq mi, mi^2)
1 hectare (he) = 10,000 square meters (m^2) = 2.5 acres

MASS - WEIGHT (APPROXIMATE)

1 gram (gr) = 0.036 ounce (oz)
1 kilogram (kg) = 2.2 pounds (lb)
1 tonne (t) = 1,000 kilograms (kg) = 1.1 short tons

VOLUME (APPROXIMATE)

1 milliliter (ml) = 0.03 fluid ounce (fl oz)
1 liter (l) = 2.1 pints (pt)
1 liter (l) = 1.06 quarts (qt)
1 liter (l) = 0.26 gallon (gal)
1 cubic meter (m^3) = 36 cubic feet (cu ft, ft^3)
1 cubic meter (m^3) = 1.3 cubic yards (cu yd, yd^3)

TEMPERATURE (EXACT)

[(9/5) y + 32] °C = x °F

QUICK INCH-CENTIMETER LENGTH CONVERSION

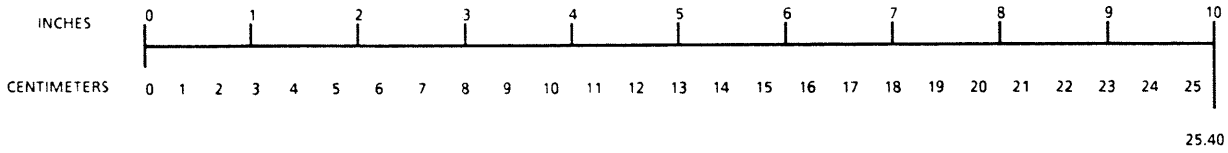

QUICK FAHRENHEIT-CELSIUS TEMPERATURE CONVERSION

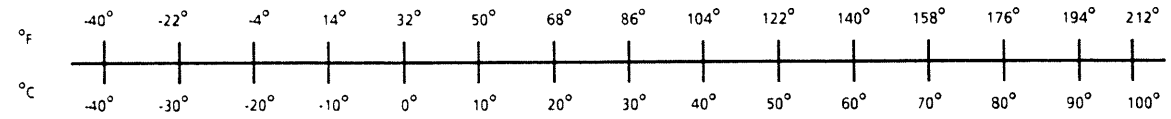

For more exact and or other conversion factors, see NBS Miscellaneous Publication 286, Units of Weights and Measures. Price $2.50. SD Catalog No. C13 10286.

TABLE OF CONTENTS

TABLE OF CONTENTS (cont.)

LIST OF FIGURES

LIST OF FIGURES (cont.)

LIST OF TABLES

1. INTRODUCTION

From February through October 1980, wake-vortex data were collected on aircraft departing from O'Hare International Airport. Runway 22L was equipped with an extensive array of wake-vortex sensors. The primary sensing systems were the Ground-Wind Vortex Sensing System (GWVSS) and the Monostatic Acoustic Vortex Sensing System (MAVSS). This data collection effort was the last in a series of tests which were designed to accumulate statistics on the decay of wake vortices generated by aircraft during normal airport operations. Such data have been used for several different purposes:

- To set or evaluate separation standards,
- To justify the wake-vortex classification of particular aircraft types, and
- To support the development of wake-vortex avoidance systems which adjust aircraft separations according to the actual duration of the vortex hazard.

Earlier work on wake vortices from landing aircraft at Heathrow, O'Hare and other airports is described in References 1-9. Vortices from landing aircraft received the first priority in airport studies because most of the reported accidents and incidents occurred on landing where aircraft are constrained to follow one another along the glideslope and runway centerline. However, to achieve a full understanding of the wake-vortex hazard near the ground, the takeoff operation eventually had to be addressed. The first study of takeoff vortices was carried out at the Toronto International Airport and is described in Reference 10. The present report describes the O'Hare study of takeoff vortices near the ground.

1.1 PURPOSE OF REPORT

The purpose of this report is fourfold:

First, it provides documentation for the O'Hare takeoff data collection effort. The O'Hare takeoff tests expanded the takeoff data collected at Toronto to include a greater number of aircraft, especially wide-body types, and to provide greater spatial coverage of the possible areas where wake vortices can drift before they decay.

Second, this report presents an analysis of O'Hare takeoff data which supports reclassifying all B-707 and DC-8 aircraft as Large (in lieu of the current classification which segregates each into the Large and Heavy Wake-Vortex classes in accordance with their maximum certificated gross takeoff weight lying below or above 300,000 lbs.). The O'Hare measurements for B-707 and DC-8 aircraft recorded whether the aircraft was Large or Heavy, a distinction not made at Toronto. Thus, for the first time, takeoff data could be used to compare the vortex behavior for the Large and Heavy B-707 and DC-8 models. Although these aircraft are now rare, they illustrate the problem encountered in defining the wake-

vortex classification from a single aircraft parameter, using a somewhat arbitrary breakpoint.

Third, this report presents results of a preliminary analysis of the probability of vortices being detected by the MAVSS at various lateral transport distances. In addition, this report considers the characteristics of wake vortices detected at the last MAVSS antenna, 1300 feet (396 meters) away from the runway centerline.

Fourth, this report presents results of an improved GWVSS analysis method, based on new software for generating plots of crosswind amplitude versus time (termed stripcharts) at each of the GWVSS sensors. The new stripchart software permits more concise visualization of the data.

1.2 SCOPE

The remainder of this report consists of four sections, each devoted to one of the four report purposes: Section 2, documentation of the O'Hare takeoff data collection process; Section 3, analysis of the potential for reclassification of B-707 and DC-8 aircraft based on takeoff data; Section 4, analysis of MAVSS wake-vortex transport data; and Section 5, analysis of GWVSS data using the new stripchart software. The scope of each of these sections is described below.

1.2.1 O'Hare Data Collection

The same technology was used for the O'Hare takeoff tests as for the earlier Toronto tests. Consequently, the description of the sensors, data collection equipment, and data reduction methods will be very limited in this report. The reader will find a complete description in Reference 10 and the earlier reports referenced there. In particular, this report documents what is unique about the O'Hare tests. The method of extrapolating the time history of vortex strengths is also documented here.

The complete analysis of takeoff data requires an additional parameter, the aircraft height (determined from photographs), which is not important for landings where aircraft generally follow the glideslope to touchdown. On takeoff, the aircraft height at a particular sensing line can vary dramatically depending upon the aircraft type and weight and the temperature.

1.2.2 Reclassification of B-707/DC-8 Aircraft

The introduction of wide-body aircraft into service in 1969 and 1970 resulted in a substantial increase in the potential wake-vortex hazard to following aircraft. In order to deal with this potential safety problem, jet transport aircraft were divided into two wake-vortex classes, Heavy and Large; and the separation requirements for following aircraft were increased behind the Heavy class. The dividing line between the two classes was set, somewhat arbitrarily, at 300,000 pounds maximum certificated gross takeoff weight. This choice of dividing line caused different versions of the B-707 and the DC-8 to fall into different

classes. If all versions of these aircraft types were combined into the Large category, the wake-vortex separation system would be improved, airport capacity would be increased, and the anomaly of different classifications for very similar aircraft would be eliminated.

References 2 and 3 assessed the potential for reclassification of Heavy B-707's and DC-8's to Large, based on MAVSS data collected on vortices generated by landing aircraft (Reference 1). The assessment in these studies was incomplete because the lack of departure data precluded a determination of whether reclassification could be applied to all phases of flight. Thus, reclassification was postponed until this report which includes an analysis of departure data.

Section 3 of the report describes the hazard duration results from the departure MAVSS database for all aircraft types, with emphasis on the B-707 and DC-8. This section documents any observed differences between the wake vortices generated by the Heavy and Large versions of the subject aircraft. This analysis is intended to be a supplement to Reference 3 which summarizes the case for including all B-707 and DC-8 aircraft in the Large class. The various issues and supporting evidence, such as the United Kingdom experience, will not be repeated here. Only questions relating to the interpretation of the O'Hare departure data are addressed.

1.2.3 Wake-Vortex Transport

Some data from the O'Hare takeoff tests were analyzed in a prior study. The ground-wind vortex sensing system (GWVSS) data were included with landing data from Kennedy airport in a draft report on the transport of wake vortices in ground effect. (Since an extensive German study of lateral vortex transport has been published [Reference 4] since the Kennedy and O'Hare study, the U.S. data will be compared to the German data before the old report will be published.) The analysis of data from the monostatic acoustic vortex sensing system (MAVSS) is presented in Section 4.

Section 4 of the report presents the results of an analysis of the probability of vortices being detected at various lateral transport distances. Similar procedures were employed for the earlier GWVSS transport analysis. Plots are presented showing the probability that a vortex will reach a particular lateral distance. Plots are included for each generating aircraft type and comparisons are made with GWVSS results. In addition, this preliminary analysis examines specific features of long transport vortices such as the strength distribution and the ambient crosswind distribution for long transport distances.

1.2.4 GWVSS Analysis

Section 5 of this report presents results of an analysis of GWVSS data employing improved software for plotting of crosswind amplitude versus time (termed stripcharts). Issues considered in this analysis include vortex generation near the ground and its relationship to aircraft attitude (On Ground, Nose Up, Airborne, Gear Up), and the relationship of the

horizontal and vertical components of the cross-wind under conditions of pure ambient wind and when the ambient wind is disturbed by a vortex.

1.3 HAZARD MODEL

The model used to relate the wake vortex hazard to the measured vortex strength (Reference 2) is based on the assumption that the loss of roll control is the primary hazard of a wake-vortex encounter. This model contains a parameter "f" which is defined as the ratio of the maximum acceptable vortex-induced rolling moment to the roll control capability of the aircraft. For example, a value of f = 1.0 means that the aircraft can handle a vortex encounter as long as the roll control capability of the aircraft is not exceeded. The correct value of f is probably less than 1.0 according to flight simulations and other analyses. A value of f = 0.5 may appear to be closer to the actual value. Because of the uncertainty concerning the correct value of f, the sensitivity of the results to the choice of f must be examined. Thus, if the results of the analysis do not change much for different values of f, the results are not affected by uncertainties in the knowledge of the correct value of f.

Table 1-1 shows the hazard threshold values used in the standard hazard analysis and the resulting values of the parameter f. The monostatic acoustic sensor has a vortex detection threshold that is near f = 0.5 so that the data near f = 0.5 may be affected by missing measurements. The impact of missing measurements is to change the apparent duration of the hazard. However, missing measurements are a function of the sensor response characteristics, not aircraft type. Thus, they do not affect comparisons between similar aircraft.

TABLE 1-1. ANALYSIS PARAMETERS

Averaging Radius (m)	Strength Threshold (m^2/sec)	f
5	30	0.6
	50	1.0
10	50	0.5
	75	0.75
	100	1.0
15	75	0.5
	100	0.67
	150	1.0
20	100	0.5
	150	0.67
	200	1.0

2. O'HARE DEPARTURE DATA

2.1 DATA COLLECTION

2.1.1 Sensors

The sensors deployed during the tests are listed in Table 2-1. Each will be described briefly in turn. More information is contained in Reference 10 and other earlier reports. The vortex sensors were installed on the Lines shown in Figure 2-1.

The ground-wind vortex sensing system (GWVSS) consists of a linear array of anemometers installed perpendicular to the aircraft flight path. The single-axis propeller anemometers used are oriented to give a signal voltage proportional to the crosswind. When a vortex pair descends near the ground, the locations of the two vortices are taken to be the positions of the anemometers showing the most positive and most negative signals. Previous studies (unpublished) have indicated that, for low to modest crosswinds, the vortex detection threshold for the GWVSS is significantly below the level where a vortex is a hazard to another aircraft. Consequently, the GWVSS can be used to give a conservative determination of when the hazard disappears. In addition to the normal horizontal orientation of the propeller anemometers, a small number of vertically pointing propeller anemometers were installed to measure the vertical velocity profile of a vortex near the ground.

The monostatic acoustic vortex sensing system (MAVSS) consists of an array of acoustic antennas. The antenna beam is narrow and is pointed vertically. A short burst of energy at approximately 3 kHz is transmitted. The signal scattered from temperature fluctuations in the atmosphere is received and analyzed. The height of the measurement is determined by the time delay of the signal, and the vertical velocity in the measurement volume is determined by spectral analysis of the doppler shift. The measurement volume for the takeoff tests was about three meters in diameter and was set at five meters in height. The maximum height was set for 100 meters. A higher maximum height was used for takeoff rather than than for landing because the vortices are expected to be higher in some cases. The price paid for the greater height is that the period between measurements is increased from 0.4 to 0.6 second. Because the MAVSS antennas do not scan, a vortex measurement is possible only if the vortex drifts past an antenna location at a reasonable speed. Consequently, the MAVSS cannot measure the vortices stalled on the runway centerline where they could cause a hazard to following aircraft. In any case, such an installation would pose a hazard to aircraft using the runway since the antenna would need to be located on the runway surface. The MAVSS can measure vortex decay when the same vortex passes successively over several MAVSS antennas at different ages.

The laser doppler velocimeter (LDV) determines the line-of-sight velocity by measuring doppler shifts in the radiation scattered from aerosols imbedded in the flow field. Range resolution is obtained by focussing the continuous wave (cw) laser beam at the desired range

TABLE 2-1. SENSORS

Type	Height (ft)	Number
GWVSS	10	
Line A		8
Line 1		34
Line 2		33
Line 2 (vert.)		8
Line 3		39
MAVSS (Line 2)	4	10
LDV	12	1
Aircraft Detectors		3
Wind	40	2
	50	1
Acoustic Sounder		1
Temperature	10	1
Pyranometer		1
Camera		1

with a 30-cm diameter telescope. Angular coverage is achieved by scanning the beam in elevation angle through the region of interest. Because the focal region is very narrow and very long, the angular resolution is much better than the range resolution. The poor range resolution complicates the measurement of the vortex velocity profile. However, if the signal-to-noise ratio is high enough, the velocity profile can be extracted from the highest frequency observed in the spectrum of the return signal. For measuring vortices, the LDV scans a plane perpendicular to the aircraft path. Using a real-time display, the operator can adjust the scan parameters to keep the wake centered in the scan area. The LDV can operate effectively at ranges from 90 to 250 meters and has a maximum angular scan of 60 degrees. It measures vortices best when they are located directly overhead. At lower elevation angles, the response from the ambient wind interferes with the vortex measurements and the two vortices can interfere with each other.

The aircraft detectors determine the time when an aircraft passes through a plane perpendicular to the runway by measuring the sound level detected by an acoustic antenna with a fan beam response. The peak signal level was detected by the data collection computer.

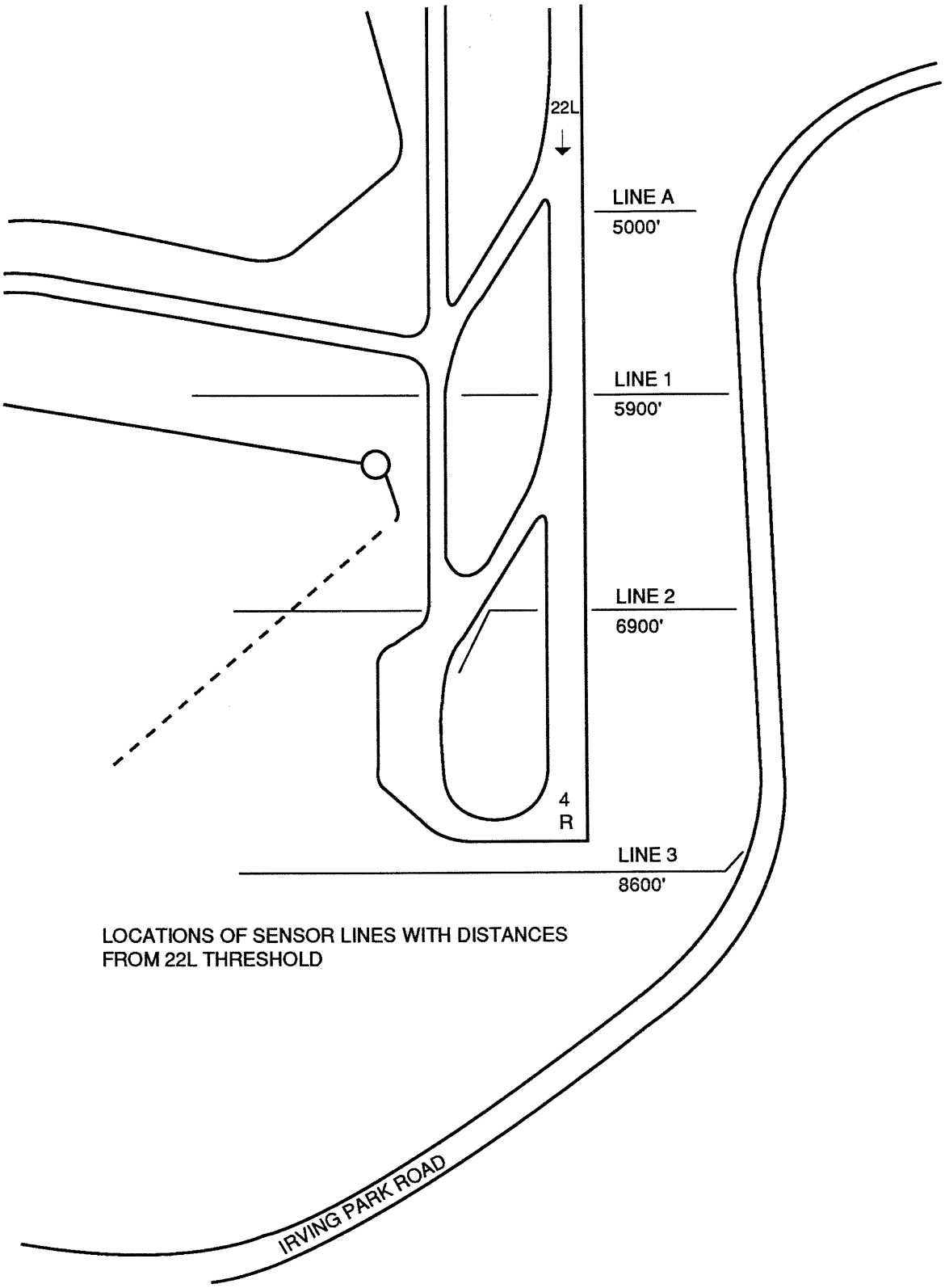

FIGURE 2-1. O'HARE TAKEOFF TEST SITE LAYOUT

The wind sensors are Bendix Aerovanes which were installed as part of the Vortex Advisory System (Reference 5). Three sensors were installed on a 50-foot (15-meter) tower located near the middle marker of Runway 32L.

The temperature sensor was mounted on the side of the data collection van.

The acoustic sounder, manufactured by AeroVironment, Inc., was installed near the data collection van. Its operation is similar to the MAVSS but with a lower frequency, a longer range, and no doppler processing. The profiles of the acoustic sounder are plotted on stripcharts and can be used to determine the height of the inversion layer.

The pyranometer measured the intensity of the solar radiation.

The sensor data were recorded on three separate data tapes: a digital data tape for the GWVSS, a 14-channel analog tape for the MAVSS, and another digital tape for the LDV. All the meteorological data, other than that from the acoustic sounder, were recorded on the GWVSS tape, which is considered to be the primary data tape.

A 35-mm motorized camera was used to take photographs of the aircraft taking off in order to determine their flight path. The camera was located inside the van and was triggered by the aircraft detector on Line 1. For each run, five pictures were taken at intervals of about one second. The date and run number were included in each picture to assist in the data analysis.

2.1.2 Layout

The sensor layout is shown in Figure 2-1. The GWVSS anemometers were installed on four baselines: Line A, Line 1, Line 2, and Line 3, located 5000, 5900, 6900, and 8600 feet (1520, 1800, 2100, and 2620 meters) respectively from the end of Runway 22L. The lateral locations of the anemometers are listed in Table 2-2. Because of an adjacent taxiway, the uniform sensor spacing could not be continued between 480 and 730 feet. Closer spacing was used near the runway where higher resolution was desired to determine how quickly vortices moved away from the runway. The wider spacing at greater distances was adequate to determine how far the vortices could travel before they could no longer be detected. Lines 1 through 3 were the primary vortex sensing locations. Line A was intended to measure the wake near the rotation point of the aircraft. Vertically pointing anemometers were installed at some locations on Line 2 (labeled Line 2(V) in Table 2-2). An aircraft detector was located on each numbered baseline. The MAVSS array was installed next to Line 2 at the lateral locations listed in Table 2-3. The uneven spacing at Antenna 7 was necessary to avoid the nearby taxiway.

2.1.3 Operation

The data collection operation made use of the Volpe Center mobile vortex data acquisition facility (MVDAF). The MVDAF trailer housed the computer that controlled the aircraft

TABLE 2-2. GWVSS ANTENNA LATERAL LOCATIONS
(Feet)

Line	A	1	2(V)	2	3
		-800		-800	-800
		-700		-700	-700
		-600		-600	-600
		-500	-500	-500	-500
	-450	-450	-450	-450	-450
	-400	-400	-400	-400	-400
	-350	-350	-350	-350	-350
	-300	-300	-300	-300	-300
	-275				
	-250	-250	250	-250	-250
	-200	-200	-200	-200	-2200
	-165	-165	-165	-165	-150
					-100
					-50
					0
		165		165	150
		200		200	200
		250		250	250
		300		300	300
		350		350*	350
		400		400*	400
		450		450*	450
		480		480*	500
		730		730	600
		760		760	700
		800		800	800
		900		900	900
		1000		1000	1000
		1100		1100	1100
		1200		1200	1200
		1300		1300	1300
		1400		1400	1400
		1500		1500	1500
		1600		1600	1600
		1700		1700	1700
		1800		1800	1800
		1900		1900	1900
		2000		2000	2000

*Displaced longitudinally to avoid taxiway.

TABLE 2-3. MAVSS ANTENNA LOCATIONS

Antenna	Lateral Position	
	(m)	(Feet)
1	-244	-800
2	-183	-600
3	-122	-400
4	-61	-200
5	61	200
6	91	300
7	232	760
8	274	900
9	335	1100
10	396	1300

camera and recorded the aircraft type and data from the GWVSS anemometers and the meteorological sensors. The processing and recording equipment for the MAVSS sensors were also located in the trailer.

During data collection, the site operator remained in the MVDAF trailer, which was oriented so that the aircraft taking off could be viewed through a window. For each takeoff run, the operator identified the aircraft type visually and entered it into the computer. For B-707 and DC-8 aircraft, the classification as Heavy or Large was determined by monitoring air traffic control on VHF radio. Log sheets were used to record each aircraft type, departure time, and attitude (on ground, nose up, airborne, gear up) at Line A. The general weather conditions and equipment failures were also logged. Data collection began on February 11, 1980, and terminated on October 31, 1980.

The LDV was housed in its own self-contained mobile van and was operated by a separate crew. Separate data log sheets were maintained for the LDV.

The various data collection systems used synchronized clocks or time code generators for data correlation. A common Start-of-Run signal was generated by the MVDAF computer from the aircraft detector signals and sent to the other recording facilities.

2.2 DATA REDUCTION

The data reduction methods for the O'Hare takeoff data differed very little from those described in Reference 10 for the Toronto tests. To understand the details of the data reduction procedures, consult that report. The following sections will point out any differences and will include a further discussion of relevant issues.

2.2.1 Ground-Wind Data

The GWVSS data were processed by computer to determine the vortex trajectories. Computer plots of the trajectories were analyzed visually to determine the positions at 30, 60, 90, and 120 seconds and to determine the time and position of the vortex "death." The vortex death is deemed to occur when the GWVSS no longer shows consistent tracking data.

In addition to plots of vortex trajectories, typical GWVSS analyses include plots of crosswind amplitude versus time at each of the GWVSS sensors (termed stripcharts in Volpe Center wake-vortex analyses). The stripcharts are useful in the identification of true wake-vortex signatures. New software was developed to provide stripcharts in a more concise form, thereby allowing easier comparison between stripcharts and vortex trajectory plots. With this new software, analyses of vortex trajectories based upon vortex trajectory plots can be more easily checked against corresponding stripcharts to ascertain whether apparent vortices in the vortex trajectory plots have true wake-vortex signatures.

Figure 2-2 shows part of the vortex trajectory plot for a B-727 takeoff. Ground-wind data from Lines 1 and 2 (Line 3 data are omitted from this figure) are used to construct the plots on the left and right portions of the figure. At two-second intervals, an S (starboard) is placed at the location of the anemometer with the highest reading, and a P (port) at the location of the anemometer with the lowest reading.

The analyst has marked the output to indicate that at Line 1, the port vortex died at 250 feet after 36 seconds and the starboard vortex died at 300 feet after 22 seconds. The analyst detected both vortices at Line 2 and neither at Line 3 (in the part of the plot omitted from the figure). The numbers written at the beginning of the tracks are residence times indicating how many seconds it took the vortices to exit a 200-foot corridor centered at the runway centerline.

Figures 2-3, 2-4, and 2-5 are stripcharts of the horizontal wind velocities measured at Lines 1, 2, and 3. Takeoff Number 43 at the beginning of each stripchart is the same takeoff as in the vortex-track print of Figure 2-2. The stripcharts agree reasonably well with the vortex-track print. Each display method shows short-lived vortices at Line 1, longer-lived vortices at Line 2, and no vortices at Line 3.

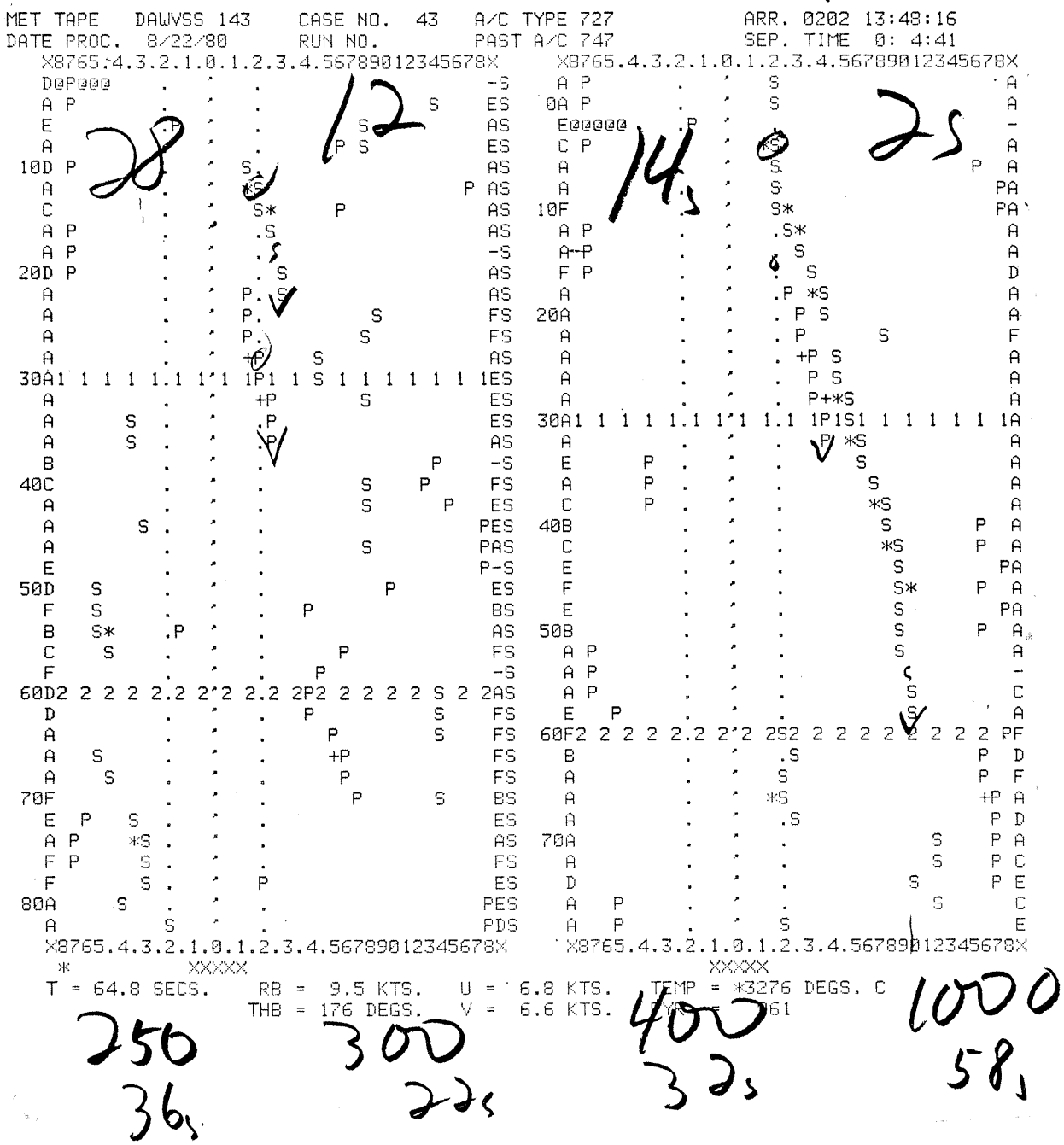

FIGURE 2-2. SAMPLE VORTEX TRACK OUTPUT

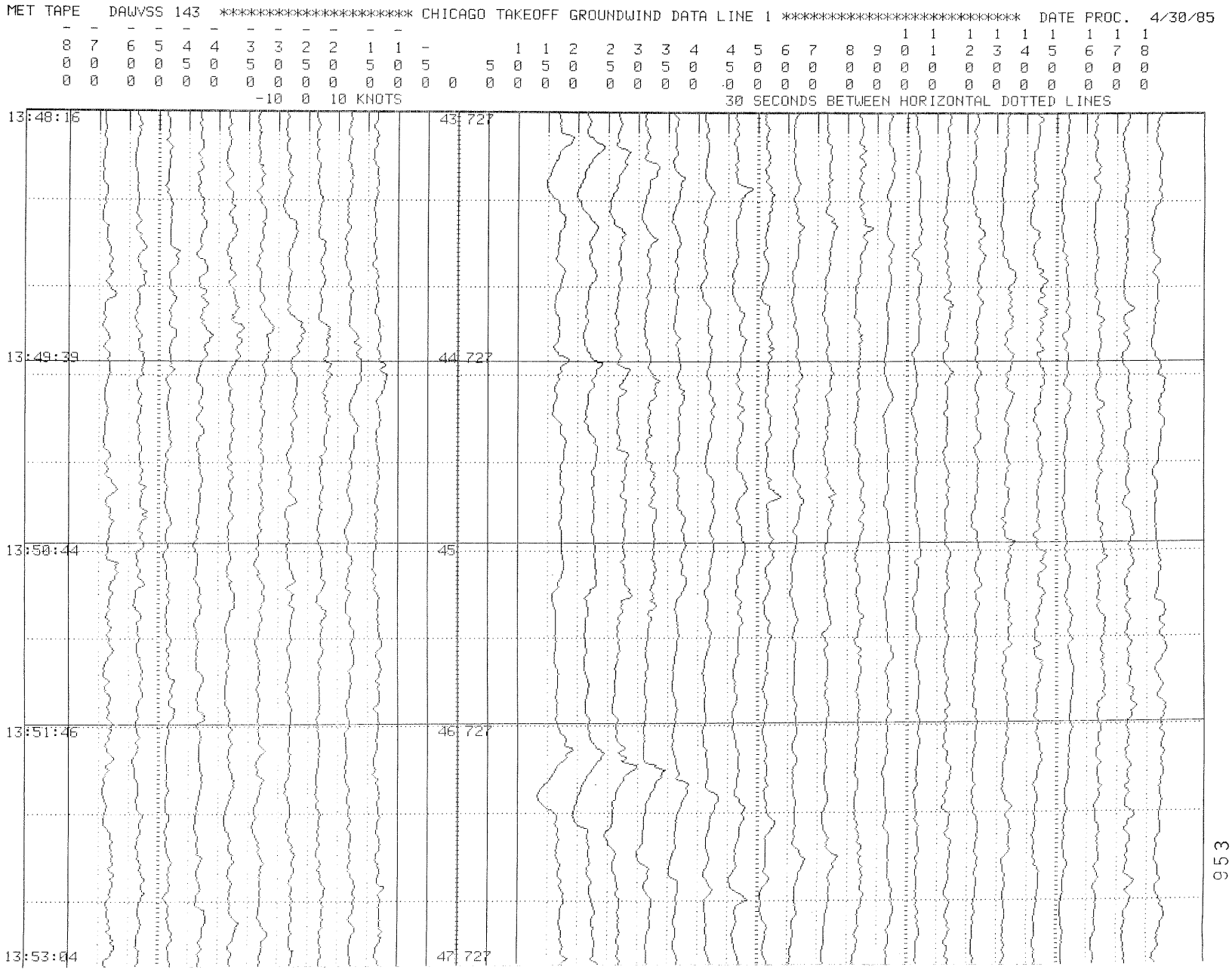

FIGURE 2-3. SAMPLE GROUND-WIND STRIPCHART (LINE 1)

FIGURE 2-4. SAMPLE GROUND-WIND STRIPCHART (LINE 2)

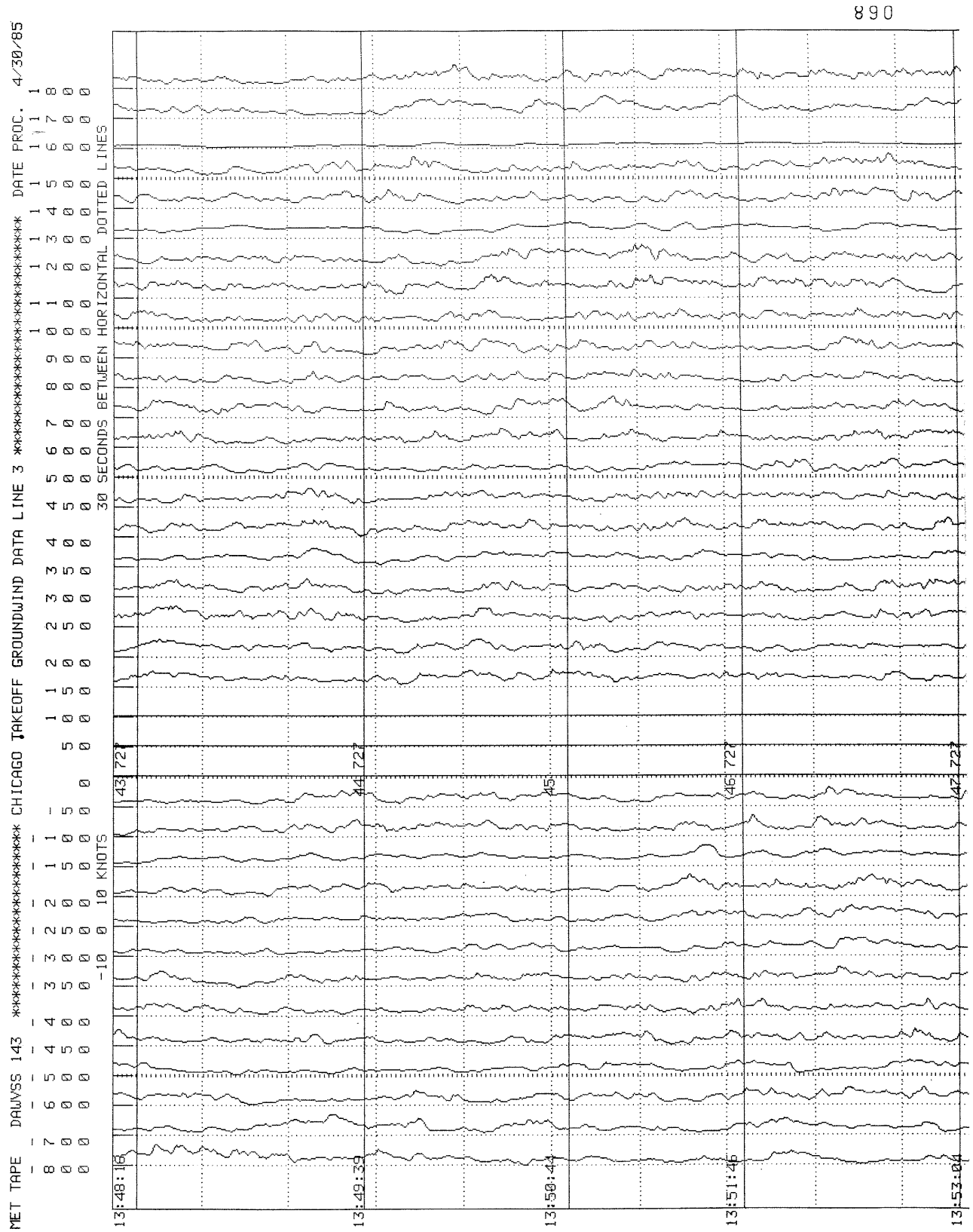

FIGURE 2-5. SAMPLE GROUND-WIND STRIPCHART (LINE 3)

2.2.2 Monostatic Acoustic Data

The MAVSS data reduction program used for landing data had to be modified somewhat to deal with takeoff data. The landing vortices generally showed the classic vertical velocity signatures of an updraft followed by a downdraft for the first vortex to arrive and a downdraft followed by an updraft for the second vortex to arrive. For takeoff vortices, the updraft portions of the vortex signature were often much weaker. Figures 2-6 and 2-7 show sample outputs from the MAVSS processing. Figure 2-6 shows the averaged data used by the correlator to detect vortices. Figure 2-7 shows the vortex velocity and spectral width profiles and the vortex tracks. Reference 1 describes the plots in more detail. The correlator used to detect landing vortices required a substantial updraft component in order to filter out false detections. For takeoff vortices, the updraft requirement had to be relaxed considerably to avoid missing many vortices. The likely explanation for this difference is that the height of the vortices was greater for takeoff than for landing. When the vortex pair is out of ground-effect, the downwash component of each vortex is enhanced and the upwash component diminished by the induced velocity from the other vortex. The relaxation of the updraft requirement resulted in many more false vortex detections for the takeoff data, which therefore required more extensive editing than the landing data.

The MAVSS data received considerable screening and editing before they were entered into the database. First, the MAVSS data plots were compared to the GWVSS plots to make sure that the correct MAVSS antennas had been processed. Only six of the ten antennas could be processed in a single pass. The vortex detections were checked for errors by examining the plots generated during the computerized detection process (Figures 2-6 and 2-7). False detections and strength measurements were deleted and obviously missed detections were added. After the visual screening, a computer screening was carried out to flag possible inconsistencies such as unrealistically high transport velocities or the same vortex being detected on both sides of the runway. The computer screening was then used to guide a final visual check on the data.

The MAVSS database includes the following data for each vortex detection:

- Age
- Height,
- Transport speed, and
- Strengths for 5-, 10-, 20-, and 30-meter averaging radii.

Strength values for 15-meter averaging radii are obtained by interpolation between the 10-meter and 20-meter values from the original MAVSS data.

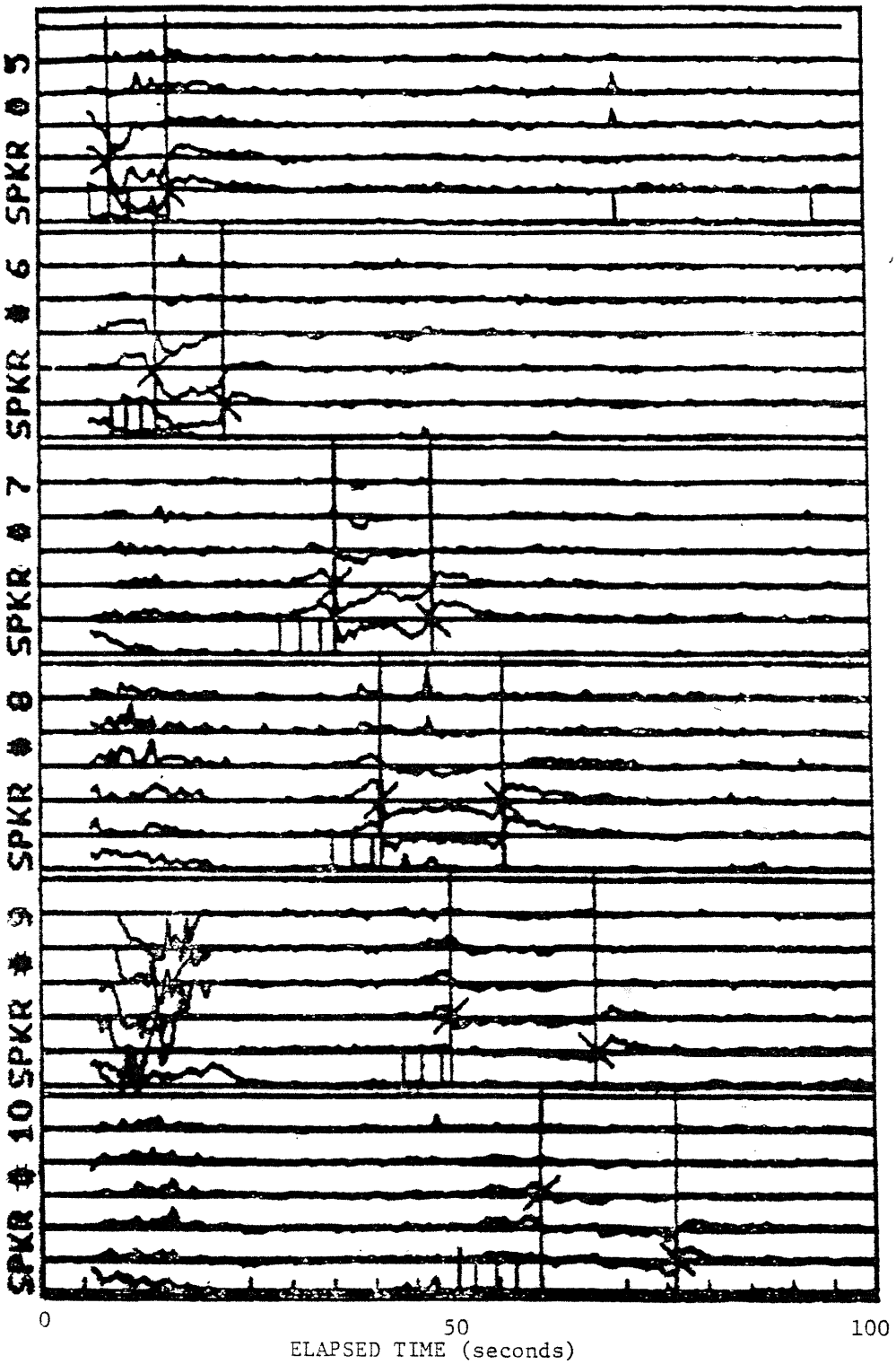

FIGURE 2-6. SAMPLE VORTEX DETECTION CORRELATIONS

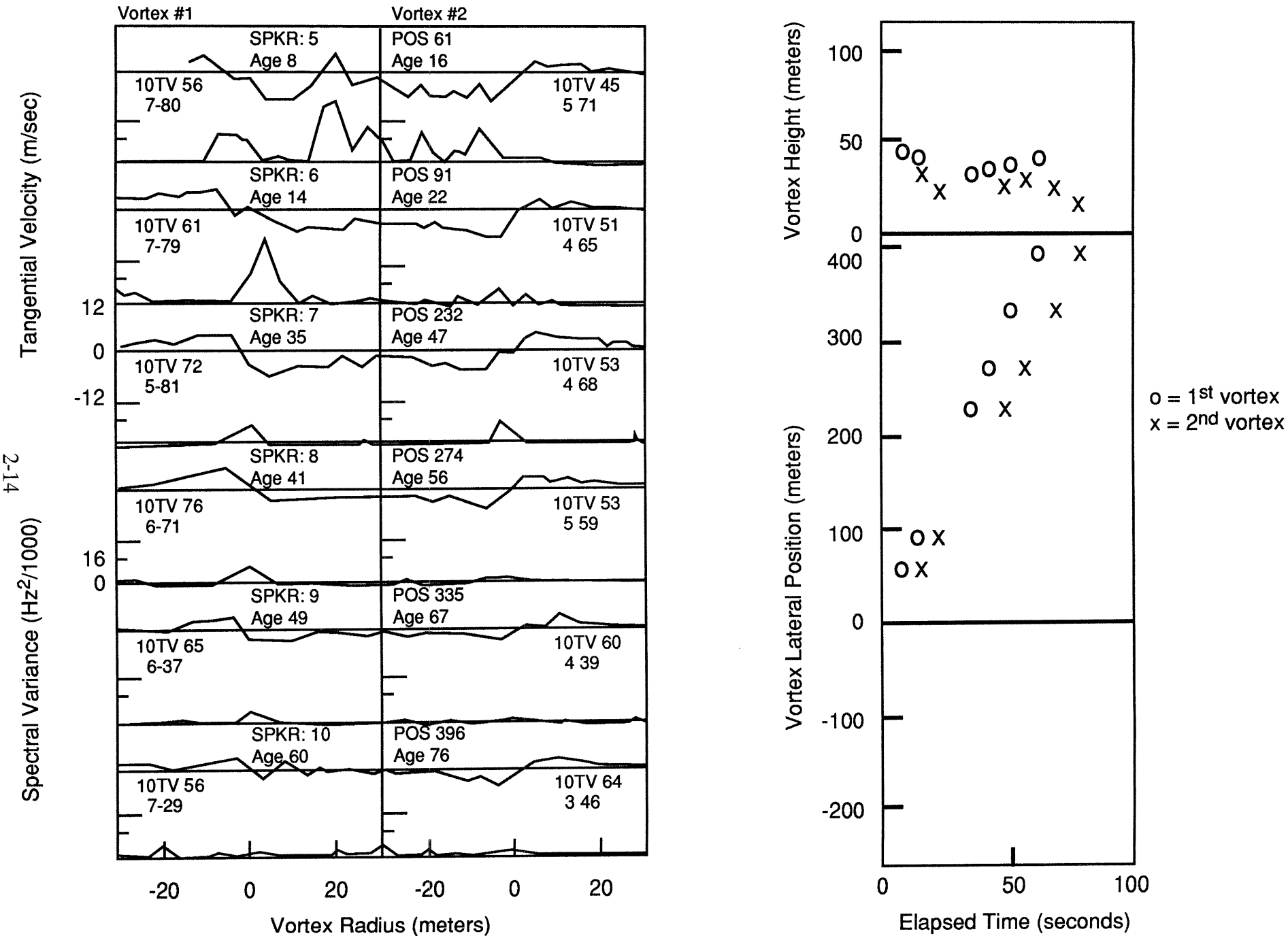

FIGURE 2-7. SAMPLE VORTEX PROFILE (VELOCITY AND SPECTRAL VARIANCE) AND VORTEX MOTION PLOTS

Time histories of the wake-vortex strength were developed for each vortex with at least two detections. The time history estimates vortex strength at 10-second time intervals from zero to 200 seconds using the interpolation/extrapolation procedure described below:

a. For times between valid detections, the strength is estimated by linear interpolation.

b. If the last detection does not occur at the end of the sensor line, then the vortex strength is extrapolated to zero at the speaker following the last valid detection. The arrival time at the speaker following the last valid detection is estimated as:

$$T_E = T_L + D/V_T$$

where:

T_E = estimated vortex arrival time at next speaker
T_L = last detection time
D = distance to next speaker
V_T = vortex transport speed at last speaker

This extrapolation procedure is subject to the following restrictions:

1. The estimated arrival time at the next speaker must occur no more than 60 seconds after the last valid detection;

2. The estimated arrival time at the next speaker must occur at least 10 seconds before the next aircraft arrival.

c. The initial vortex strength is assumed to be equal to the first detection occurring within 20 seconds. If no detection occurs within 20 seconds, then no initial vortex strength is assigned.

Considerable effort was directed at insuring that this algorithm was properly programmed into the data analysis software.

2.2.3 Photographic Data

The photographic data were processed to determine the aircraft height over each numbered sensor line. The height was defined by the position of the root of the aircraft wing.

2.2.4 Databases

The data reduction for the three sensors discussed above resulted in three independent ASCII databases which had to be merged for much of the data analysis. The ground-wind database was the primary database because it contained the only accurate identification of aircraft type. The merging process for the ground-wind and monostatic-acoustic databases was based on matching the arrival times recorded by the two systems. A difference of five seconds was allowed. The photographic database was merged by means of date and run number. The LDV data were never processed into a database because of the intense labor involved.

Although some of the MAVSS data statistics to be presented in the next sections required the use of the full database, most of the analysis employed a simplified binary database using one disk block per run which included only runs with at least two MAVSS detections. This truncated database could be accessed very quickly and contained all of the MAVSS data considered to be valid for analysis. At least two MAVSS detections are required to obtain accurate transport speeds and, hence, accurate strength values, since the strength value is proportional to the transport speed.

The two wake vortices generated by an aircraft are designated in MAVSS data as "Vortex 1" and "Vortex 2" according to their arrival order at a particular MAVSS antenna. This distinction is related to the point of vortex generation (port or starboard with respect to the aircraft) and the direction of vortex transport. The lateral transport direction of each of the two wake vortices is determined by the ambient crosswind. Useful MAVSS measurements are generally obtained only on the downwind side of the runway. The downwind vortex is the first to reach a particular MAVSS antenna and is termed "Vortex 1." If the crosswind is large enough, the upwind vortex will also move with the wind and will arrive second at a particular MAVSS antenna and hence be termed "Vortex 2." If the crosswind is small, however, the upwind vortex will drift in the opposite direction from the downwind vortex because of its induced motion in ground effect. If it reaches a MAVSS antenna, it would also be termed "Vortex 1." If the crosswind magnitude is exactly right, the upwind vortex will stall on the runway centerline where it poses a potential hazard to an aircraft following on that runway. Thus, it is the duration of the upwind vortex, measured as Vortex 2 by the MAVSS system, that best characterizes the wake vortex-hazard to an aircraft following on the same runway. The experimental data show that second vortices last longer than first vortices.

3. RECLASSIFICATION OF B-707 AND DC-8 AIRCRAFT

3.1 DEPARTURE DATA ANALYSIS METHODS

3.1.1 Aircraft Weights

In contrast to the landing tests (References 1 and 2), actual B-707 and DC-8 departure weights were not obtained for the departure tests. Consequently, the various statistical analyses of the effects of aircraft weight on wake vortex strength and persistence cannot be repeated for the departure data. Fortunately, there is no reason to expect any significant difference in these results for departing aircraft. The departure data analysis will be limited to comparing the decay of the wake-vortex hazard for the Large and Heavy versions of the B-707 and DC-8 and for other aircraft types.

3.1.2 Hazard Decay Analyses

The decay of the wake-vortex hazard is based on the hazard model outlined in Section 1.3. The new time-history algorithm (see Section 2.2.2) was first discussed in Reference 6, but was not used for much of the data analysis in that report. The primary algorithm change was to eliminate the use of vortex detections after 20 seconds to estimate the initial vortex strength. Since the vortices can decay significantly after 20 seconds, the prior algorithm included many low strengths in the initial strength distribution. Thus, earlier plots of the vortex-hazard probability showed lower initial values than observed in the corresponding plots of this report. Figure 3-1 shows a sample plot of the vortex-hazard probability versus time. The hazard probability is estimated as the ratio of the number of vortices with strength above the hazard threshold at a given time divided by the number of valid measurements at that time. The time-history algorithm is used to determine these numbers for the ensemble of vortices. The analysis software uses six threshold values: 30, 50, 75, 100, 150, and 200 m^2/s. Table 1-1 shows how these values are related to the hazard model parameter f for the four averaging radii: 5, 10, 15, and 20 meters. The data for a particular value of averaging radius pertain to an encountering aircraft with a wingspan equal to twice the averaging radius. For example, the 15-meter radius data would be used for a DC-9 which has a wingspan of approximately 30 meters. Figure 3-1 plots the hazard probability for Vortex 2, which is the vortex that might stall on the runway centerline and thereby pose a hazard to a following aircraft using the same runway. The figure contains two plots. The left plot shows the decay of the hazard probability for all ten aircraft types so that all can be compared. The right plot isolates the B-707 and DC-8 data so that detailed comparisons can be made.

The hazard decay plots for the O'Hare takeoff data are shown in Appendix A. For comparison, hazard decay plots using the same time-history algorithm are shown for the O'Hare landing data in Appendix B.

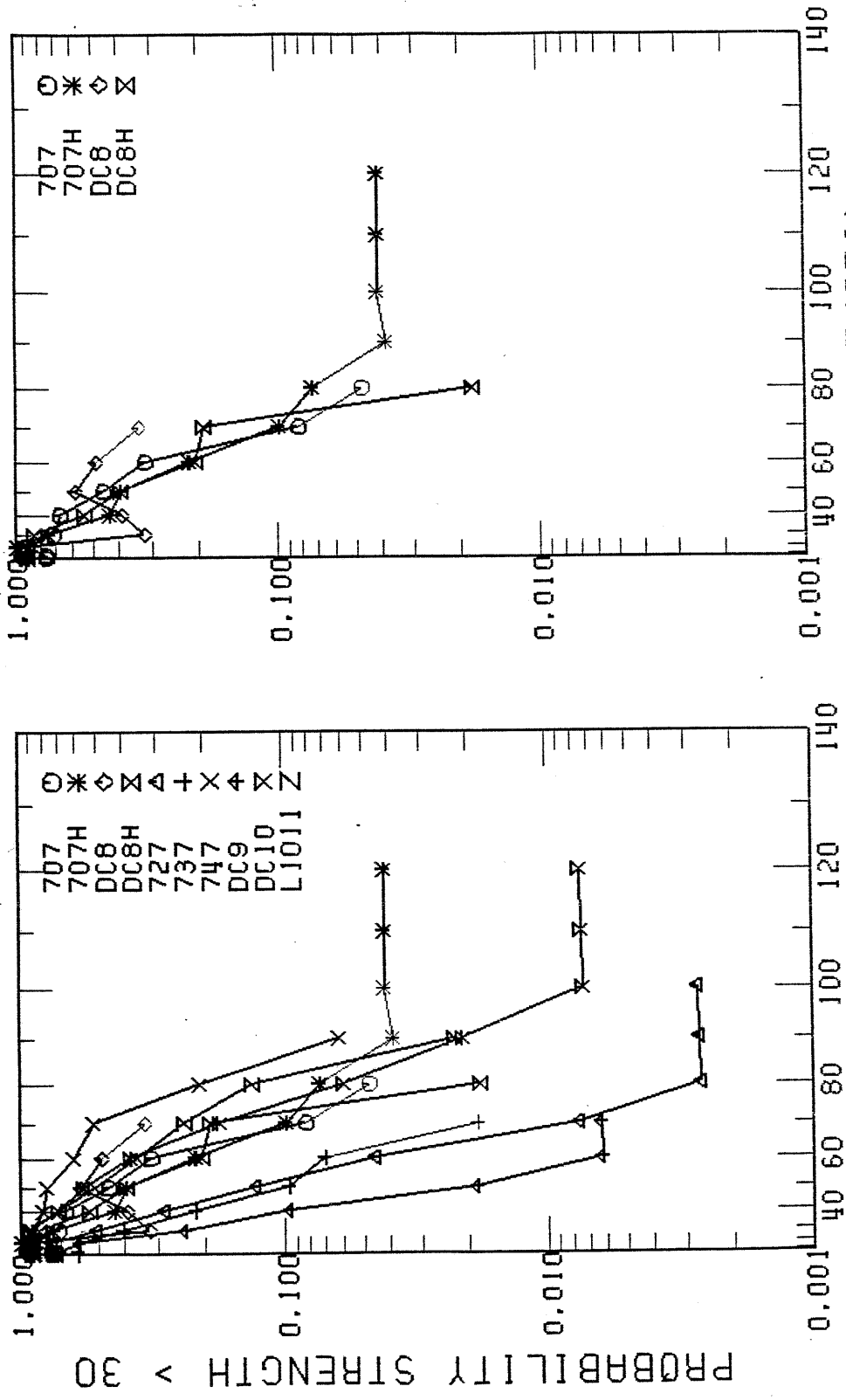

FIGURE 3-1. VORTEX HAZARD PROBABILITY VERSUS TIME BY AIRCRAFT TYPE

The interpretation of the hazard decay requires some care since statistical fluctuations can produce dramatic effects which are not statistically significant. The most obvious effect occurs when one vortex lasts for an abnormally long time. One such vortex will add a horizontal tail to the end of the decay curve. Such stragglers occasionally appear in the plots and will be ignored in the discussion. The calculated fractional standard deviation (Reference 2) of a particular probability point is simply one divided by the square root of the number of hazardous vortices at that point. Thus, the data have virtually no statistical significance at the level of one hazardous vortex.

3.2 HAZARD DECAY RESULTS

3.2.1 Landing

The original results of the hazard decay analysis for landing (Reference 2) showed comparable hazard persistence for B-707, DC-8, and DC-8H vortices (H denotes the Heavy versions). Some plots for small averaging radii showed somewhat longer persistence for B-707H vortices. This difference was not, however, statistically significant. On the other hand, B-707 vortices showed a statistically significant faster hazard decay than the B-707H for small averaging radii and low hazard thresholds. The similarity of the DC-8H and B-707H wake decay to that of the DC-8 was used to support the reclassification of the Heavy versions into the Large class. Comparisons between aircraft showed that the B-707/DC-8 versions had more rapid hazard decay than most of the Heavy class (B-747 and L1011), but had comparable hazard decay to the Heavy DC-10, and had, as expected, slower hazard decay than smaller Large aircraft such as the B-727, B-737, and DC-9.

The analysis of landing data using the new time-history algorithm (see data in Appendix A) produced some noticeable changes in the comparisons of vortex decay for different aircraft. First, the plots for all aircraft types are more likely to show a hazard probability of one at time zero. The net effect of this change was to reduce the difference between the Large and Heavy classes. Nevertheless, in most cases, the B-747 and L1011 have a more persistent hazard than the B-707/DC-8 types. The other noticeable change produced by the new algorithm is a shuffling of the decay rates for the B-707/DC-8 types for 5-meter averaging radius and for the 50 and 75 m^2/s thresholds at 10-meter averaging radius. For these four plots, the difference between the B-707H and DC-8 hazard persistence has increased to the degree that the B-707H may have a significantly longer persistence at some points on the decay curves. Since the total number of B-707H cases is only 10, it is not realistic to place much weight on these results which, in fact, show the B-707H decay to be identical to the B-747 and L1011. Thus, the re-analysis suggests that the Heavy B-707H *may* have a more persistent wake-vortex hazard than the Large DC-8 for following aircraft with wingspans of 20 meters or less. To put these B-707H observations in perspective, it should be noted that a similar long hazard persistence was observed for DC-8 takeoff vortices, for which only six vortex 2 cases were measured. These DC-8 takeoff measurements are too few to be worth discussing in the next section.

TABLE 3-1. COMPARISON OF WIND DISTRIBUTIONS

Aircraft	Number of Cases	Fraction of Winds Below 9 Knots
B-707H	9	1.00
B707	53	0.58
DC-8	31	0.52
DC-8H	17	0.82

One hypothesis for explaining the abnormal persistence of B-707H wake vortices is that the meteorological conditions for the ten B-707H runs were more favorable to long vortex persistence than those for the other aircraft types. This hypothesis was tested by examining the distribution of the ambient wind speed for the cases where Vortex 2 was detected at age 70 seconds or older. Selecting the age limit of 70 seconds gives about the same number of cases as shown in the hazard decay plots. The wind distribution results are shown in Table 3-1.

The wind magnitude was abnormally low for the B-707H cases. Since long vortex persistence is correlated with low wind speed, it is not surprising that the hazard persistence in these test results is longer for the B-707H.

3.2.2 Takeoff

Table 3-2 shows the number of departure vortices from each aircraft type for which at least two successive measurements were made on the same vortex. Very few DC-8 aircraft were measured so that it is not possible to use the DC-8 to define the upper limit of the Large class, as was done in the original landing analysis. Fortunately, the departure data can be analyzed successfully without the DC-8 data. It was found that the B-707H and DC-8H vortex decay was indistinguishable (within expected statistical variations) from that for the B-707. Thus, for departure, the B-707 can be used as the reference for the upper end of the Large class.

The data on the measured hazard decay for departure wake vortices is shown in Appendix A. Only vortex 2 is considered since the primary goal of the study is to analyze separations for aircraft using the same runway. The B-707, B-707H, and DC-8H data points cluster closely together in all plots. No significant difference is discerned between Heavy and Large versions.

Comparisons between B-707/DC-8 versions and other aircraft are generally similar to the landing observations. One minor difference is that the L1011 results generally look more like

TABLE 3.2. DEPARTURE VORTICES MEASURED

Aircraft	First Vortex	Second Vortex
B-707	85	46
B-707H	98	55
DC-8	8	6
DC-8H	135	86

the DC-10 rather than the B-747. The DC-10 and L1011 plots are often close to the DC-8/B-707 plots. In many figures, particularly for low hazard thresholds, the B-747 plots show dramatically longer hazard persistence than all other aircraft.

3.2.3 Comparison Of Takeoff And Landing

Hazard persistence appears to be greater on landing than on takeoff for all DC-8/B-707 versions for all averaging radii except the 20-meter value, where the persistence is similar for takeoff and landing. Because of differences in meteorological conditions and in the methods of collecting and analyzing the two data sets, such an observed difference does not necessarily represent an actual difference in the rate of the hazard decay.

3.3 CONCLUSIONS

The decay of the wake-vortex hazard from departing Heavy B-707 and DC-8 aircraft was observed to be similar to that from Large B-707 aircraft. As expected, the decay of the wake-vortex hazard for B-707/DC-8 aircraft is consistently faster than that for the B-747 which is the heaviest member of the Heavy class. Two other members of the Heavy class, the DC-10 and the L1011, showed hazard durations similar to those of the B-707/DC-8. Note, however, that the monostatic acoustic sensor responds to thermal fluctuations in the wake and therefore may respond differently to aircraft whose engine exhaust is injected near the vortex core (B-707, DC-8, and B-747 with four wing-mounted engines) than to those with no engines located near the origin of the vortex core. In particular, the lack of injected exhaust may produce poor signal-to-noise ratios which could result in erroneously low vortex velocity measurements. Consequently, it would be a mistake to use the similarity of B-707/DC-8 and DC-10/L1011 data to justify putting the latter aircraft into the Large category. These two aircraft were observed to exhibit abnormally slow vortex decay on landing, according to Reference 6.

The data on the decay of the wake-vortex hazard from departing B-707 and DC-8 aircraft showed no unexpected results which would question the safety of including all B-707 and

DC-8 aircraft in the Large class under all conditions. According to the analysis of Reference 3, no important impact on safety would result from such a reclassification. In any case, the accident/incident reporting statistics show that wake-vortex encounters are more likely on landing than on departure, probably because the landing aircraft are restricted to a small amount of airspace near the glideslope and runway centerline, while departures use much more airspace as a result of differing rotation points and vectoring.

The question of the relative duration of the landing wake-vortex hazard from a Heavy B-707 and a Large DC-8 was revived by a re-analysis of the landing data. The results suggested more strongly than in the previous analysis (Reference 2) that the wake-vortex hazard duration *may* be longer for a Heavy B-707 than for a Large DC-8. The small number of data points for the B-707H prevented a definitive answer to this question, particularly since the B-707H cases occurred during abnormally low wind conditions. If this observation were verified, it could cast some doubt upon the safety of reclassifying the Heavy B-707 as Large. Fortunately, the recent United Kingdom experience, discussed in the next section, can be used to bypass this question. The cost of additional data collection could not be justified on the basis of this question alone.

3.4 RECOMMENDATIONS

It is recommended that all B-707 and DC-8 aircraft be classified as Large for all operations. This classification has been in operation safely since January 1982 in the United Kingdom. According to the UK incident reporting system (Reference 7), the effect of transferring Heavy B-707 and DC-8 aircraft to the Large class has been twofold:

a) The incident rate for Heavy B-707 and DC-8 aircraft behind other Heavy aircraft (e.g., the B-747) was drastically reduced from a relatively high level to the point of being negligible.

b) The incident rate for other aircraft behind the Heavy B-707 and DC-8 aircraft increased somewhat, as might be expected since the separations were reduced. The incident rate, nevertheless, remained at an acceptable level.

The UK experience has thus shown the safety of the reclassification. The analyses contained in this report and those of References 2 and 3 have not established any significant safety problems that would result from such a change in the separation standards.

4. WAKE-VORTEX TRANSPORT ANALYSIS

This section of the report analyzes the probability of vortices being detected at various lateral transport distances. The procedures for analyzing the MAVSS vortex transport data are similar to those employed for the earlier GWVSS transport analysis (unpublished). Plots are included that indicate the probability of vortex arrival as a function of distance from the runway centerline. Separate plots are presented for each generating aircraft type. Comparisons are made between landing and takeoff results and with GWVSS results. Specific features of long transport vortices, such as strength distribution and the ambient crosswind distribution, are also examined.

4.1 METHODOLOGY

The probability of a vortex moving laterally some specified distance (coinciding with the distance from the runway centerline to a MAVSS speaker) is estimated as the number of vortices detected at that distance divided by the total number of vortices generated. Separate transport probabilities are computed for each direction of motion (with respect to the runway centerline). For purposes of computing probabilities, it was therefore necessary to determine the direction of motion of the wake vortices. Where wake vortices were detected at one or more speakers, the direction of motion is clear. For wake vortices that were never detected, the direction of transport was taken to be the direction of the crosswind. Note: For low values of crosswind, this assumption may not be valid; however, the error introduced by this assumption is likely to be very small.

A requirement for inclusion of an observation in the analysis was that the vortices be generated below the height (approximately 350 feet) where the normal vortex descent would bring them within the range of the MAVSS. In addition, it was required that the generating aircraft be off the ground for inclusion in the analysis. Thus, only vortices generated between 0 and 350 feet at line 2 were considered. Table 4-1 shows the number of wake vortices included in the database for each generating aircraft type and direction of motion.

If a wake vortex was detected at a given distance, it can be inferred that it existed but was undetected at all lesser distances. In a number of instances, the data show that a vortex was not detected at one or more speakers located closer to the runway centerline than the speakers where it was detected. Table 4-1 shows by aircraft type, the number of cases in which detections could be reasonably inferred but did not exist in the original data. The subsequent plots and analysis calculate probabilities of detection including all inferred detections.

Table 4-1 indicates that it would have been useful to have additional speakers spaced farther from the runway centerline. Note that 80 of the 467 (more than 1/6) of the DC-10 generated vortices moving in the positive direction were observed at the 1300-foot (farthest) speaker. Thus, for future experiments designed to observe the spacial boundaries encompassing the complete demise of the wake-vortex hazard, speakers should be placed beyond 1300 feet,

TABLE 4-1. COUNTS OF ACTUAL AND INFERRED DETECTIONS

Positive Direction

A/C Type	Distance from Runway Centerline (Feet)												Total+
	200		300		760		900		1100		1300		
	A*	I	A	I	A	I	A	I	A	I	A	I	
DC-10	345	122	419	11	219	14	176	7	114	0	80	0	467
DC-9	400	133	442	17	115	10	60	4	20	5	12	0	533
DC-8	2	0	2	0	2	0	1	0	0	0	0	0	2
DC-8H	85	27	97	5	52	2	37	0	19	2	16	0	112
L1011	70	12	72	1	39	0	24	0	14	1	6	0	82
707	61	37	88	2	31	1	20	1	11	0	10	0	98
707H	74	35	100	3	36	0	25	2	16	0	9	0	109
727	1374	414	1538	41	449	42	276	16	116	20	69	0	1788
737	195	46	198	6	55	5	30	3	7	4	8	0	241
747	35	14	43	0	23	1	16	1	10	0	7	0	49

Negative Direction

A/C Type	Distance from Runway Centerline (Feet)								Total
	-200		-400		-600		-800		
	A*	I	A	I	A	I	A	I	
DC-10	265	48	232	13	167	7	88	0	313
DC-9	230	70	179	26	120	4	22	0	300
DC-8	2	3	5	0	4	0	2	0	5
DC-8H	47	10	47	3	25	1	9	0	57
L1011	58	6	46	1	35	0	15	0	64
707	54	19	55	1	29	0	14	0	73
707H	40	25	51	4	40	0	11	0	65
727	741	279	653	51	397	19	141	0	1020
737	101	36	95	4	50	1	14	0	137
747	41	11	42	2	27	0	16	0	52

+. Total includes undetected vortices, thus is greater than or equal to row total.
*. A - actual data I - inferred data.

possibly as far as 2500 feet. Future analyses of the currently available MAVSS data, including detailed strength analyses, comparison of the MAVSS and GWVSS transport probability results, and detection thresholds may yield a better estimate of how far the MAVSS speakers should be located from the runway centerline in future experiments.

In addition, missed detections seem to be disproportionately high at the closest speakers to the runway centerline. This effect is probably due to a higher proportion of vortices being above the range of the MAVSS speakers closer to the runway centerline.

An additional problem with the data used in this analysis is interference in the measurement due to the arrival of another aircraft. A vortex that arrives at a MAVSS speaker within 10 seconds of the arrival of the next aircraft may not be shown to have been detected by the speaker in this database. An estimate was made of the prevalence of this condition in the database using the vortex velocity at the time of last detection, the distance to the next speaker, and the time from the last detection to the next aircraft arrival. The condition exists for 25% of DC-10, 36% of B-727, and 26% of B-747 Port vortices. The condition exists for 26% of DC-10, 41% of B-727, and 16% of B-747 Starboard vortices. Although various methods were tried, no satisfactory algorithm was found to alleviate this problem. As a result, the vortex transport plots show a vortex hazard distance that is less than the actual distance.

4.2 VORTEX TRANSPORT RESULTS

Unpublished earlier analyses of ground wind data indicated that the log of the probability of detection was roughly proportional to the square of the distance. Thus, the plots were scaled accordingly: probability of arrival has a log scale, and distance has a square scale. Detection probabilities were computed separately for vortices moving in each direction from the runway centerline, and for each sensor type: MAVSS and GWVSS.

Figures 4-1, 4-2 and 4-3 show the transport probability plots for the aircraft types with the most data: the DC-10, B-727, and DC-9 respectively. Plots for other aircraft types are included in Appendix C. The plots are approximately linear; thus, the choice of scaling for the axes was appropriate. Vortices appear to decay somewhat faster on the negative (short) side of the runway centerline, although this effect is not highly pronounced. The last speaker on the negative side may have been adversely affected by highway noise (see Figure 2-1). A substantial proportion (17 percent) of the DC-10 vortices were transported to the end of the positive (long) side of the centerline. By comparison with the GWVSS results, the vortices appear to decay significantly more slowly with distance in the MAVSS data. Note the steeper descent of the GWVSS curves (Figures 4-1, 4-2, 4-3). This discrepancy is worsened by the problem of measurement interference due to arrival of the next aircraft (see Section 4.1 above), which results in a MAVSS curve steeper than it should be; hence the discrepancy is even greater than shown in the Figures. This analysis indicates that the MAVSS is more sensitive to wake vortices in motion than the GWVSS.

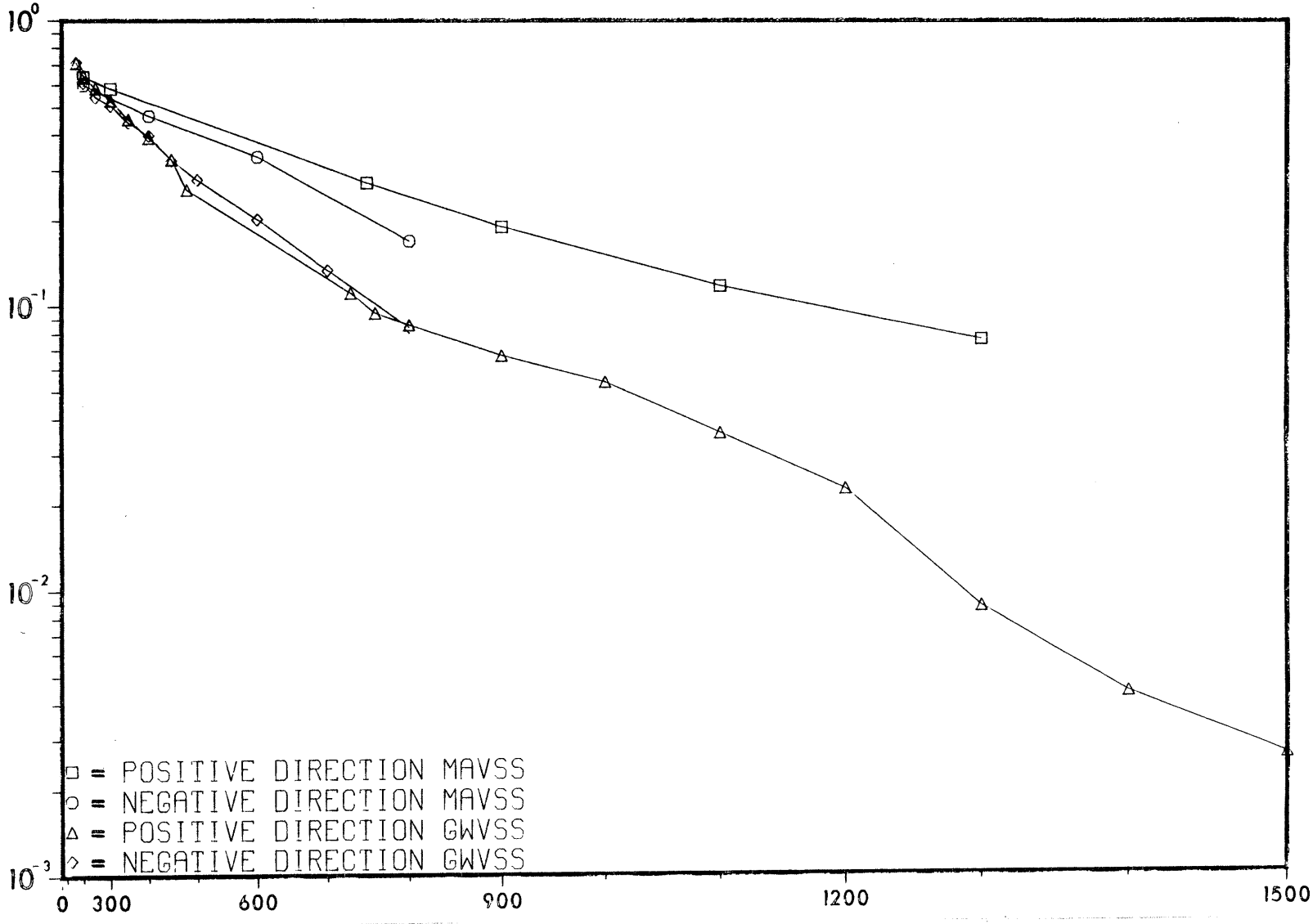

FIGURE 4-1. PROBABILITY OF DETECTING A VORTEX AS A FUNCTION OF DISTANCE FROM THE RUNWAY CENTERLINE: AIRCRAFT TYPE, DC-10

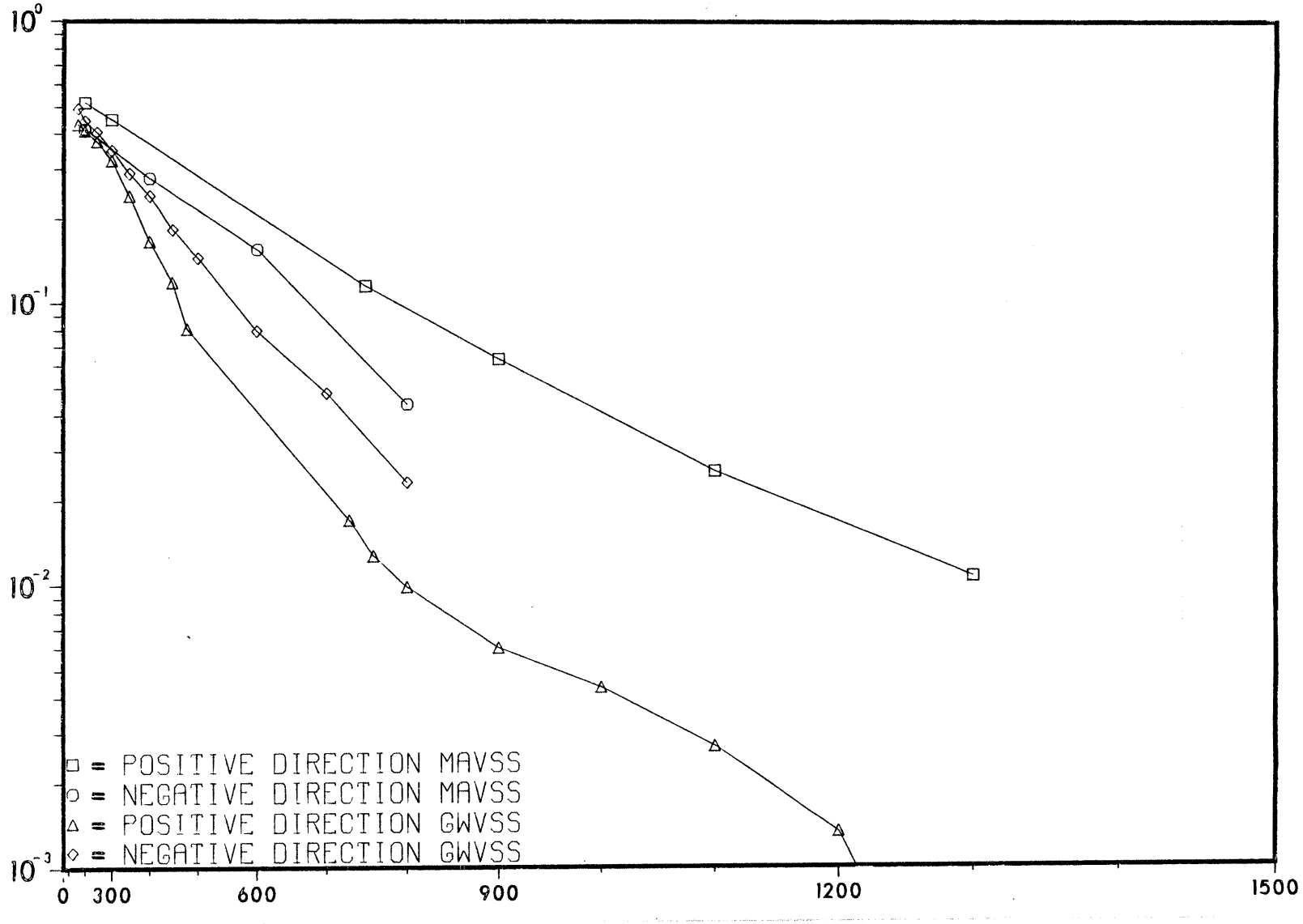

FIGURE 4-2. PROBABILITY OF DETECTING A VORTEX AS A FUNCTION OF DISTANCE FROM THE RUNWAY CENTERLINE: AIRCRAFT TYPE, B-727

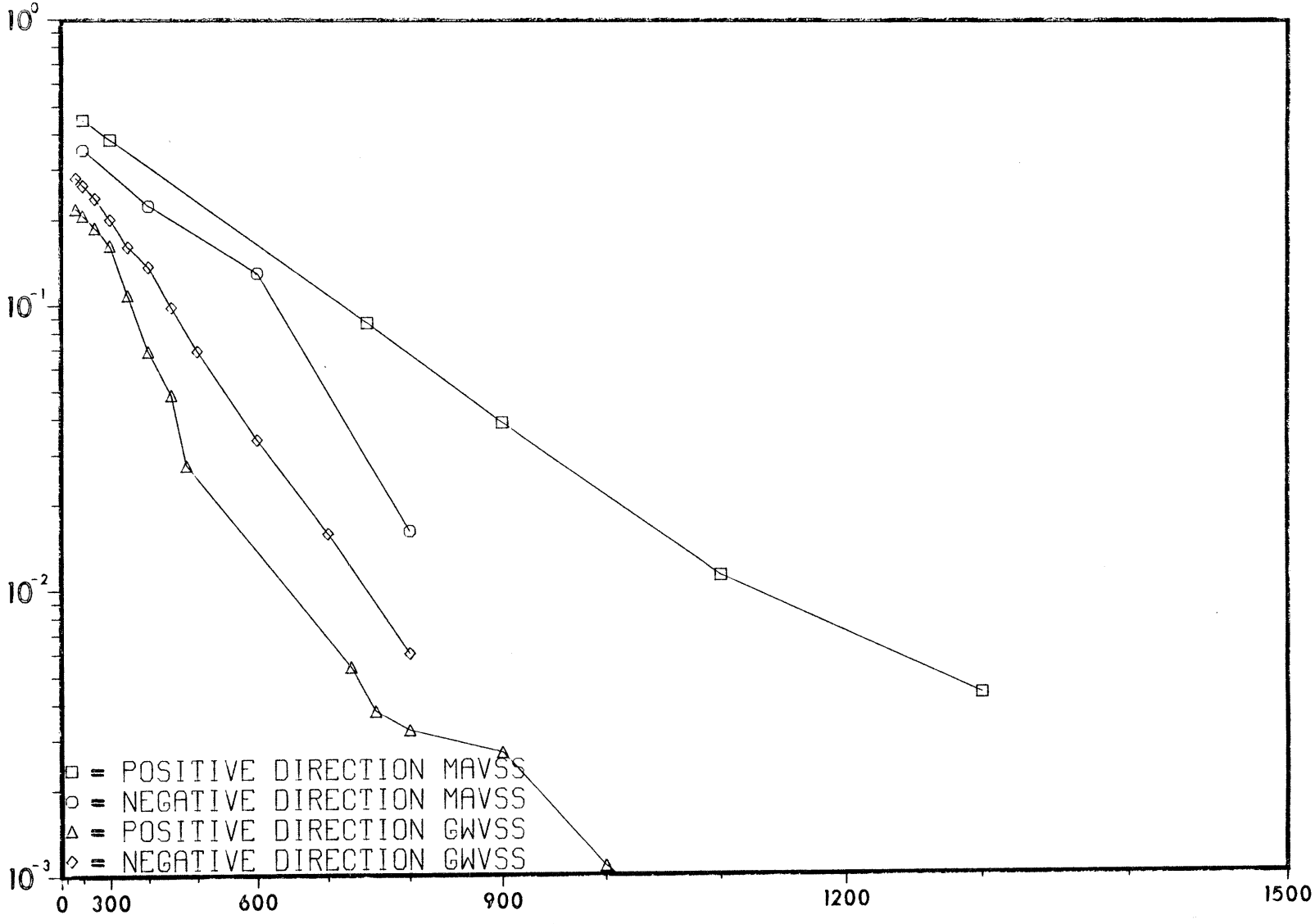

FIGURE 4-3. PROBABILITY OF DETECTING A VORTEX AS A FUNCTION OF DISTANCE FROM THE RUNWAY CENTERLINE: AIRCRAFT TYPE, DC-9

The crosswind distribution for vortices transported to the MAVSS speaker at 1300 feet (positive direction) from the runway centerline is shown in Figure 4-4. Approximately two-thirds of the vortices transported to the 1300-foot speaker had crosswinds in excess of seven knots. By comparison, approximately three-fourths of the crosswinds occurring when one or more vortices moved in the positive direction were less than seven knots (Figure 4-5). Thus, it is evident that long transport of vortices requires relatively high crosswinds.

Figures 4-6, 4-7, and 4-8 show the strength distribution for vortices transported to the 1300-foot speaker (all aircraft types) at averaging radii of 5, 10, and 20 meters respectively. Note, the sign of the strength distinguishes Vortex 1 from Vortex 2 (see discussion in Section 2.2.4). Using the conventions of this analysis, first vortices have negative strengths and second vortices have positive strengths. If vortices exceeding 50 percent of the roll control authority of the following aircraft are considered hazardous (Reference 2), then vortices of strength in excess of 25, 50, and 100 m^2/s are hazardous to following aircraft of 5-, 10-, and 20-meter semispans, etc. By this criteria, 31 percent of those vortices transported to 1300 feet were hazardous to 5-meter semispan follower aircraft. Twenty-five percent were hazardous to 10-meter semispan follower aircraft and 16 percent were hazardous to 20-meter semispan aircraft.

4.3 RECOMMENDATIONS

For parallel runway analyses, the MAVSS data appear to be better suited than GWVSS, because the MAVSS measures the strength of vortices directly and because the MAVSS appears to have a lower detection threshold as illustrated by the high proportion of vortices detected at 1300 feet. For single runway analyses, the GWVSS data are superior, because MAVSS strength determinations rely on vortex lateral motion. Future analyses should make more extensive use of the MAVSS strength data. For example, the decay of the vortex hazard with transport distance could be analyzed with respect to various strength hazard thresholds. In addition, correlations should be made between MAVSS and GWVSS data to ascertain the reliability of the two sensing systems and their respective data. Future analyses should make more extensive use of meteorological data, to gain further insight into the relationship of meteorological conditions and the decay of the vortex hazard.

The slow demise of vortices, as exhibited, for example, by the proportion of B-747 vortices detected at the 1300-foot (farthest) speaker, indicates that a useful long range research effort would be to instrument one or more runways with MAVSS speakers, perhaps as far as 2500 feet from the runway centerline. This effort could provide information useful in the determination of maximum vortex transport.

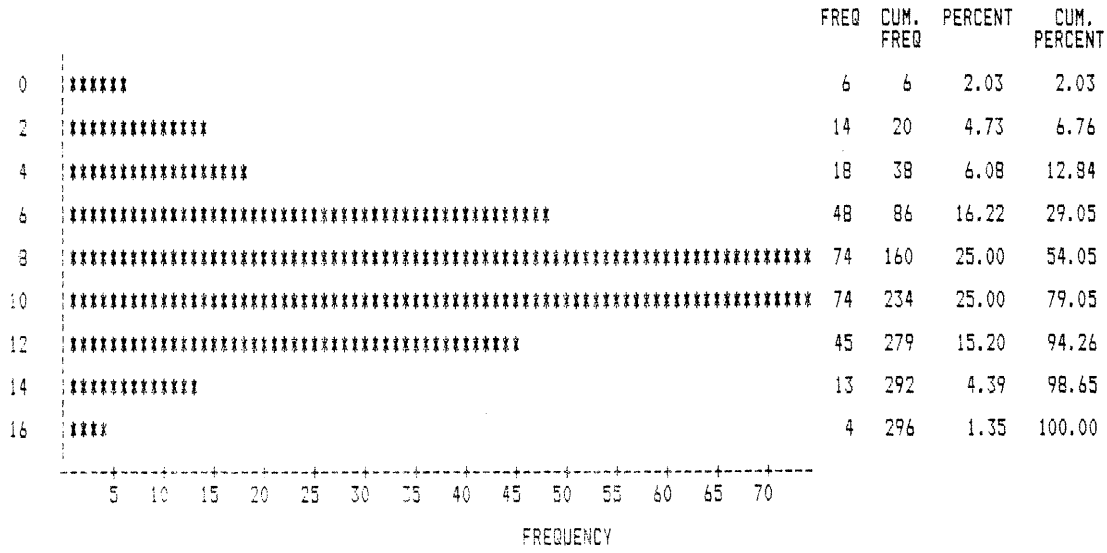

FIGURE 4-4. CROSSWIND DISTRIBUTION FOR VORTICES DETECTED BY THE MAVSS SPEAKER 1300 FEET FROM THE RUNWAY CENTERLINE

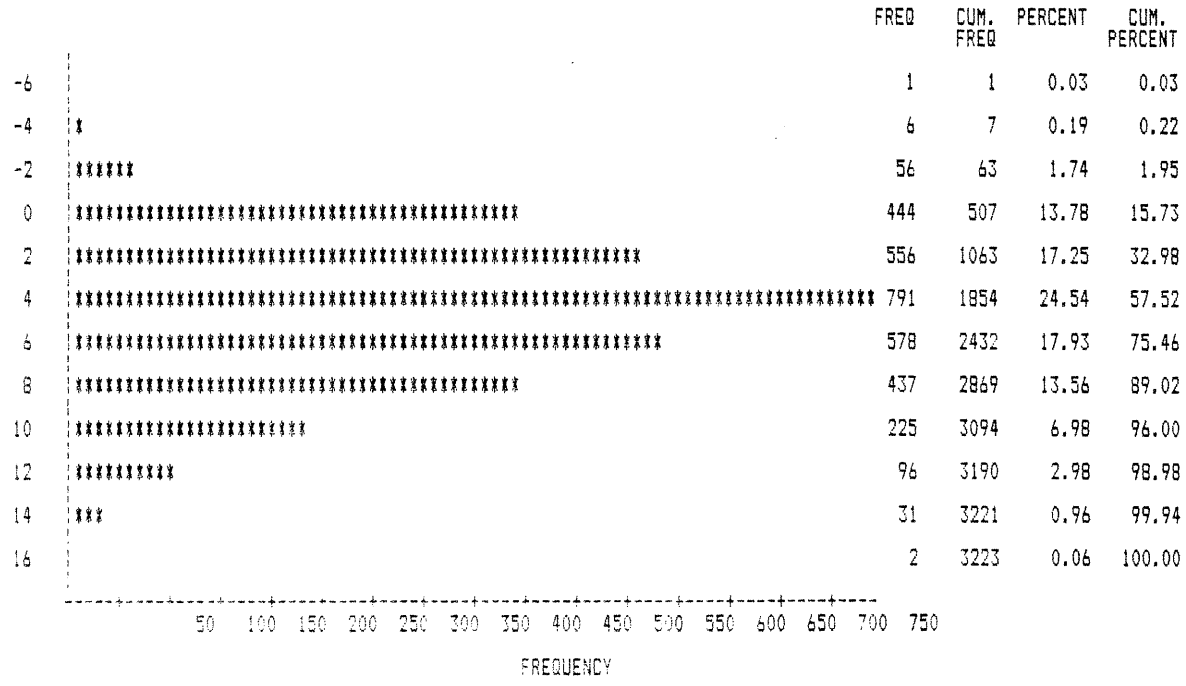

FIGURE 4-5. CROSSWIND DISTRIBUTION FOR VORTICES MOVING IN POSITIVE DIRECTION

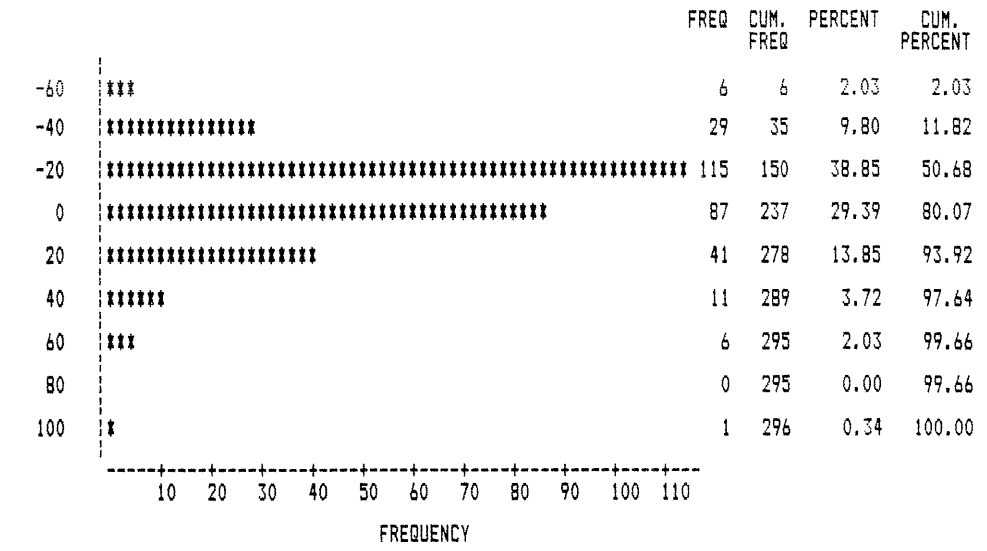

FIGURE 4-6. STRENGTH (m^2/s) OF VORTICES TRANSPORTED 1300 FEET ALL AIRCRAFT TYPES, FIVE-METER AVERAGING RADIUS

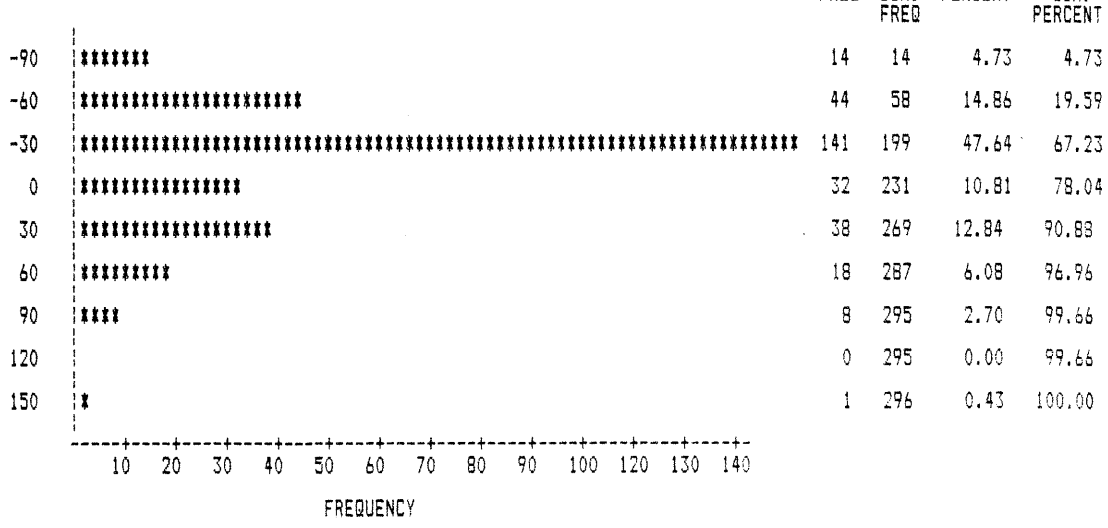

FIGURE 4-7. STRENGTH (m^2/s) OF VORTICES TRANSPORTED 1300 FEET ALL AIRCRAFT TYPES, TEN-METER AVERAGING RADIUS

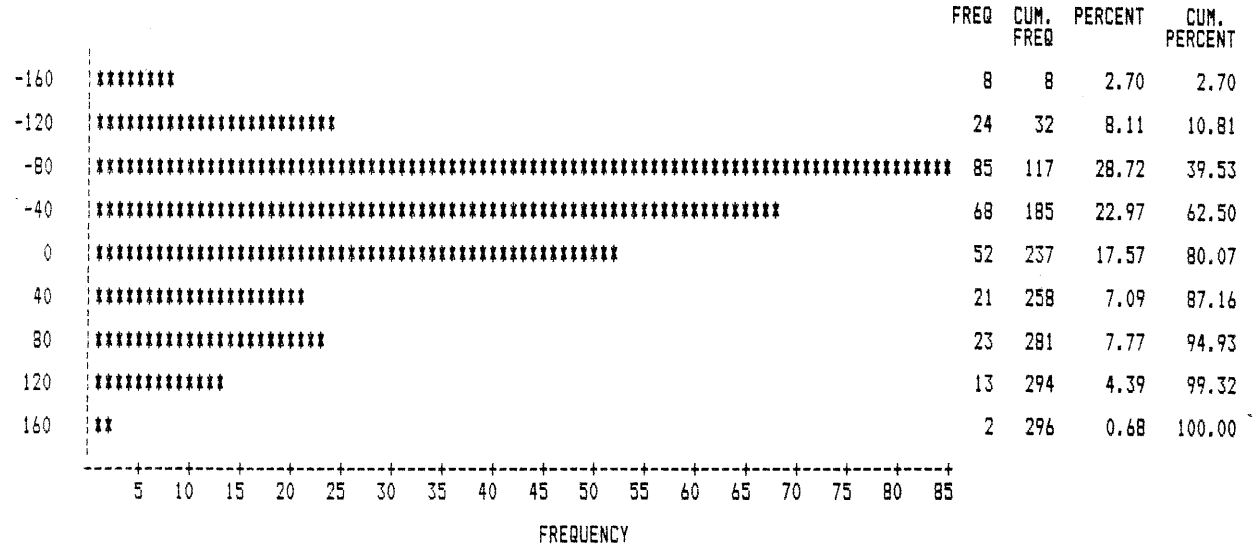

FIGURE 4-8. STRENGTH (m^2/s) OF VORTICES TRANSPORTED 1300 FEET ALL AIRCRAFT TYPES, TWENTY-METER AVERAGING RADIUS

5. GWVSS ANALYSIS

The groundwind data from Lines 1, 2, and 3 of Figure 2-2 were analyzed using vortex-trajectory plots to obtain vortex death times and death positions; these values then formed the ground-wind database. The analysis of this data is in an unpublished report. Sections 5.1 and 5.2 below discuss some ground-wind data that was not included in that report.

5.1 THE AIRCRAFT ROTATION POINT - LINE A

Line A consists of eight horizontal ground-wind anemometers on the port side of the runway 5000' from the end of the runway 22L (see Figure 2-1). The locations of each anemometer are given in Table 2-2. This line was located near the expected rotation point for many of the takeoffs.

The site operator would note the attitude (On Ground, Nose Up, Airborne, Gear Up) of each aircraft as it passed Line A. Approximately one-half of the planes had an attitude of Airborne or Gear Up at Line A.

There were no MAVSS speakers at Line A, so there is no accurate way to estimate the vortex strengths near the rotation point. Stripcharts of the horizontal winds measured at Line A can show the presence or absence of a vortex, however, and the maximum wind change can be used as a crude indicator of vortex strength.

Table 5-1 below summarizes vortex detection data at Line A for 80 B-727 takeoffs. The data is for all the B-727 takeoffs on groundwind tapes 052 and 081. These two tapes were chosen because they each had many takeoffs (about 100) and the ambient crosswind was blowing toward Line A (port side) at approximately two knots.

TABLE 5-1. VORTEX DETECTIONS AT LINE A

Aircraft Attitude at Line A	Cases	% with Vortices Evident	Avg. Wind Change (Knots)	Avg. Ht. at Line 1 (Feet)
On Ground	18	83	1.5	19
Nose Up	34	79	1.8	44
Airborne	16	100	3.9	120
Gear Up	12	92	3.1	75

Since only 18 of the B-727 takeoffs have the On Ground attitude, it is clear that the median rotation point was somewhat before Line A. Vortices were visually observed in the stripcharts for the majority of takeoffs regardless of the aircraft attitude. In particular, vortices are evident while the aircraft is still on the ground. The average wind change is the difference between the maximum wind sensed along the line and the ambient wind sensed before the aircraft passed the line. Using this average wind change as a crude measure of vortex strength, it is clear that the vortices are noticeably weaker when the aircraft is still on the ground. This would be expected since full lift has yet to be achieved.

The last column in Table 5-1 shows the average aircraft heights as they flew over Line 1, which was 900 feet further down the runway from Line A. This height data was computed from a sequence of several photographs taken for each takeoff. The aircraft heights at Line 1 correlate reasonably well with the aircraft attitude at Line A and serve to indicate that the site operators were accurate in their attitude designations. Also, note the rapid decay at Line A for on-ground vortices.

Figures 5-1 and 5-2 show typical vortex groundwind signatures at Lines A and 1 respectively for two DC-10 takeoffs. The heading at the top of each stripchart gives each anemometer location in feet from the centerline. Time is measured in the vertical direction with 30 seconds between adjacent horizontal dotted lines.

In Figure 5-1, takeoff 31 (10:41:58) shows a weak port vortex at Line A generated by a DC-10 on the ground (i.e. before rotation) as it passed Line A. In Figure 5-2, the same aircraft at a 25-foot altitude shows a pair of separating vortices. The port vortex in Figure 5-2 appears stronger than the port vortex in Figure 5-1.

In Figure 5-1, takeoff 5 (9:56:19) shows the port vortex generated by a DC-10 in the Nose-Up attitude as it passed Line A. This vortex appears stronger than the port vortex of the DC-10 still on the ground (takeoff 31) and is essentially as strong as the vortex generated by the same DC-10 as it flew at 75 feet over Line 1 (takeoff 5 in Figure 5-2).

5.2 VERTICAL ANEMOMETERS - LINE V

All anemometers at Lines A, 1, 2, and 3 were oriented to measure the horizontal component of the crosswind. On the left side of Line 2, vertical anemometers were placed next to eight of the horizontal anemometers to measure the vertical component of the wind.

Table 5-2 below gives the average maximum horizontal and vertical wind changes at Line 2 due to the port vortices shed by the same B-727 takeoffs analyzed in the previous section.

The wind signals produced by the vortices are generally smaller for higher aircraft. This result can be explained by vortex decay during the time required for the vortex pairs to descend to an altitude where they can be sensed by the anemometers. The average vertical wind changes are about 30 percent as large as the average horizontal wind changes. If the anemometers

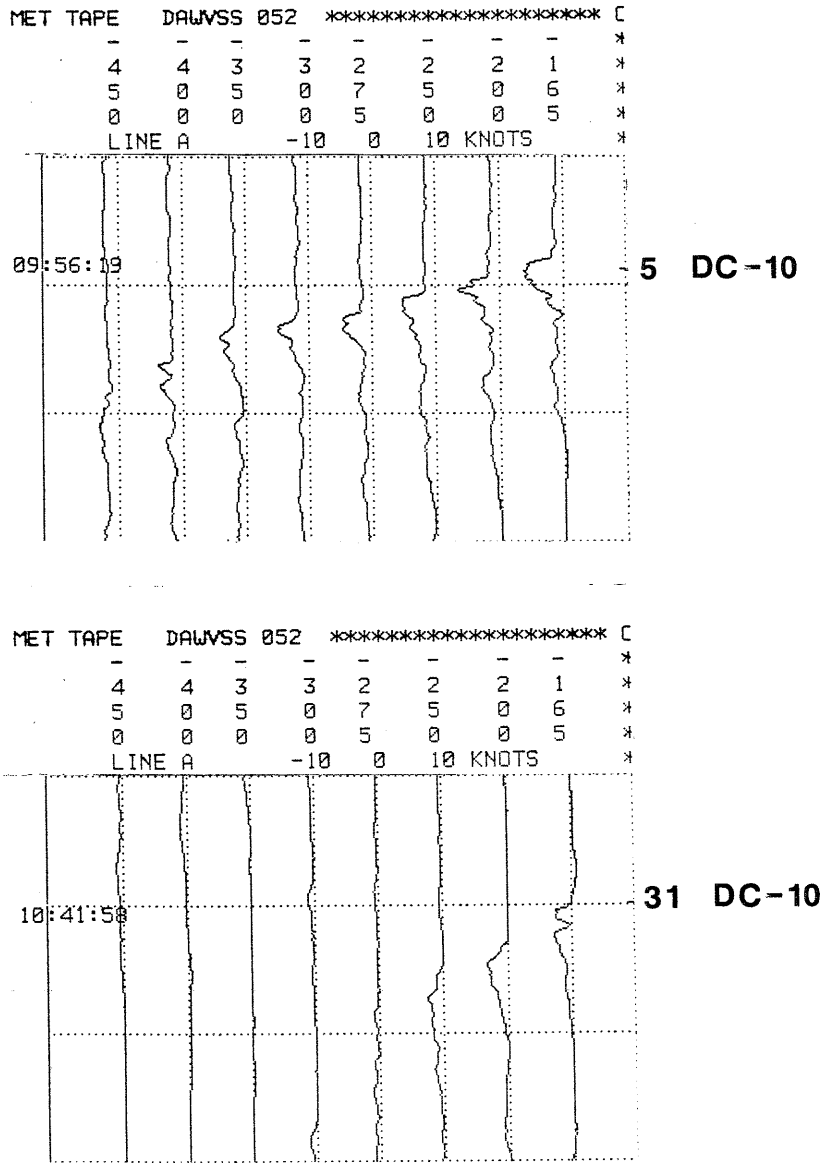

FIGURE 5-1. GROUND-WIND DATA AT LINE A

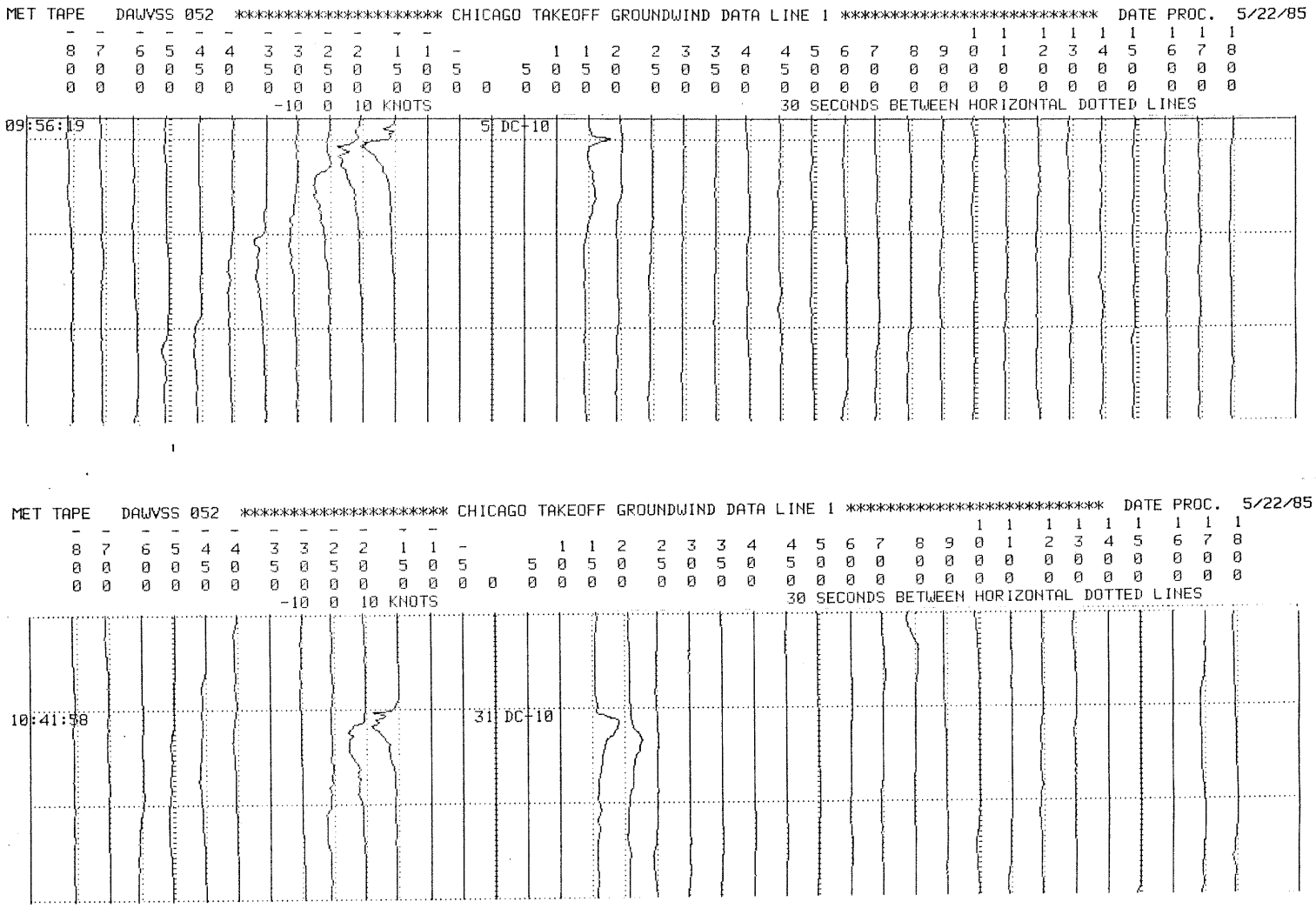

FIGURE 5-2. GROUND-WIND DATA AT LINE 1

TABLE 5-2. HORIZONTAL AND VERTICAL WINDS AT LINE 2

A/C Ht. (H) Over Line 2 (Feet)	Cases	Avg. Horiz. Wind Change (Knots)	Avg. Vert. Wind Change (Knots)
H = 0	None	---	---
0 < H < 75	4	3.8	1.3
75 ≤ H < 150	48	4.9	1.7
150 ≤ H < 225	22	3.6	1.3
225 ≤ H ≤ 300	6	1.8	1.2

were at ground level, there would be no vertical component due to the vortices since no wind can flow into the ground. The vertical winds are a result of the anemometers being ten feet above the ground. In general, the vertical winds measured are somewhat higher than the analytic model predicts, as will be discussed at the end of this section.

Figure 5-3 is a stripchart showing side-by-side, the horizontal and vertical components of the wind for 2 takeoffs on groundwind tape 052. Note that the scale for the horizontal wind, Line 2, is double the scale for the vertical wind, Line V.

The anemometers of Line 2 show an ambient crosswind of about 2 knots towards the negative side. There is effectively no vertical component to the ambient wind as would be expected so close to the ground.

Both vortices from the B-727 can be seen drifting off to the negative side in the Line 2 horizontal data. The port vortex produces a negative wind (to the left of the zero line) and the starboard vortex produces a positive wind. The two vortices can be clearly seen in the vertical data at the -250 foot anemometer. The second (starboard) vortex arrives at the anemometer about 20 seconds after the first (port) vortex. The first vortex produces an updraft followed by a downdraft. The second vortex produces a downdraft followed by an updraft. For this case, the maximum horizontal and vertical wind changes are approximately three knots each.

The bottom part of Figure 5-3 shows the port vortex shed by a DC-10 during takeoff. The starboard vortex stalled over the runway and therefore cannot be seen in the stripchart. The maximum horizontal wind change at the 200-foot anemometer is approximately nine knots. The maximum vertical wind change at the same anemometer is approximately three knots, giving a horizontal to vertical wind ratio of 3 to 1.

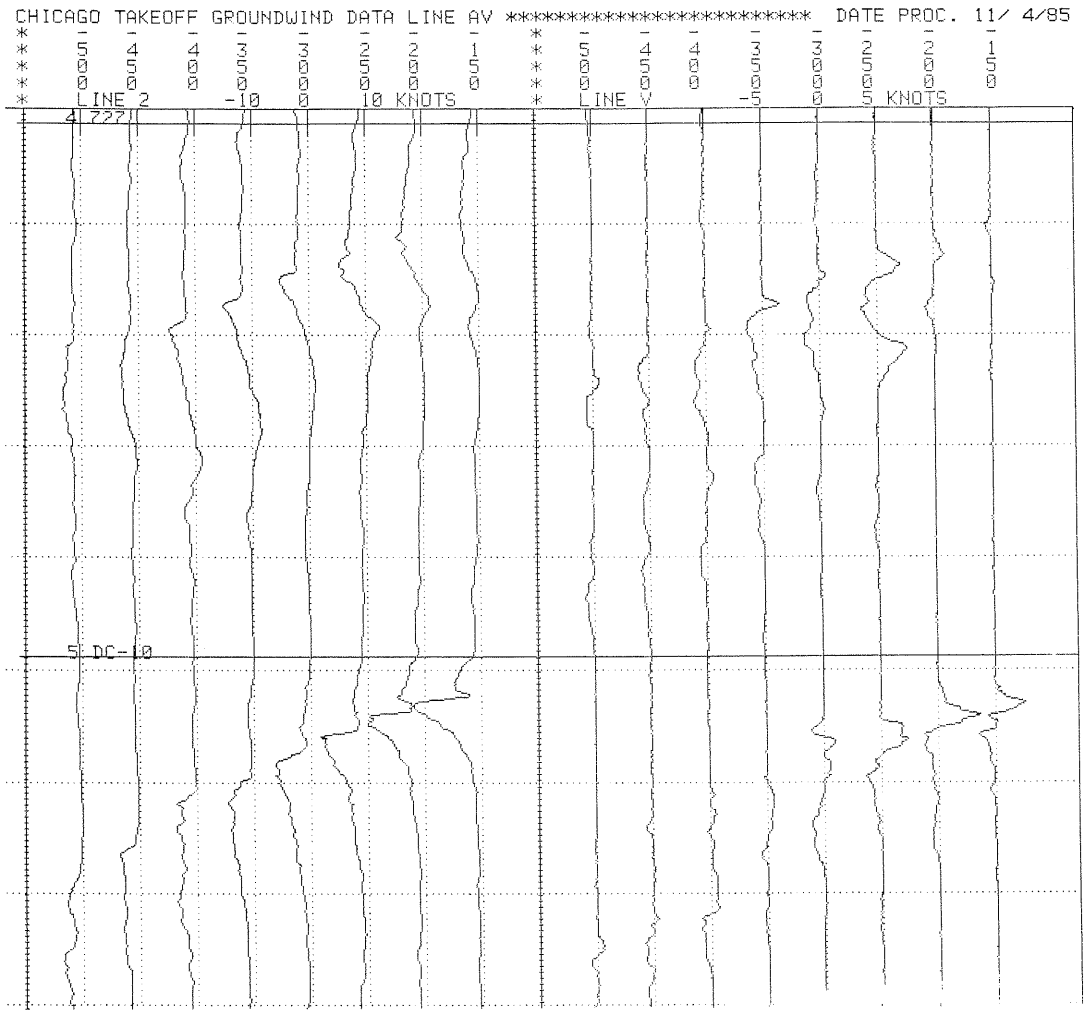

FIGURE 5-3. HORIZONTAL AND VERTICAL GROUND-WIND AT LINE 2

An analytic model program was run to compare with the measured winds for the DC-10 takeoff in Figure 5-3. The model integrates the equations of motion for a vortex pair and their image vortices to model the effect of the ground. The vortex swirl velocity outside the core is given by

$$V(r) = \Gamma_\infty/2\pi r[1+(r_c/r^2)]$$

where Γ_∞ is the vortex circulation at infinity and r_c is the radius where the maximum velocity occurs.

The MAVSS database provided values for the average circulation, $\Gamma'(5)$ and $\Gamma'(10)$, for this DC-10 vortex over averaging radii of 5 and 10 meters out from the vortex center. The average circulation is related to Γ_∞ and r_c by the following equation:

$$\Gamma'(r) = \Gamma_\infty[1-(r_c/r)\tan^{-1}(r/r_c)].$$

From this equation, values of 201 m^2/sec and 3.0 m were obtained for Γ_∞ and r_c. The initial height of the vortex pair was set at 25 meters, and the initial separation was 38 meters which is $\pi/4$ times a DC-10 wingspan and corresponds to the expected vortex separation for a wing with elliptic loading. The 25-meter height was chosen so the vortex would cross the anemometers at an altitude of 17 meters, which was the altitude measured by the MAVSS sensor next to the 200-foot anemometer.

Figures 5-4 and 5-5 show the horizontal and vertical winds from the model at the 200-foot sensor for these initial conditions. These curves are to be compared with the measured winds at the 200-foot anemometer in Figure 5-3. The horizontal wind profiles agree as well as can be expected. The maximum measured horizontal wind change was about 9 knots versus a model value of 7.7 knots. Both the model and the measured data agree that the vortex took about 30 seconds to pass over the anemometer. This transport speed results from a one-knot crosswind and the vortex motion induced by the ground.

The model predicts a maximum vertical wind from the vortex of 0.86 knots, as shown in Figure 5-5. The measured wind in Figure 5-3 is about three knots. This underestimate of the vertical wind by the model appears to occur often and will require further investigation to be clearly understood. The effect is probably related to the vortex interaction with the ground and with the ambient wind shear near the ground.

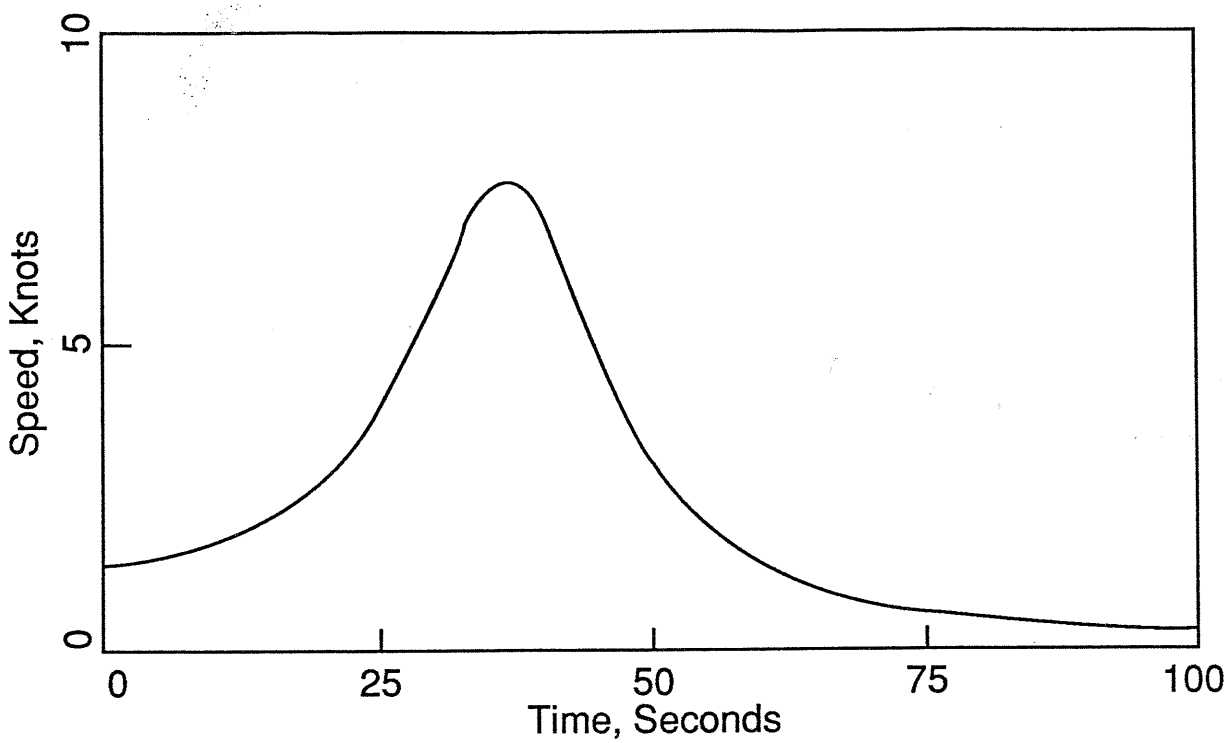

FIGURE 5-4. HORIZONTAL WIND FROM MODEL

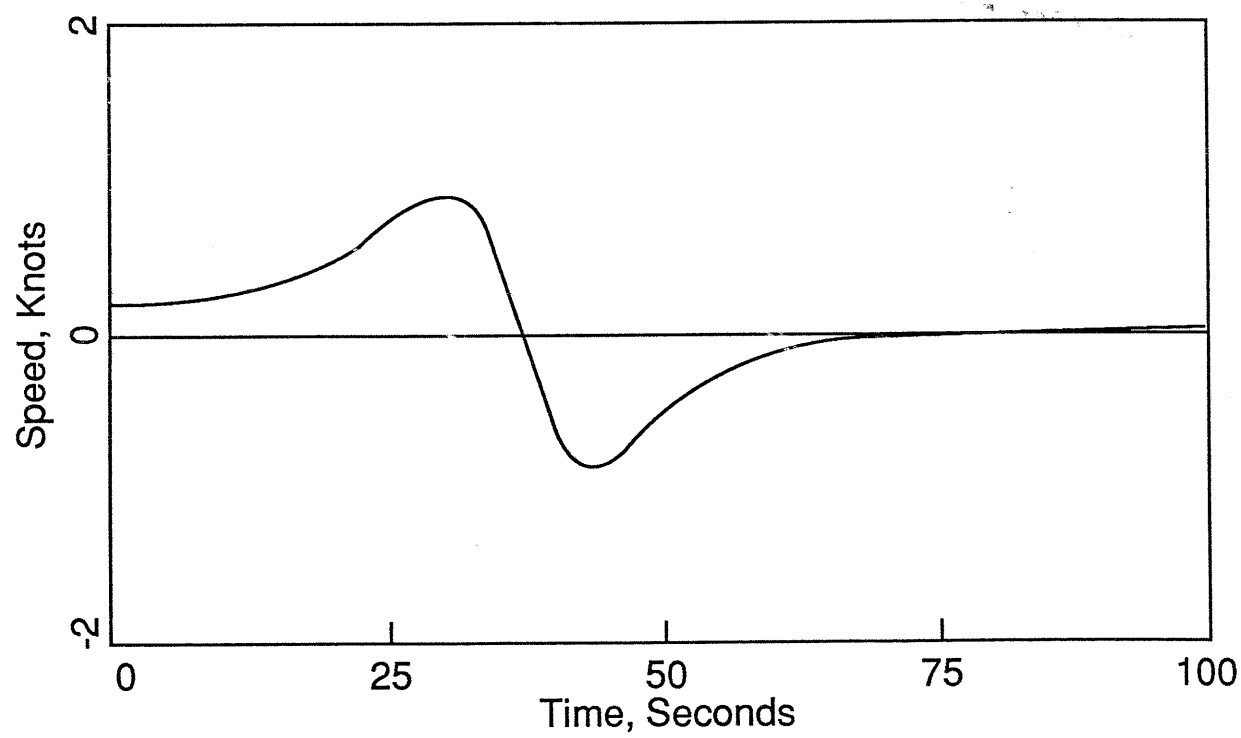

FIGURE 5-5. VERTICAL WIND FROM MODEL

APPENDIX A

TAKEOFF HAZARD PROBABILITY PLOTS

(See Section 3.1.2 for a description of these plots.)

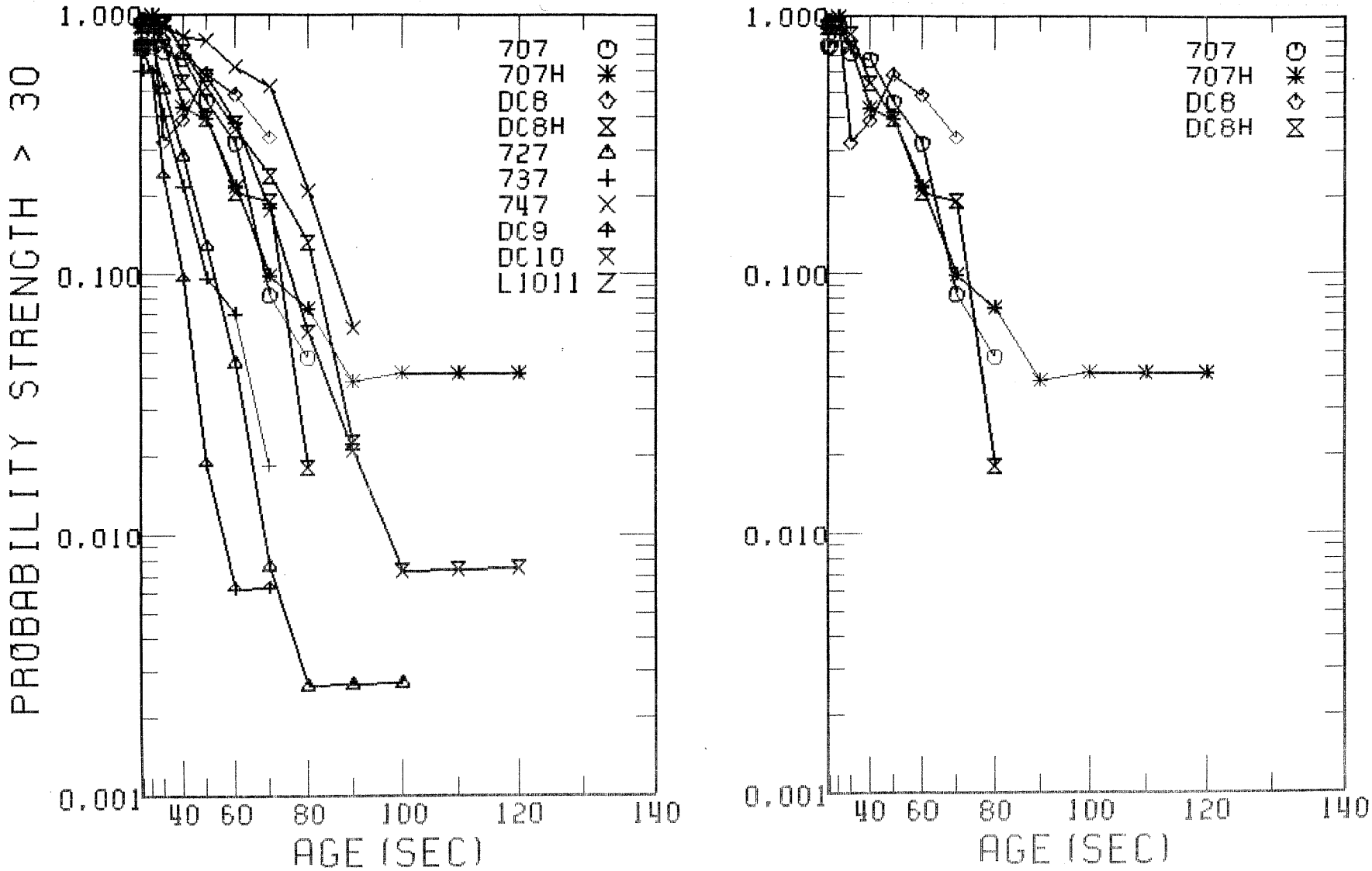

FIGURE A-1. CHICAGO TAKEOFF DATA, VORTEX #2: AVERAGING RADIUS=5m, PROBABILITY VORTEX STRENGTH >30 m^2/s VS. VORTEX AGE

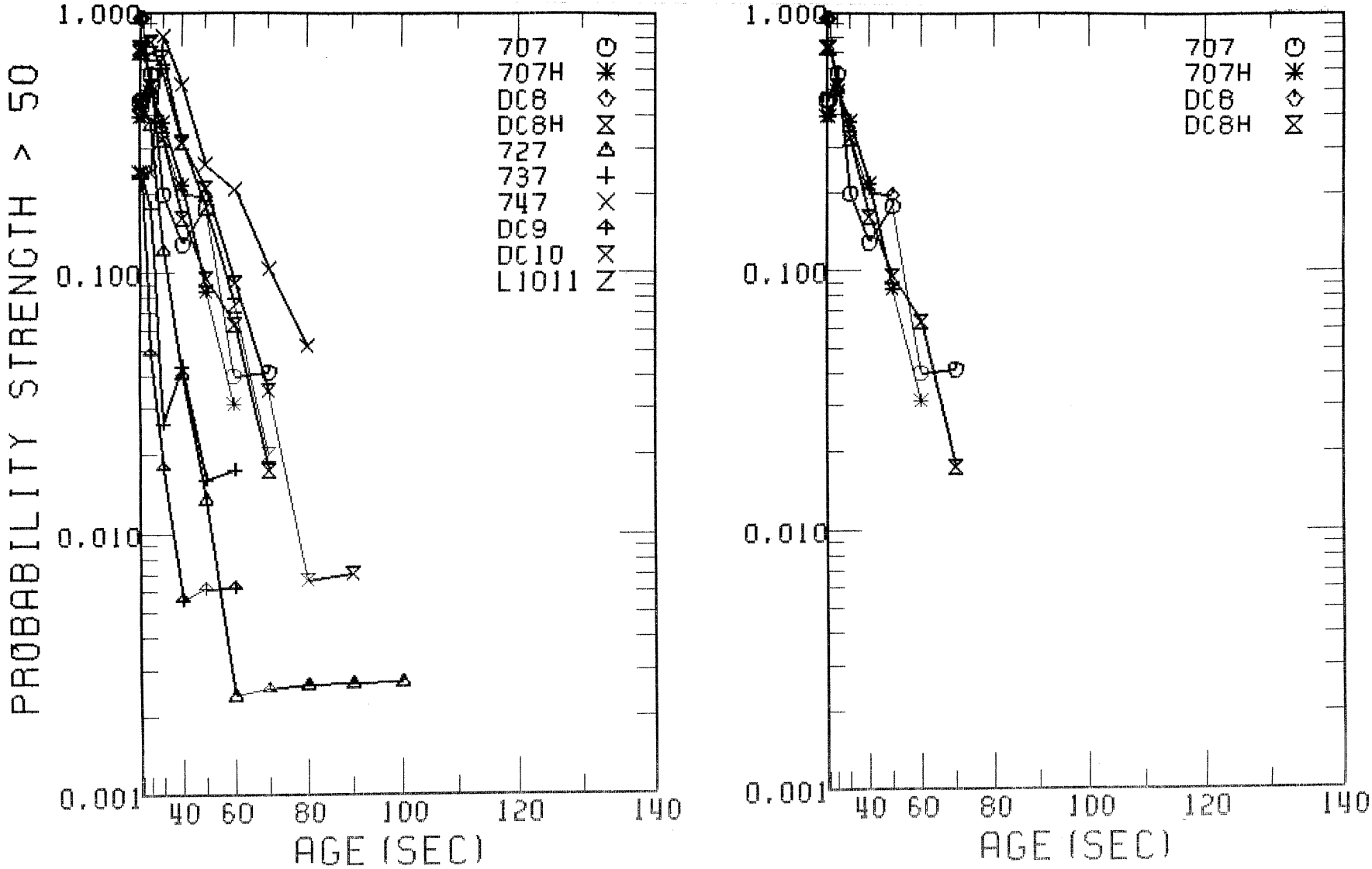

FIGURE A-2. CHICAGO TAKEOFF DATA, VORTEX #2: AVERAGING RADIUS=5m, PROBABILITY VORTEX STRENGTH>50 m^2/s VS. VORTEX AGE

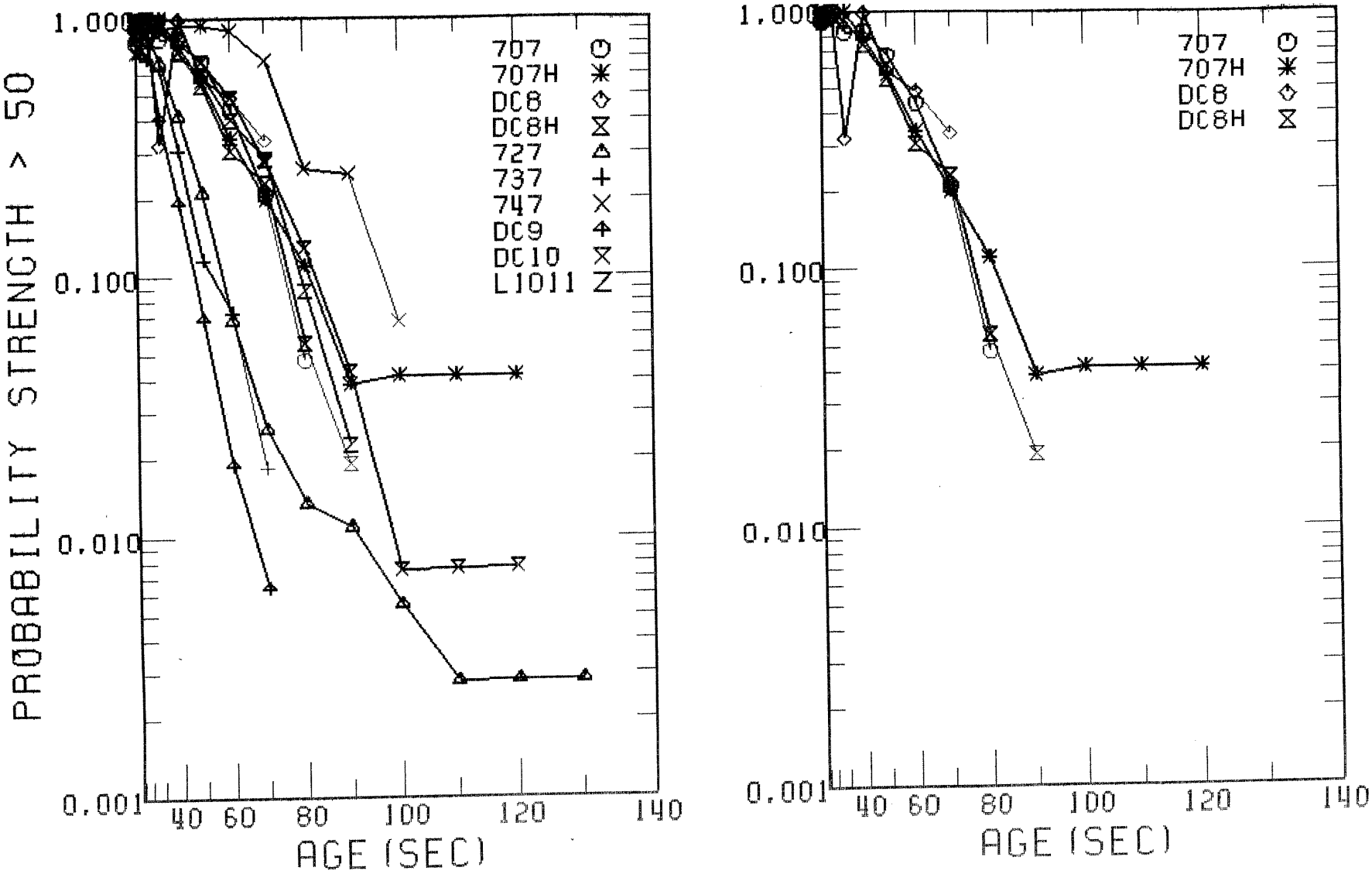

FIGURE A-3. CHICAGO TAKEOFF DATA, VORTEX #2: AVERAGING RADIUS=10m, PROBABILITY VORTEX STRENGTH>50 m^2/s VS. VORTEX AGE

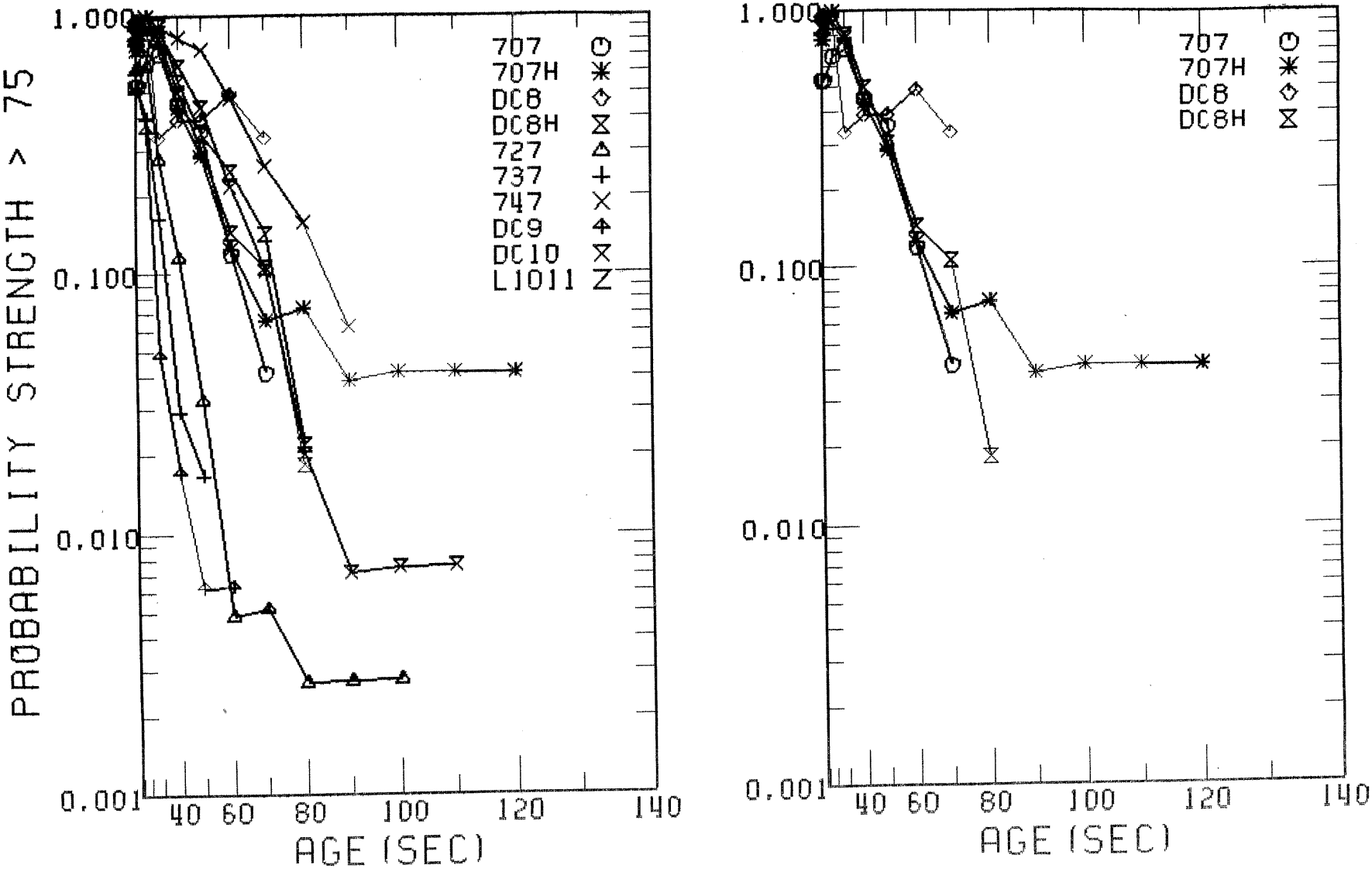

FIGURE A-4. CHICAGO TAKEOFF DATA, VORTEX #2: AVERAGING RADIUS=10m, PROBABILITY VORTEX STRENGTH>75 m^2/s VS. VORTEX AGE

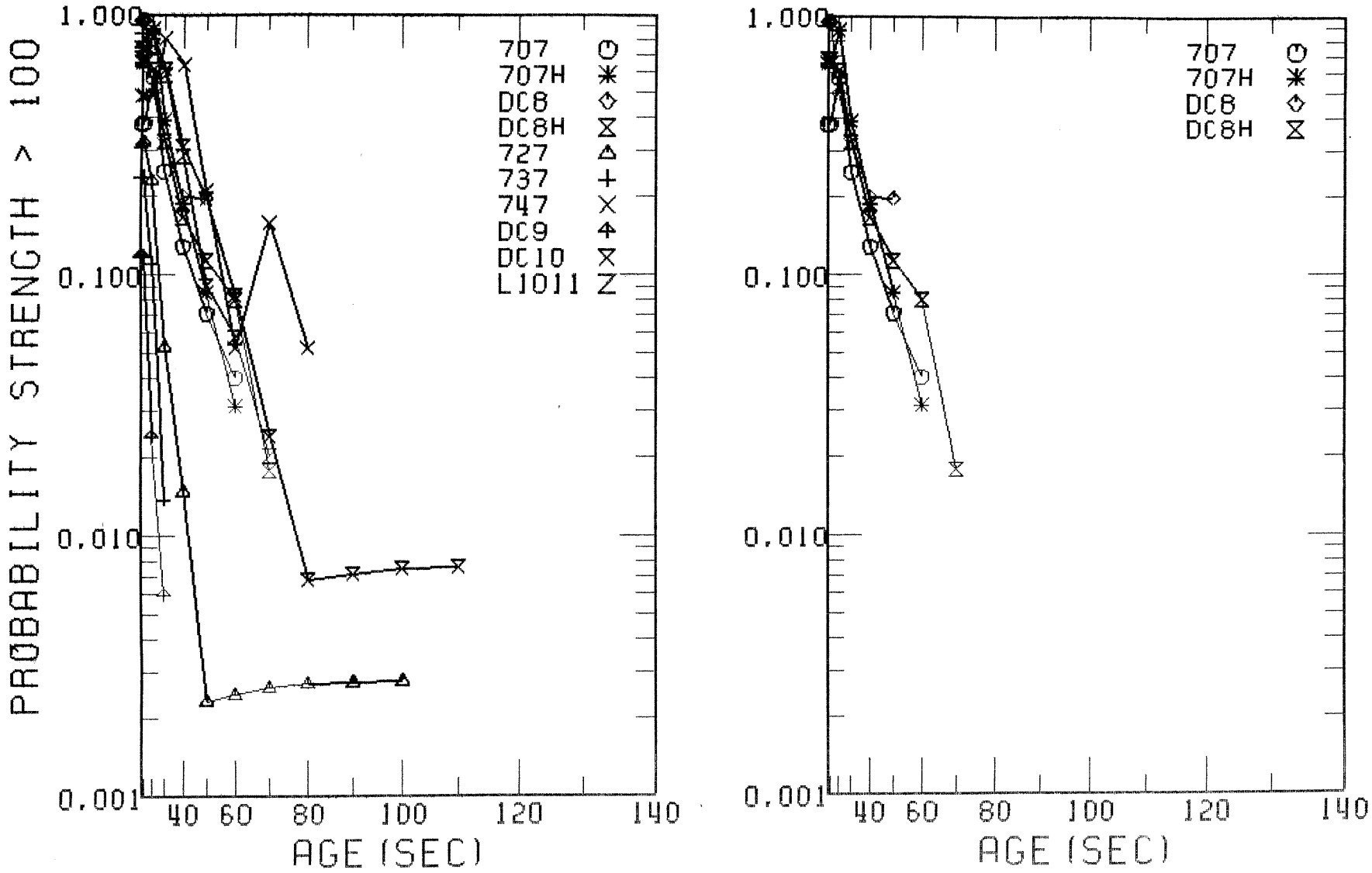

FIGURE A-5. CHICAGO TAKEOFF DATA, VORTEX #2: AVERAGING RADIUS=10m, PROBABILITY VORTEX STRENGTH>100 m^2/s VS. VORTEX AGE

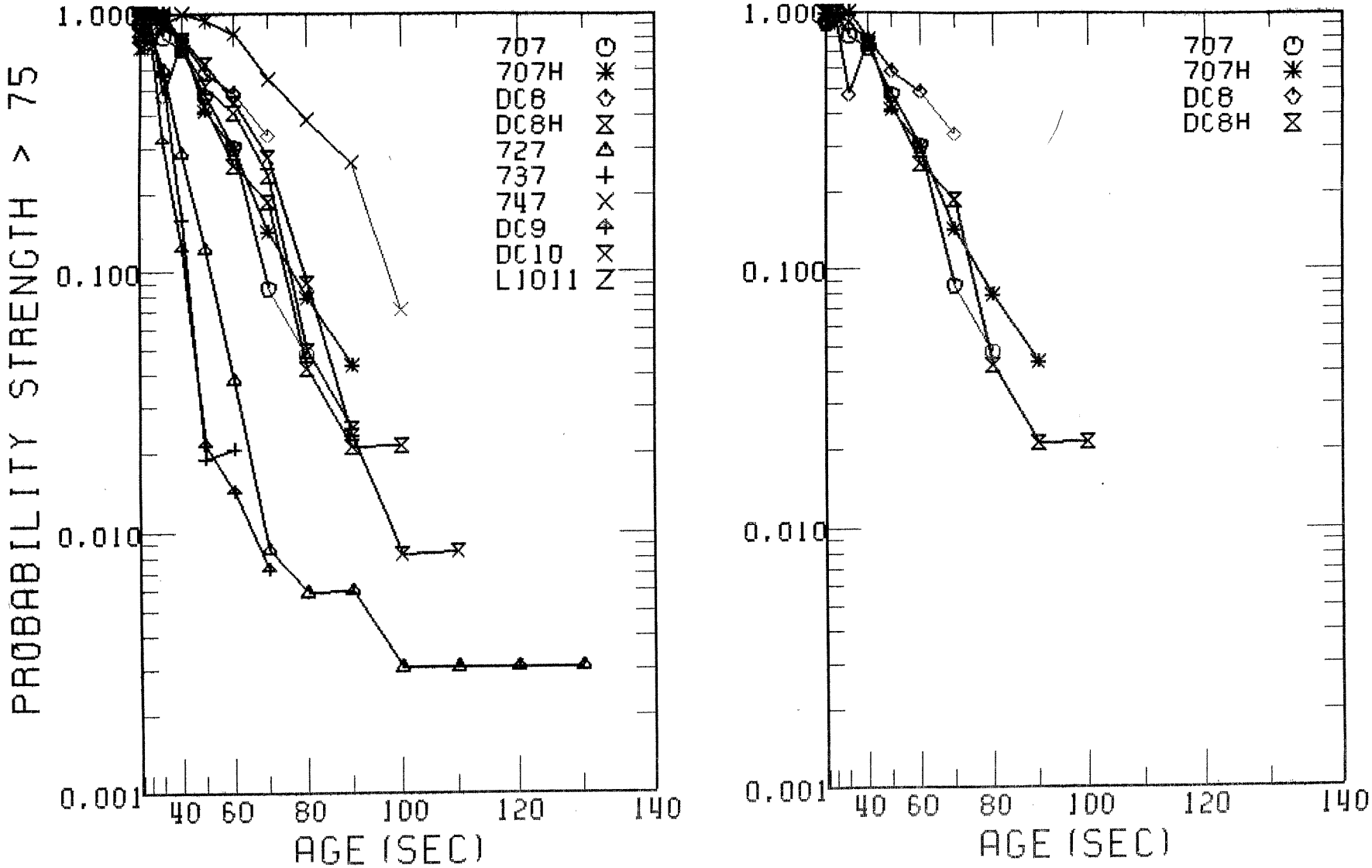

FIGURE A-6. CHICAGO TAKEOFF DATA, VORTEX #2: AVERAGING RADIUS=15m, PROBABILITY VORTEX STRENGTH>75 m^2/s VS. VORTEX AGE

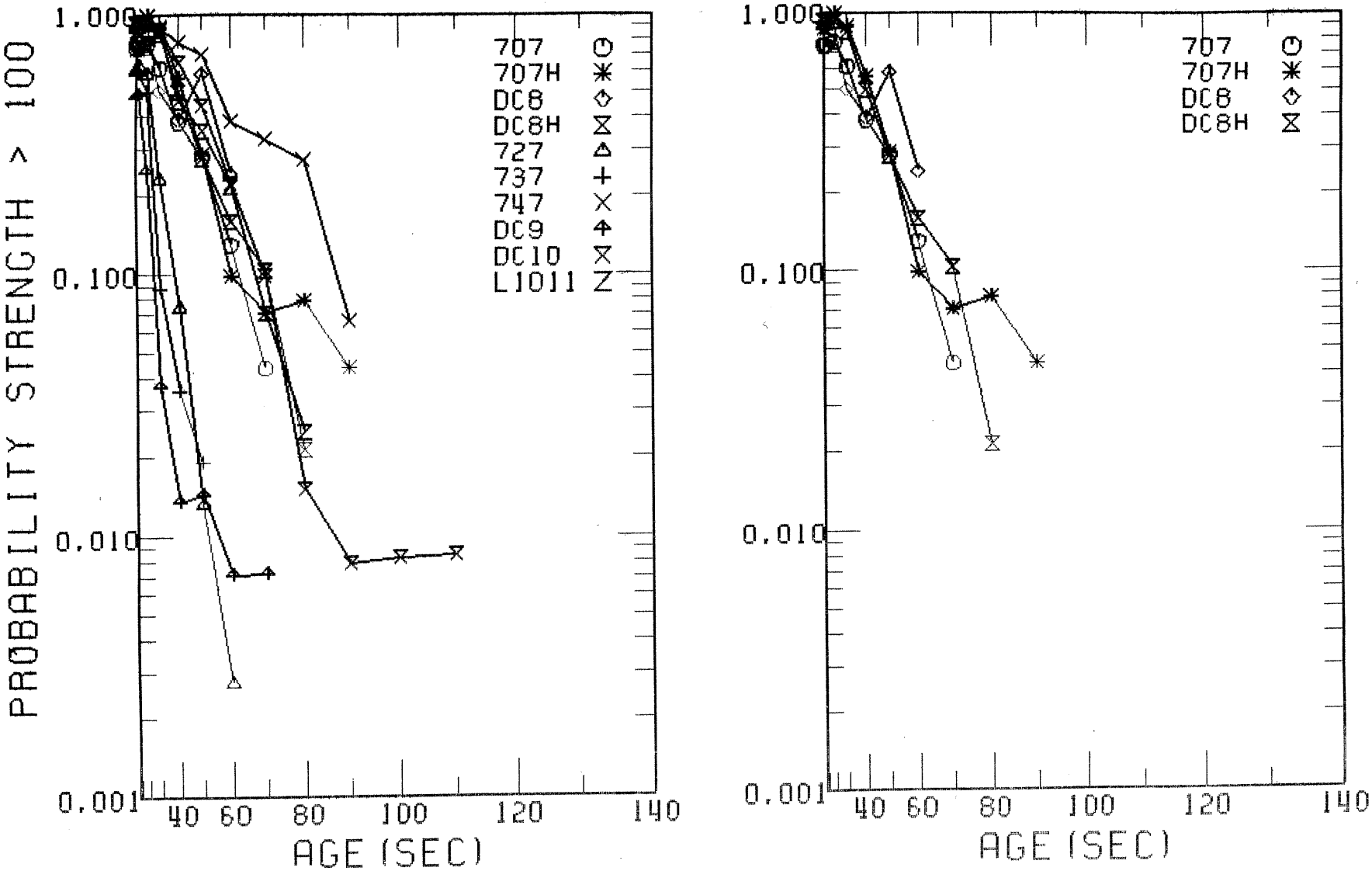

FIGURE A-7. CHICAGO TAKEOFF DATA, VORTEX #2: AVERAGING RADIUS=15m, PROBABILITY VORTEX STRENGTH>100 m^2/s VS. VORTEX AGE

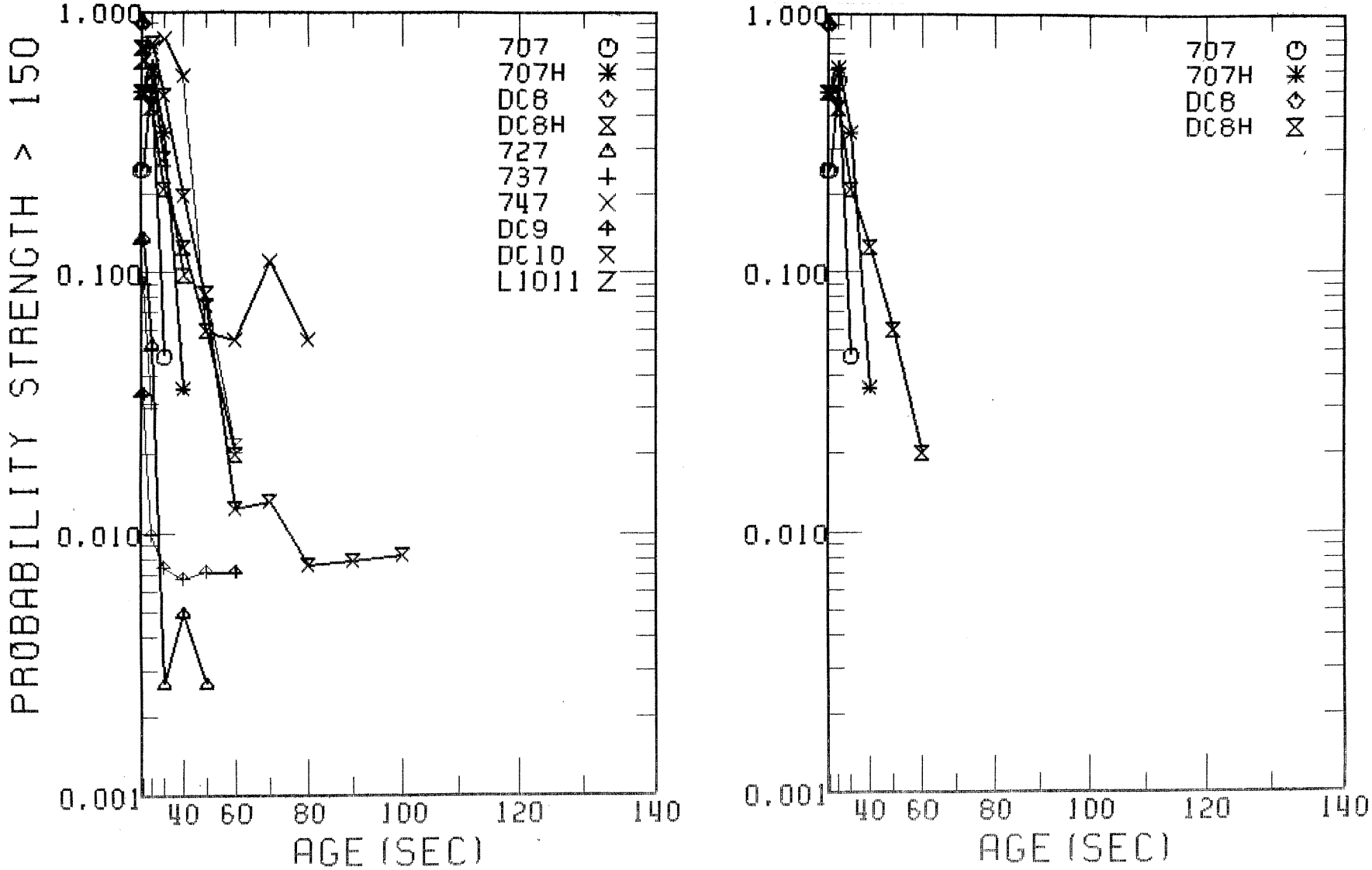

FIGURE A-8. CHICAGO TAKEOFF DATA, VORTEX #2: AVERAGING RADIUS=15m, PROBABILITY VORTEX STRENGTH>150 m^2/s VS. VORTEX AGE

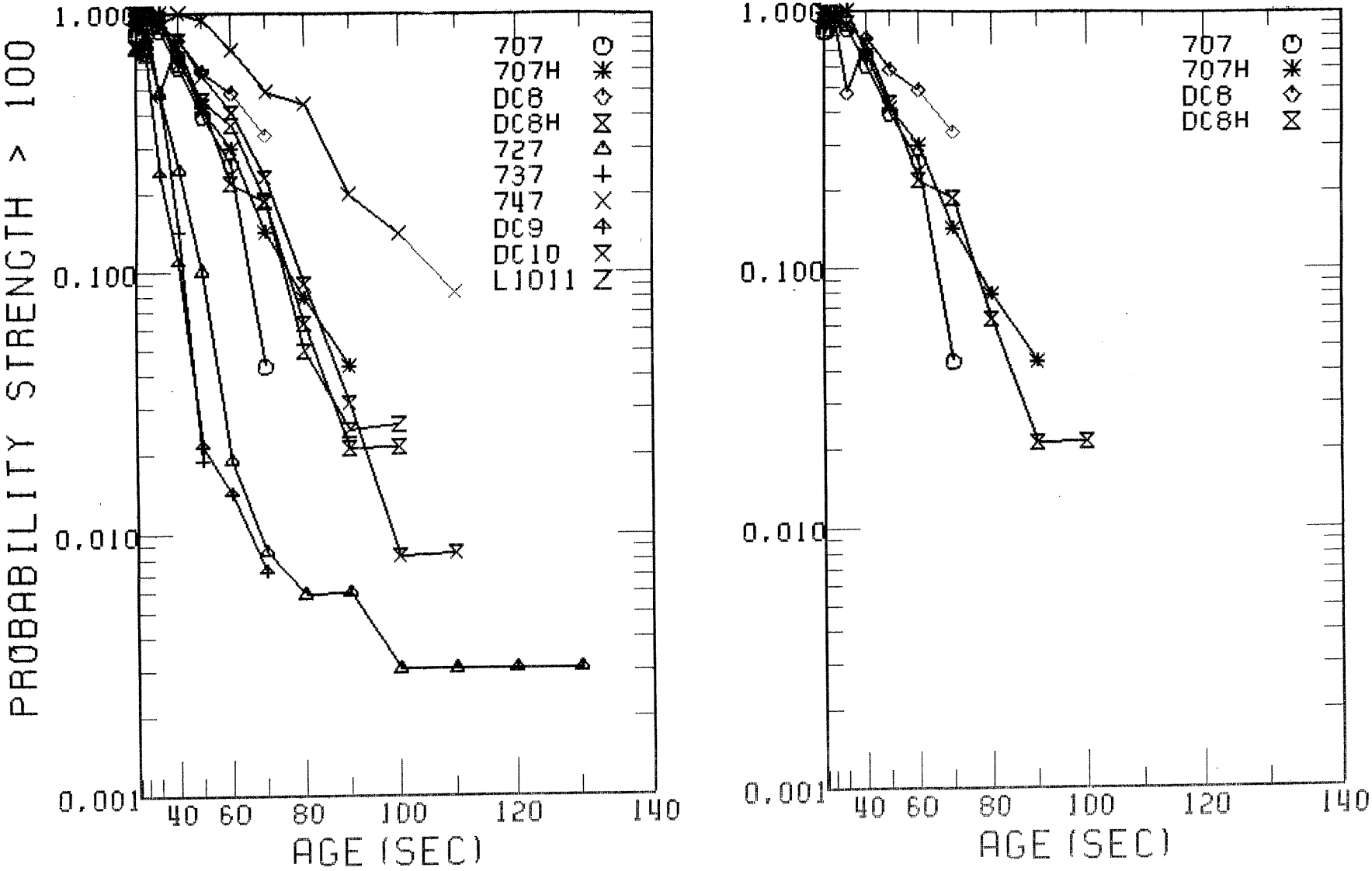

FIGURE A-9. CHICAGO TAKEOFF DATA, VORTEX #2: AVERAGING RADIUS=20m, PROBABILITY VORTEX STRENGTH>100 m^2/s VS. VORTEX AGE

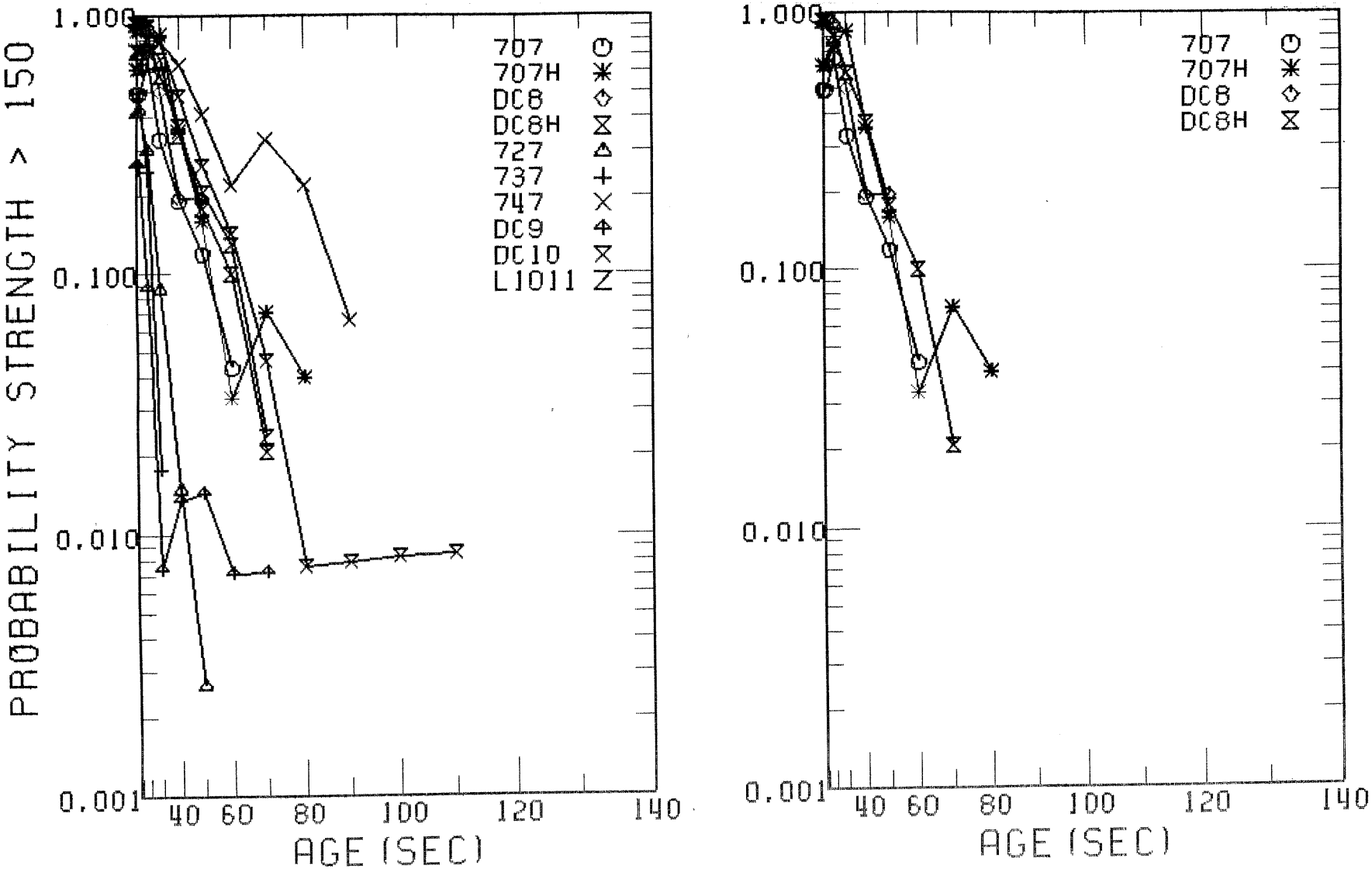

FIGURE A-10. CHICAGO TAKEOFF DATA, VORTEX #2: AVERAGING RADIUS=20m, PROBABILITY VORTEX STRENGTH>150 m^2/s VS. VORTEX AGE

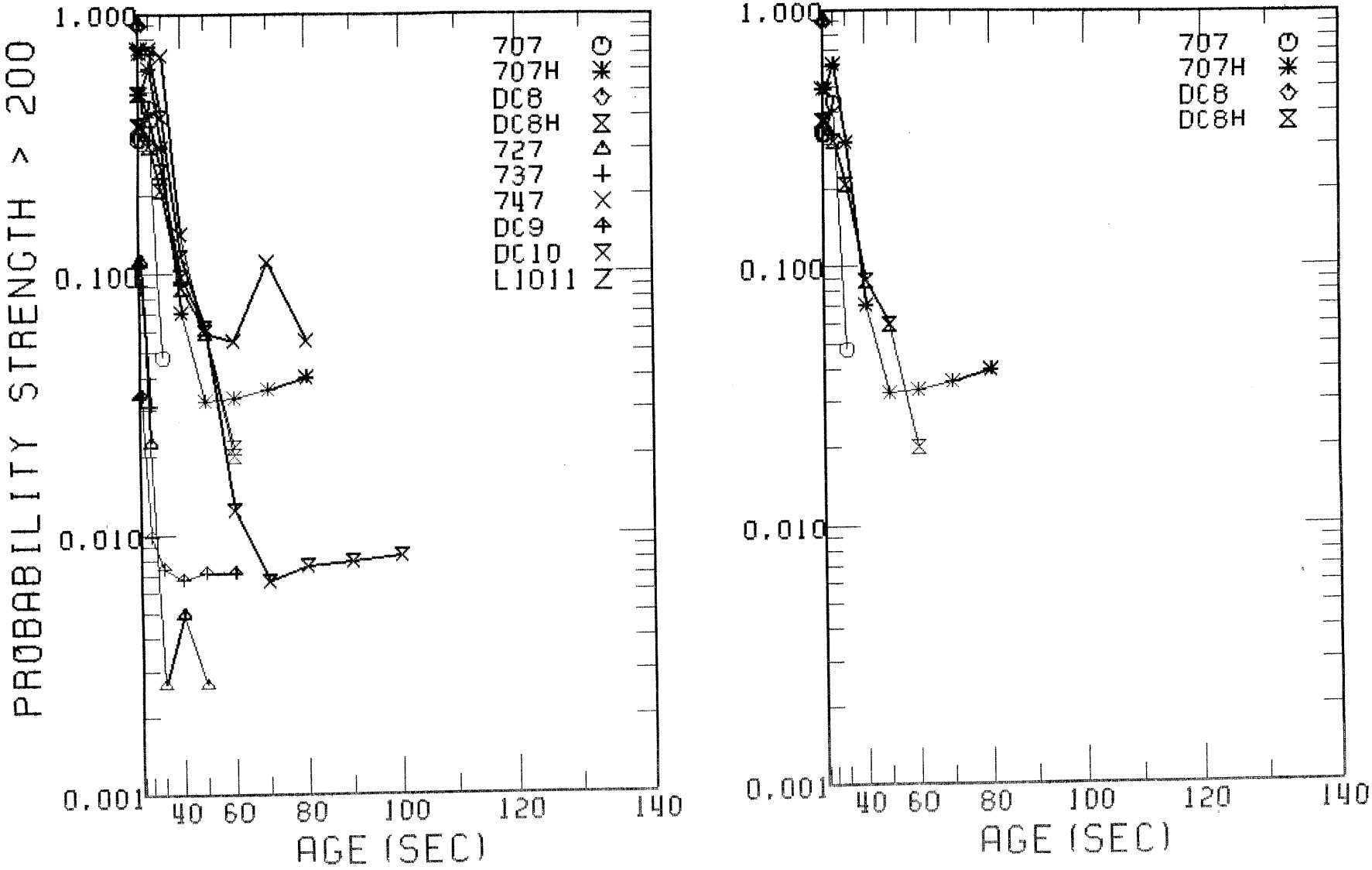

FIGURE A-11. CHICAGO TAKEOFF DATA, VORTEX #2: AVERAGING RADIUS=20m, PROBABILITY VORTEX STRENGTH>200 m^2/s VS. VORTEX AGE

APPENDIX B

LANDING HAZARD PROBABILITY PLOTS

(See Section 3.1.2 for a description of these plots.)

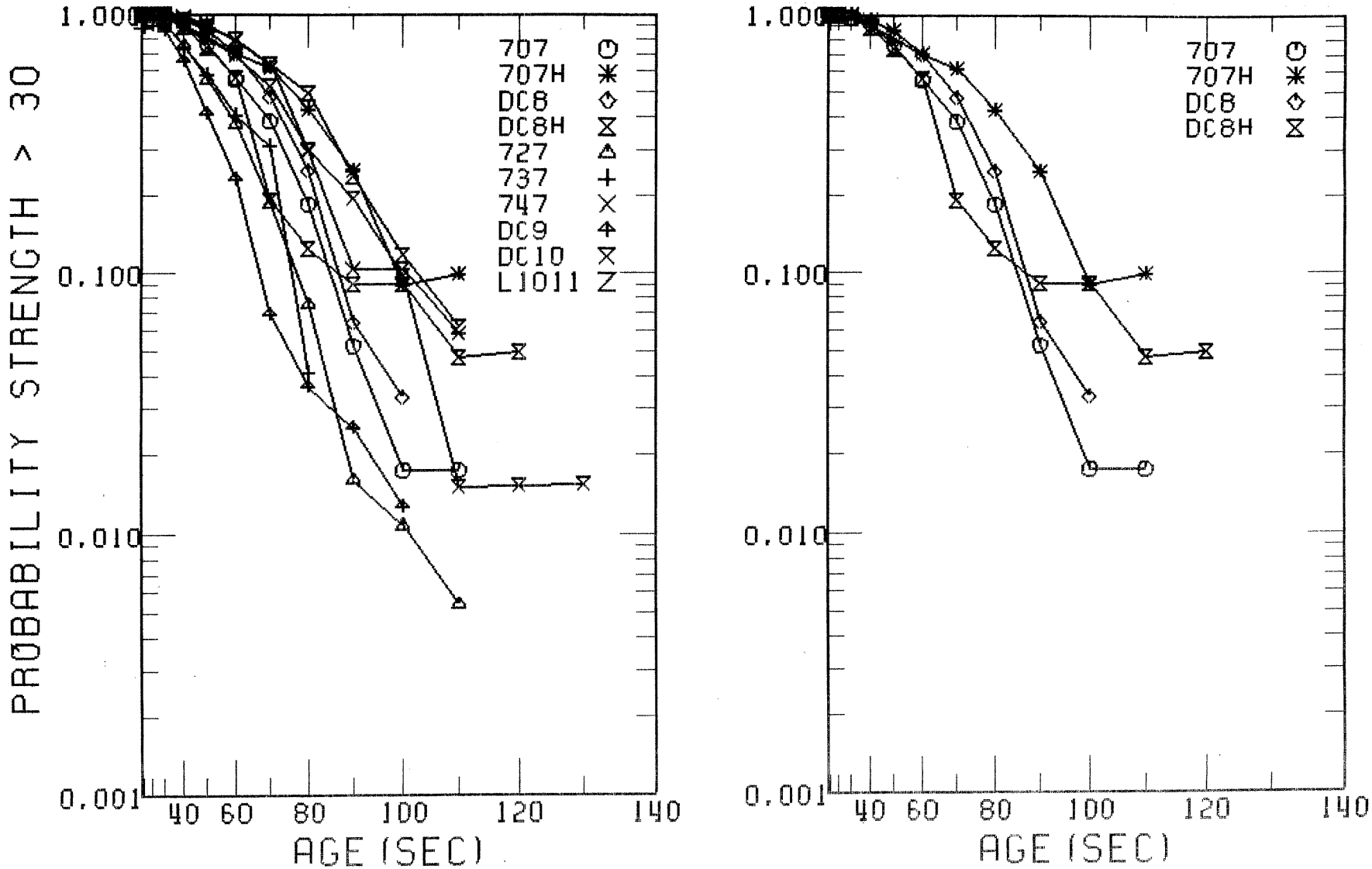

FIGURE B-1. CHICAGO LANDING DATA, VORTEX #2: AVERAGING RADIUS=5m, PROBABILITY VORTEX STRENGTH>30 m^2/s VS. VORTEX AGE

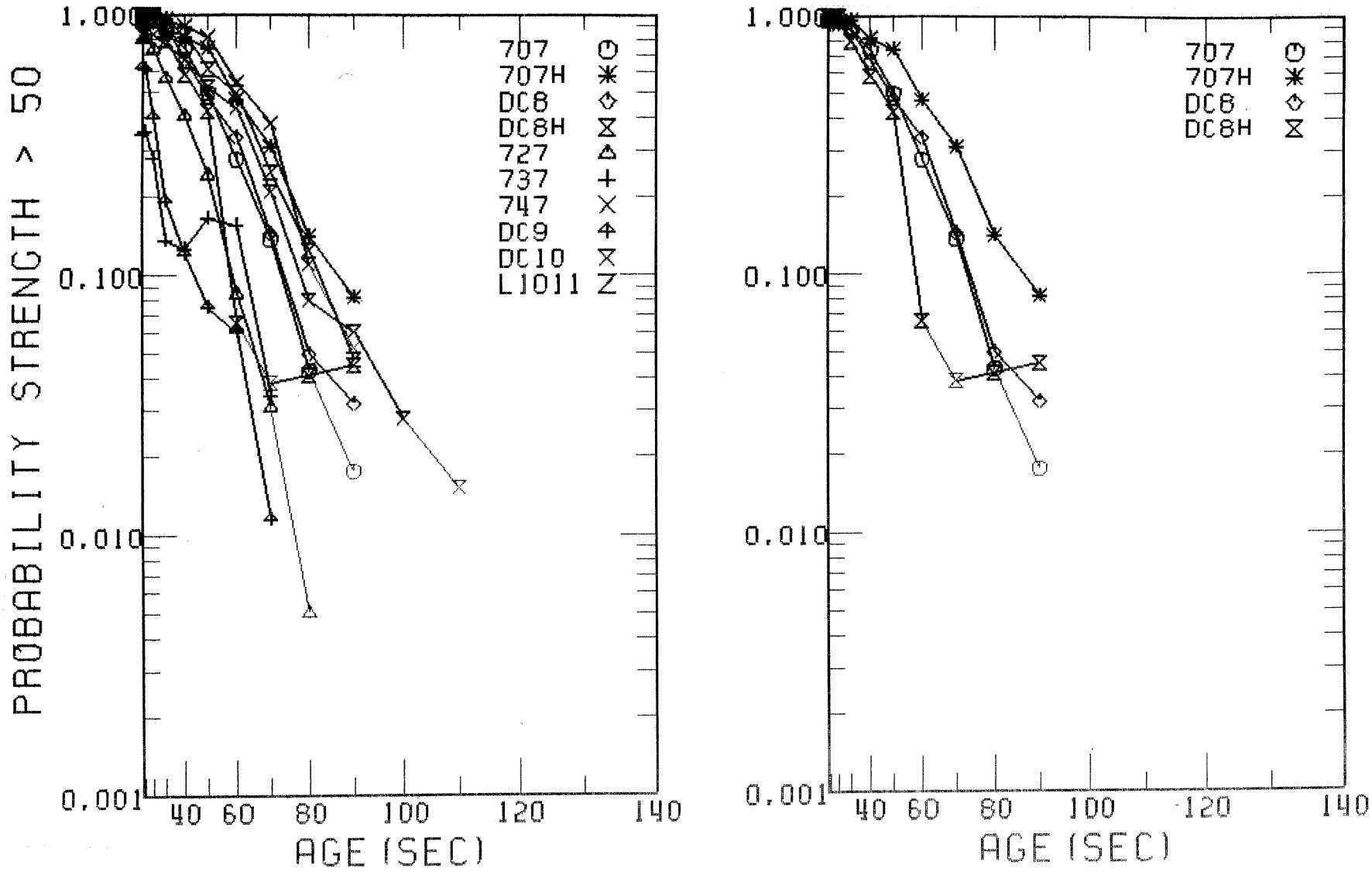

FIGURE B-2. CHICAGO LANDING DATA, VORTEX #2: AVERAGING RADIUS=5m, PROBABILITY VORTEX STRENGTH>50 m^2/s VS. VORTEX AGE

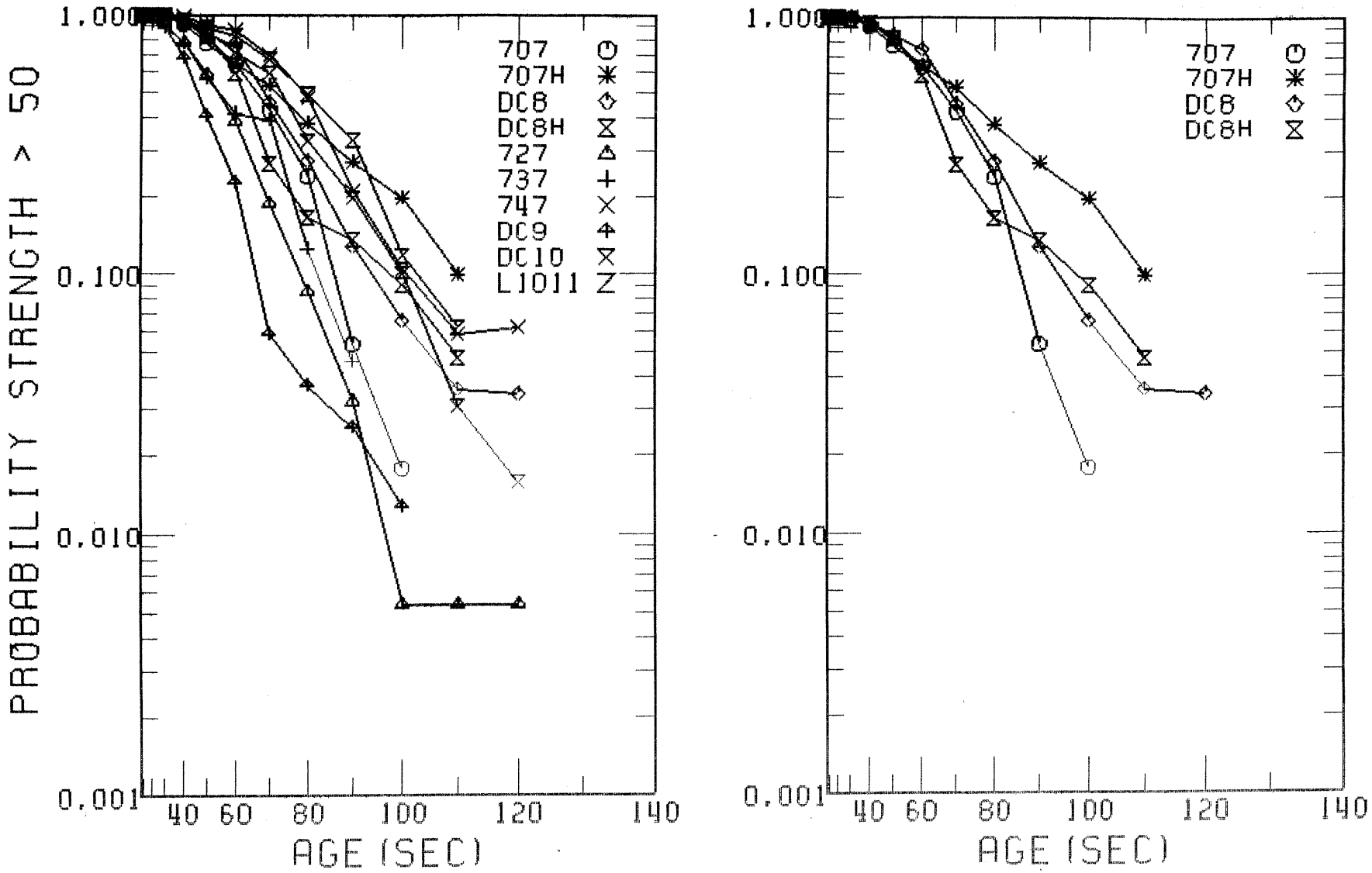

FIGURE B-3. CHICAGO LANDING DATA, VORTEX #2: AVERAGING RADIUS=10m, PROBABILITY VORTEX STRENGTH>50 m^2/s VS. VORTEX AGE

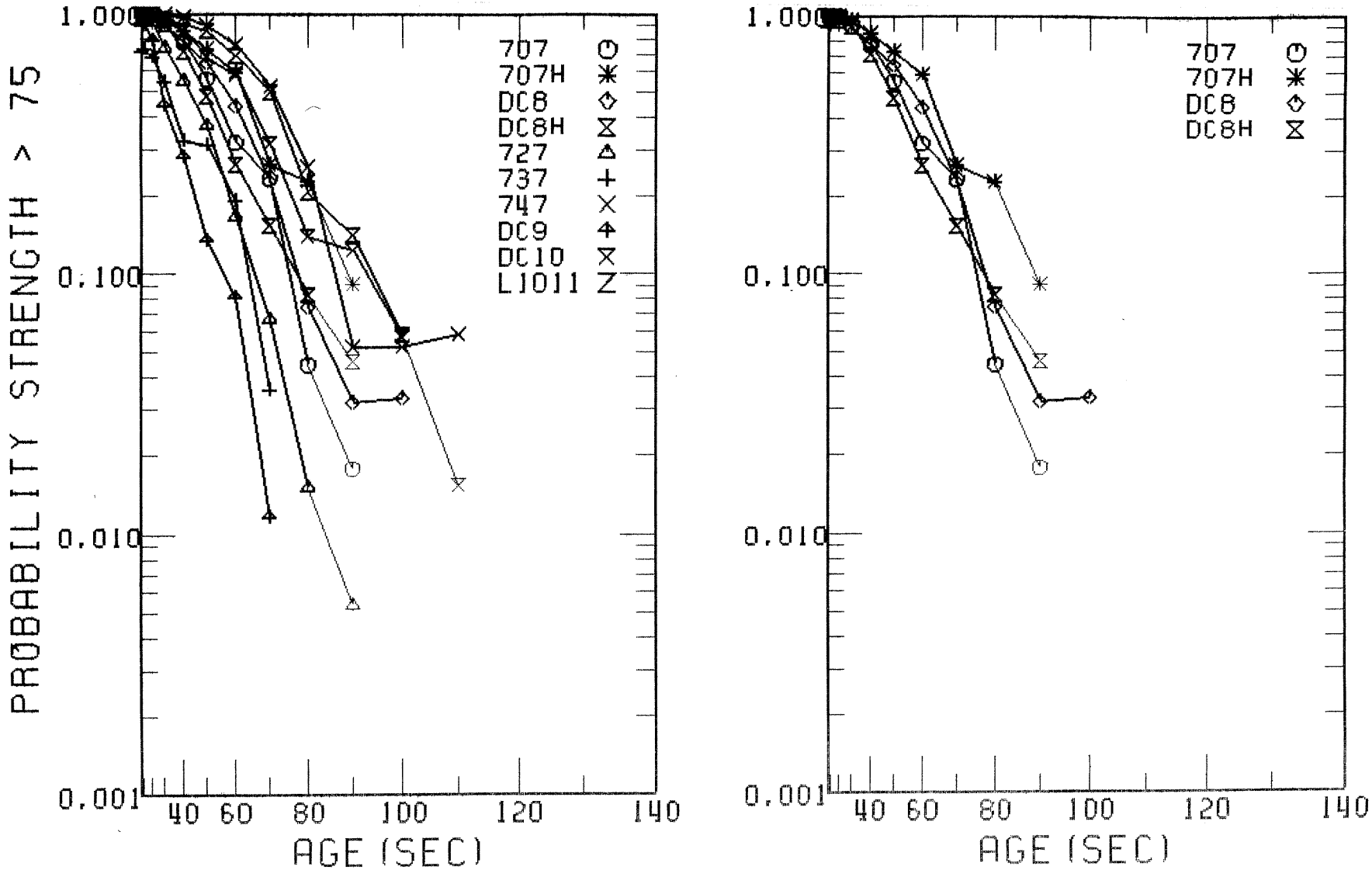

FIGURE B-4. CHICAGO LANDING DATA, VORTEX #2: AVERAGING RADIUS=10m, PROBABILITY VORTEX STRENGTH>75 m^2/s VS. VORTEX AGE

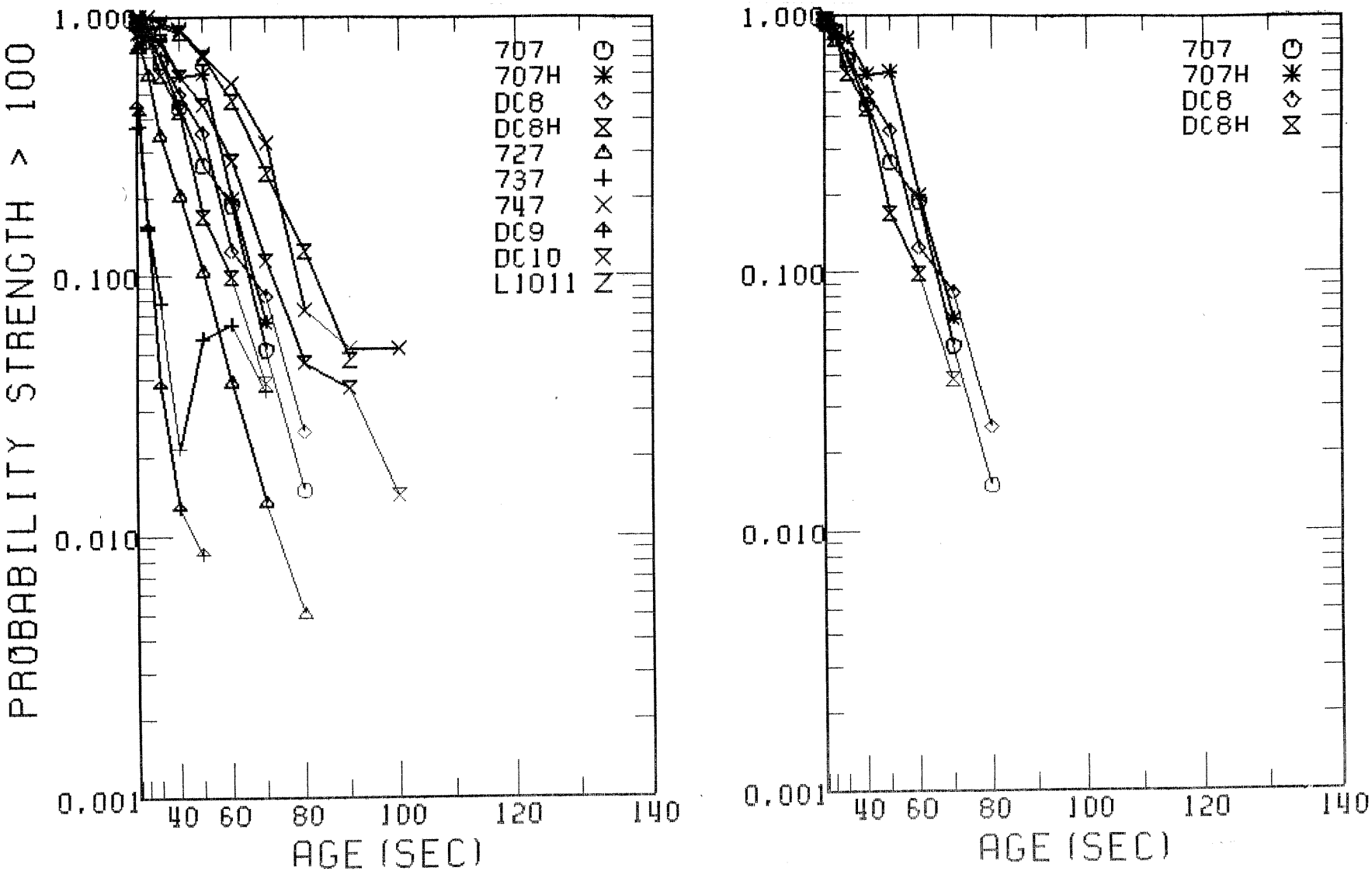

FIGURE B-5. CHICAGO LANDING DATA, VORTEX #2: AVERAGING RADIUS=10m, PROBABILITY VORTEX STRENGTH>100 m^2/s VS. VORTEX AGE

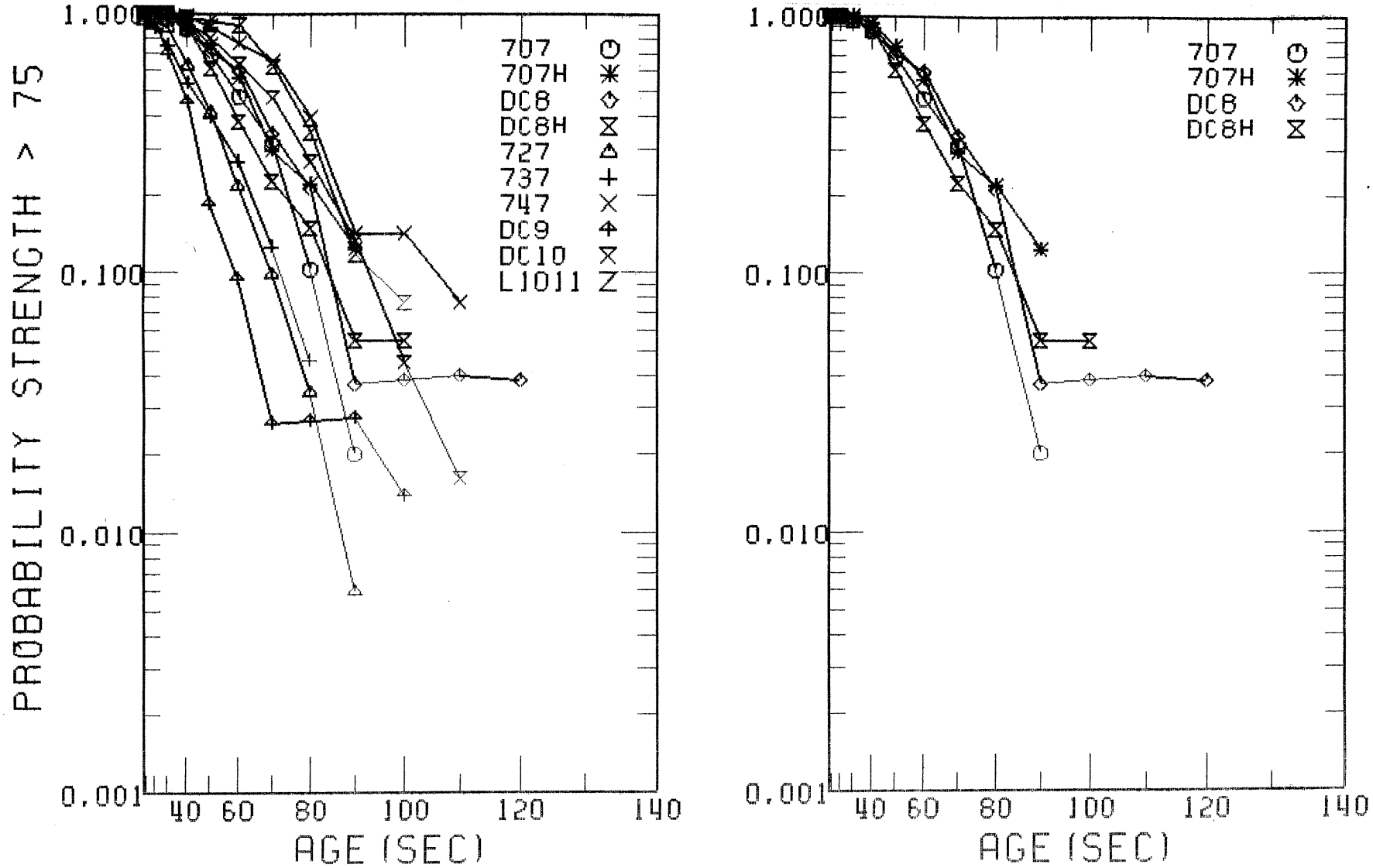

FIGURE B-6. CHICAGO LANDING DATA, VORTEX #2: AVERAGING RADIUS=15m, PROBABILITY VORTEX STRENGTH>75 m^2/s VS. VORTEX AGE

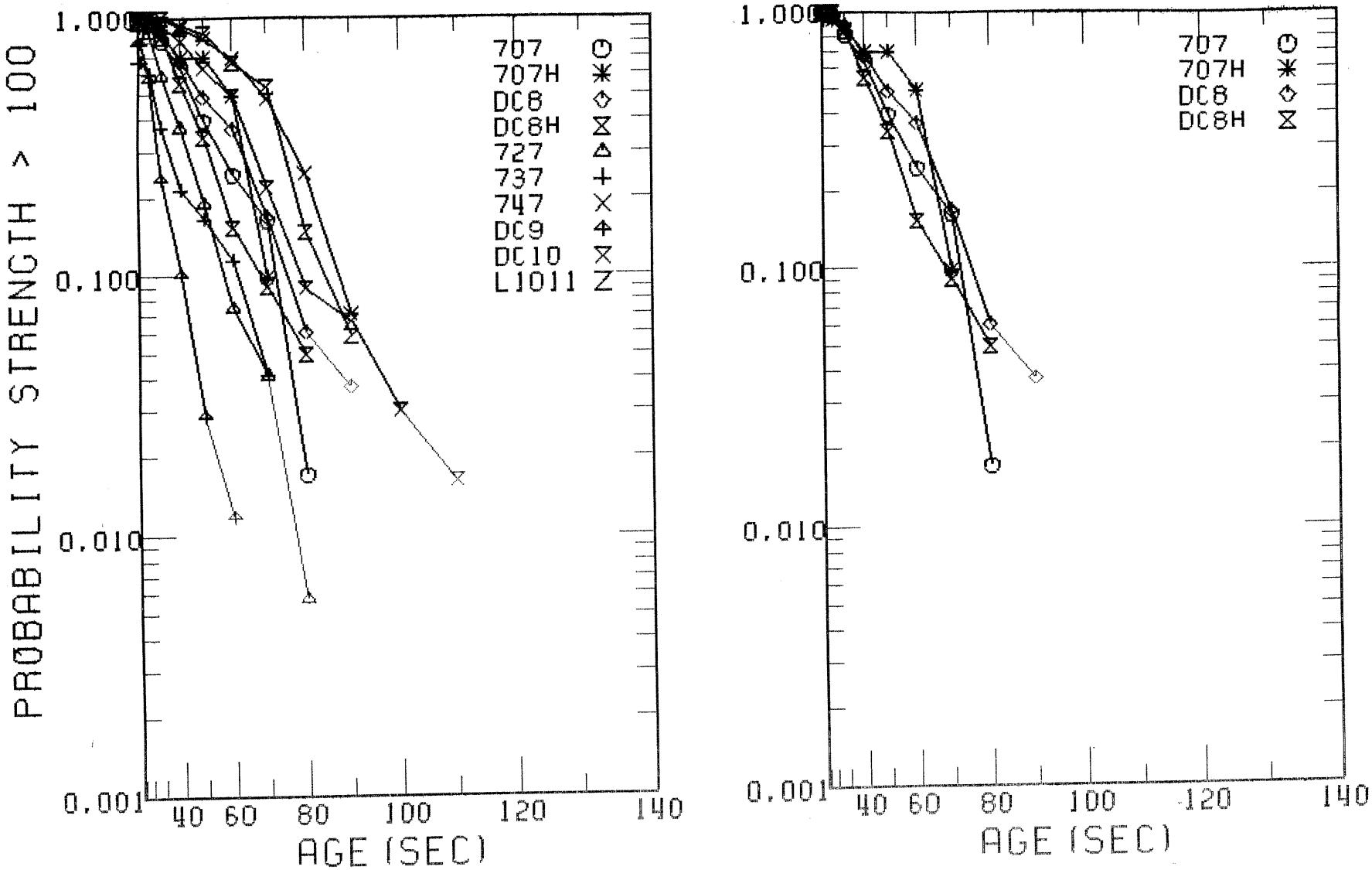

FIGURE B-7. CHICAGO LANDING DATA, VORTEX #2: AVERAGING RADIUS=15m, PROBABILITY VORTEX STRENGTH>100 m^2/s VS. VORTEX AGE

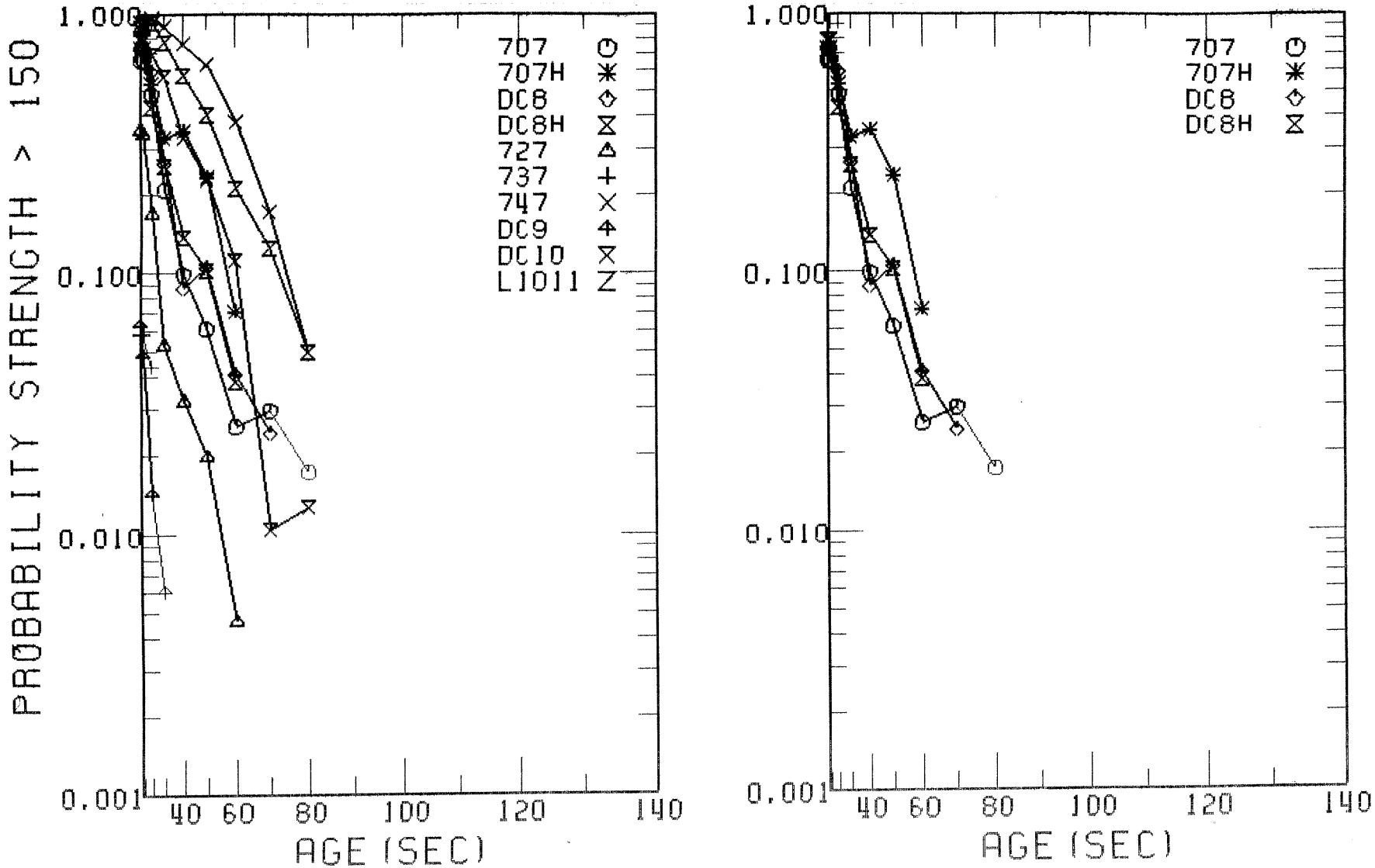

FIGURE B-8. CHICAGO LANDING DATA, VORTEX #2: AVERAGING RADIUS=15m, PROBABILITY VORTEX STRENGTH>150 m^2/s VS. VORTEX AGE

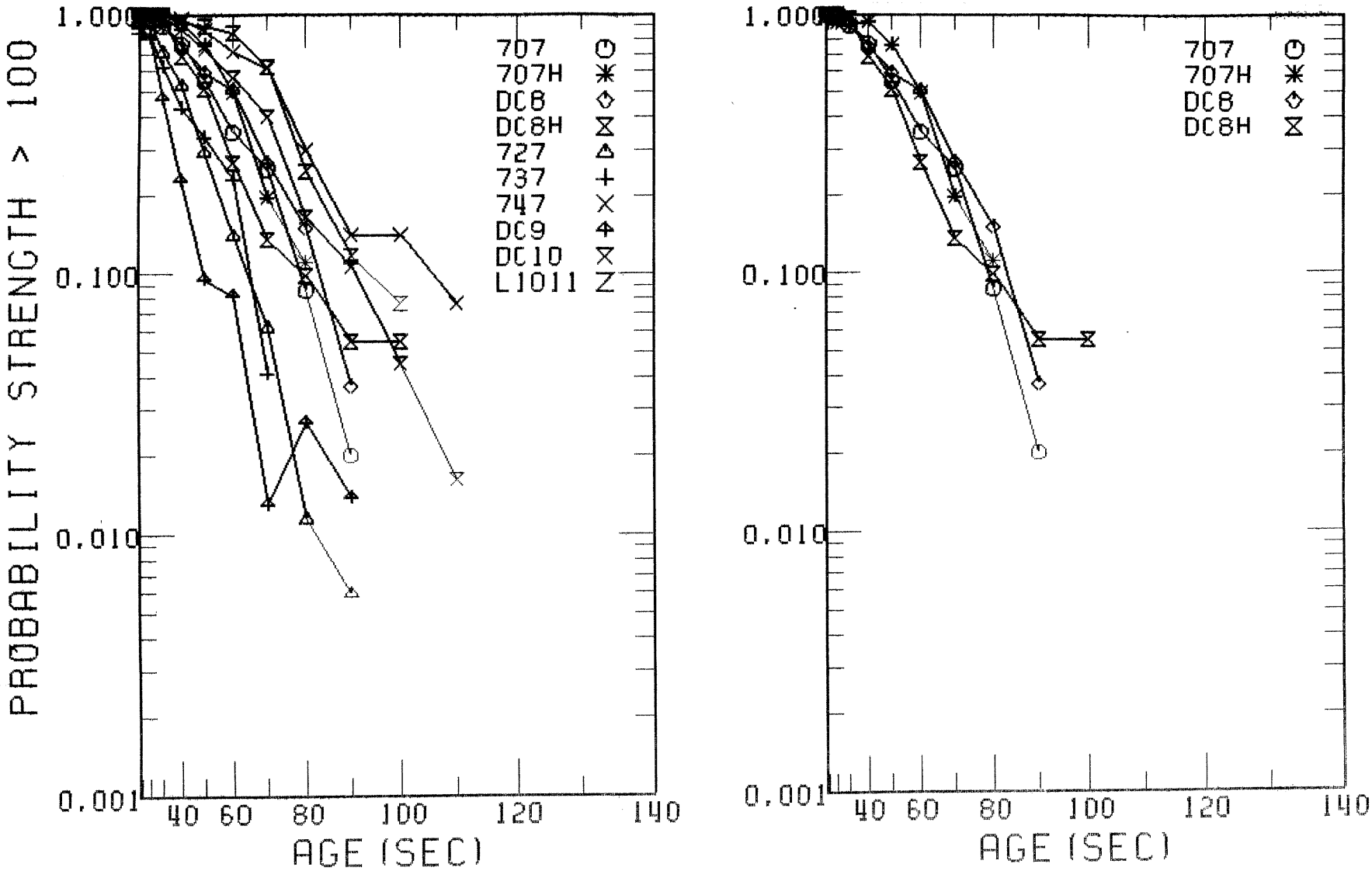

FIGURE B-9. CHICAGO LANDING DATA, VORTEX #2: AVERAGING RADIUS=20m, PROBABILITY VORTEX STRENGTH>100 m^2/s VS. VORTEX AGE

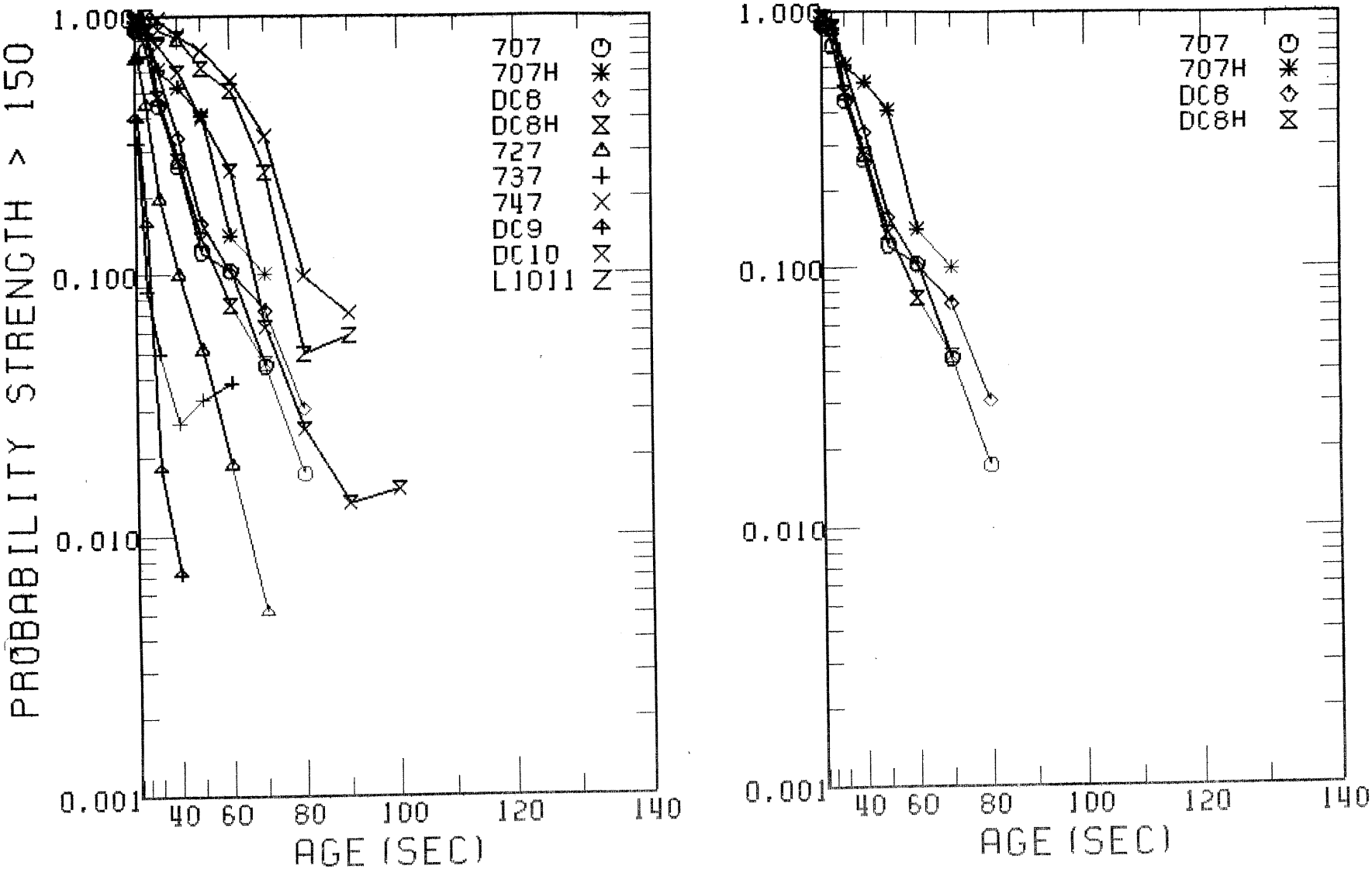

FIGURE B-10. CHICAGO LANDING DATA, VORTEX #2: AVERAGING RADIUS=20m, PROBABILITY VORTEX STRENGTH>150 m^2/s VS. VORTEX AGE

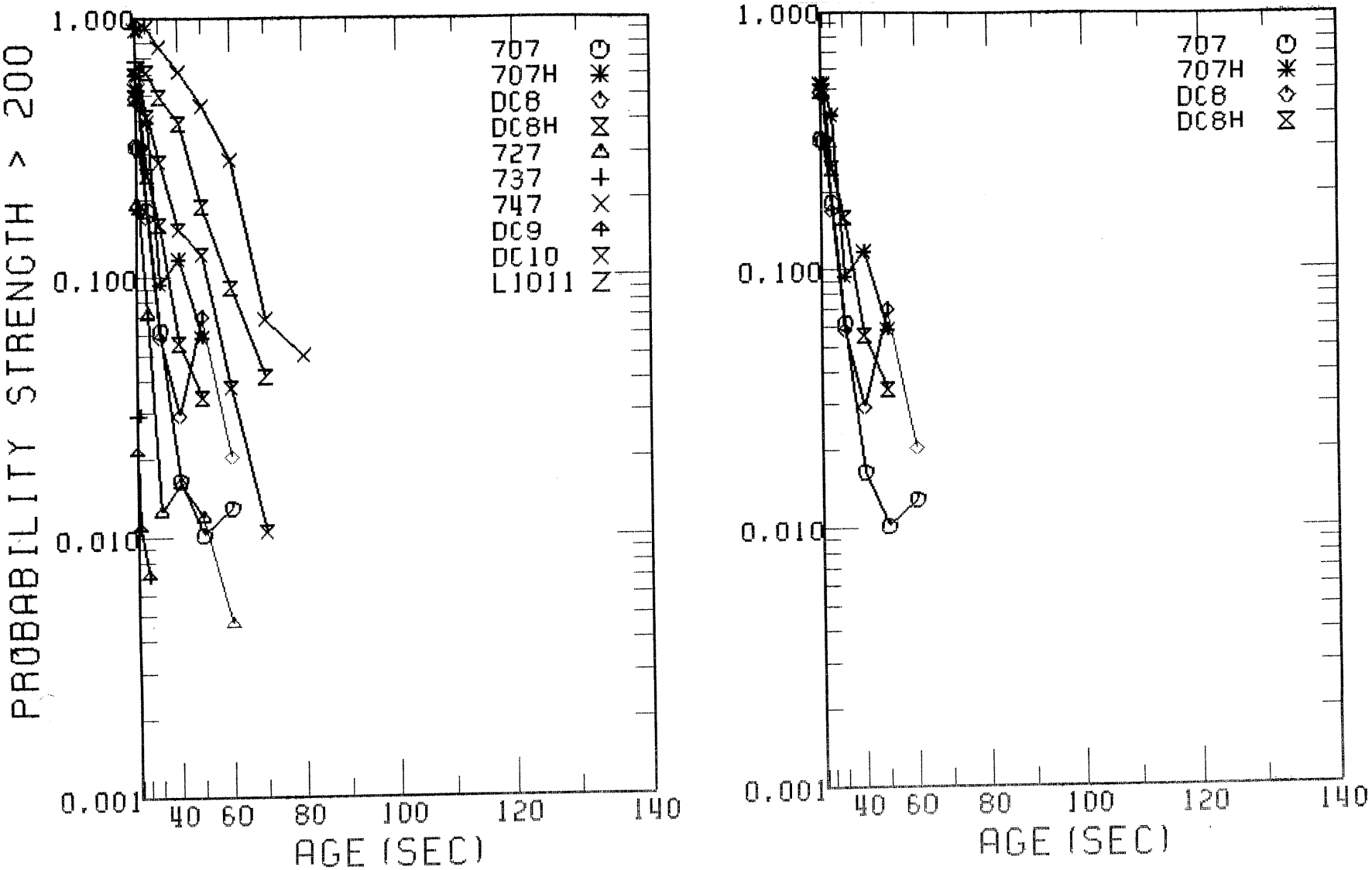

FIGURE B-11. CHICAGO LANDING DATA, VORTEX #2: AVERAGING RADIUS=20m, PROBABILITY VORTEX STRENGTH>200 m^2/s VS. VORTEX AGE

APPENDIX C

WAKE-VORTEX TRANSPORT PROBABILITY PLOTS

(See Section 4.2 for a description of these plots.)

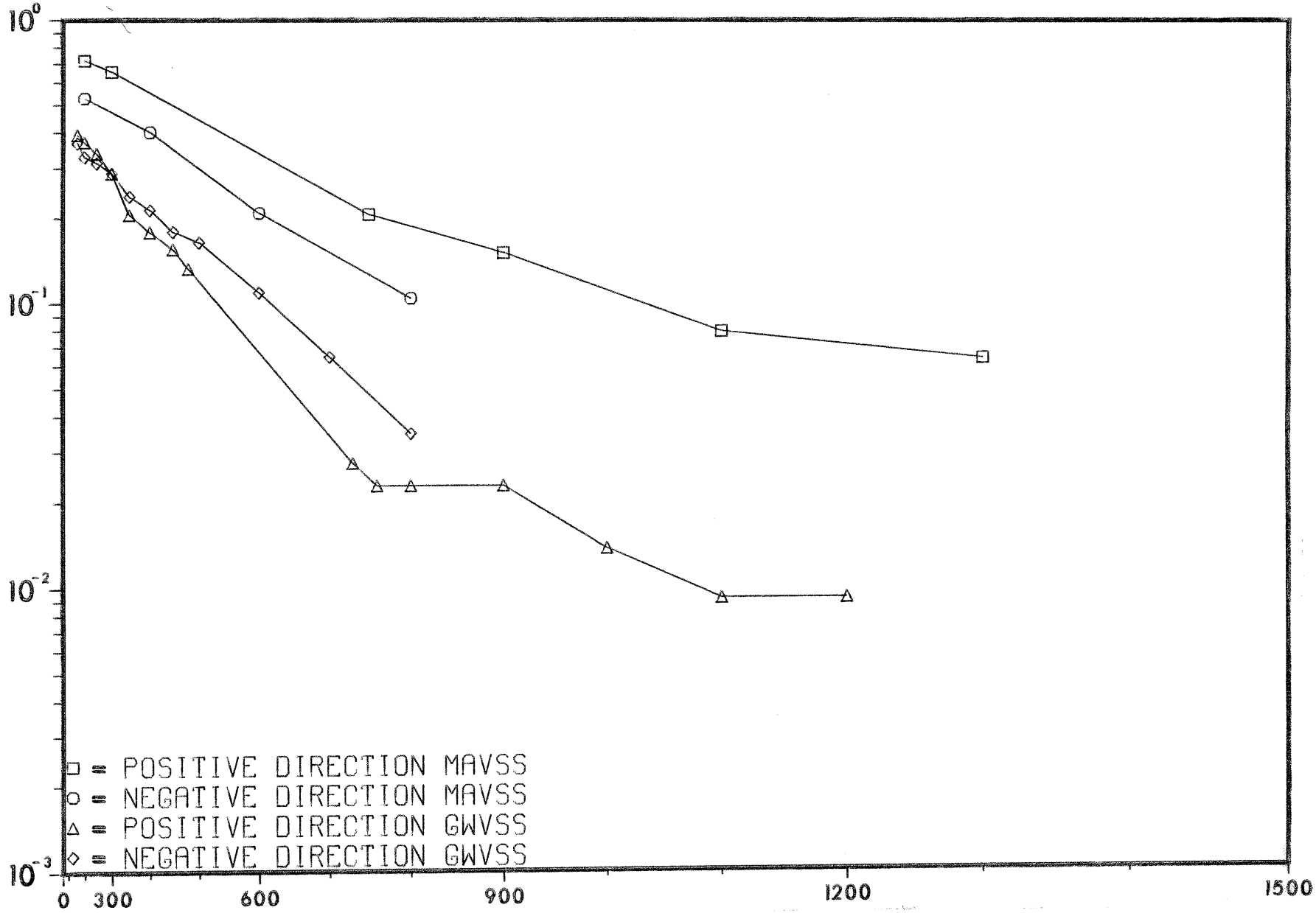

FIGURE C-1. PROBABILITY OF DETECTING A VORTEX AS A FUNCTION OF DISTANCE FROM THE RUNWAY CENTERLINE: AIRCRAFT TYPE = B-707

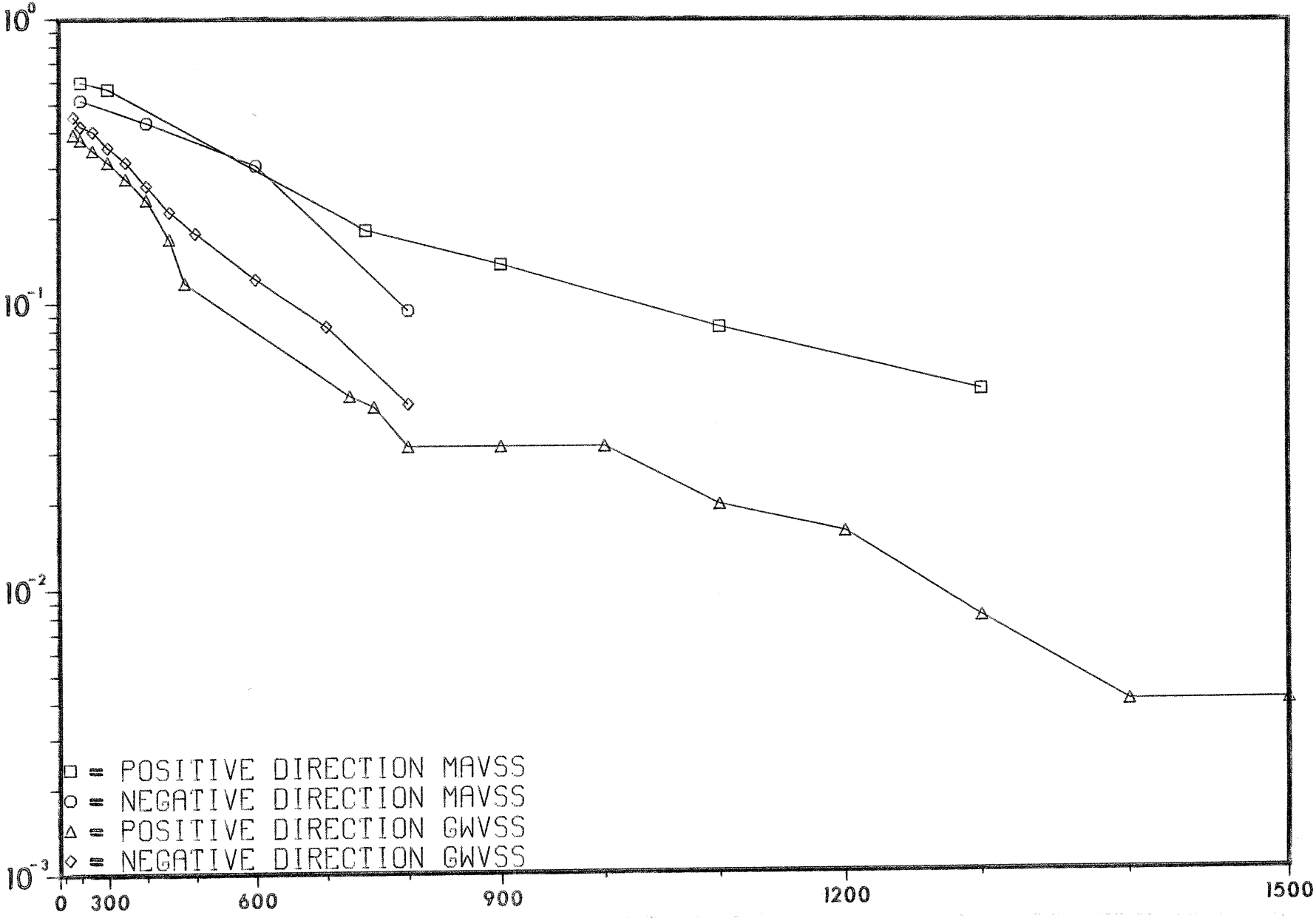

FIGURE C-2. PROBABILITY OF DETECTING A VORTEX AS A FUNCTION OF DISTANCE FROM THE RUNWAY CENTERLINE: AIRCRAFT TYPE = B-707H

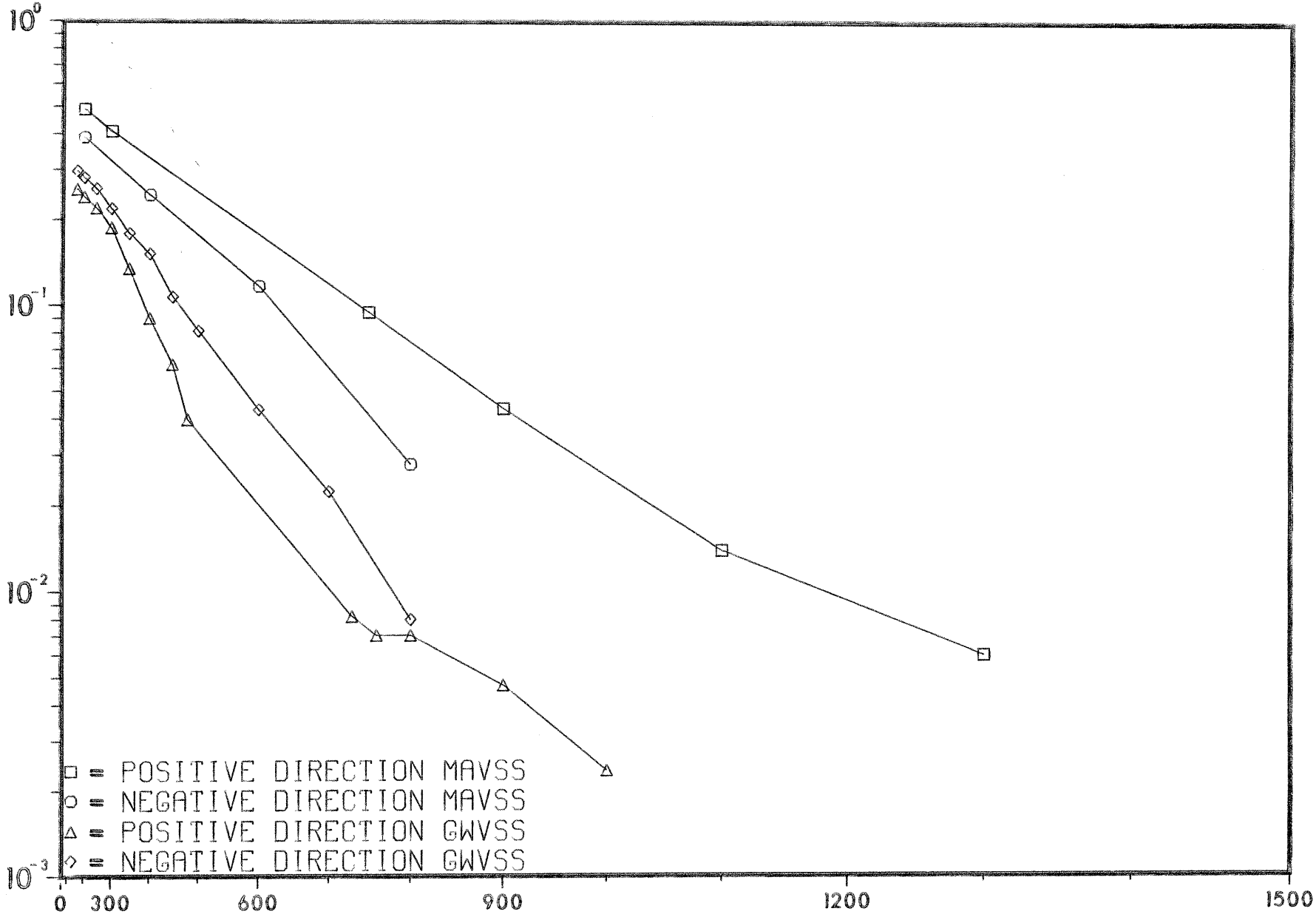

FIGURE C-3. PROBABILITY OF DETECTING A VORTEX AS A FUNCTION OF DISTANCE FROM THE RUNWAY CENTERLINE: AIRCRAFT TYPE = B-737

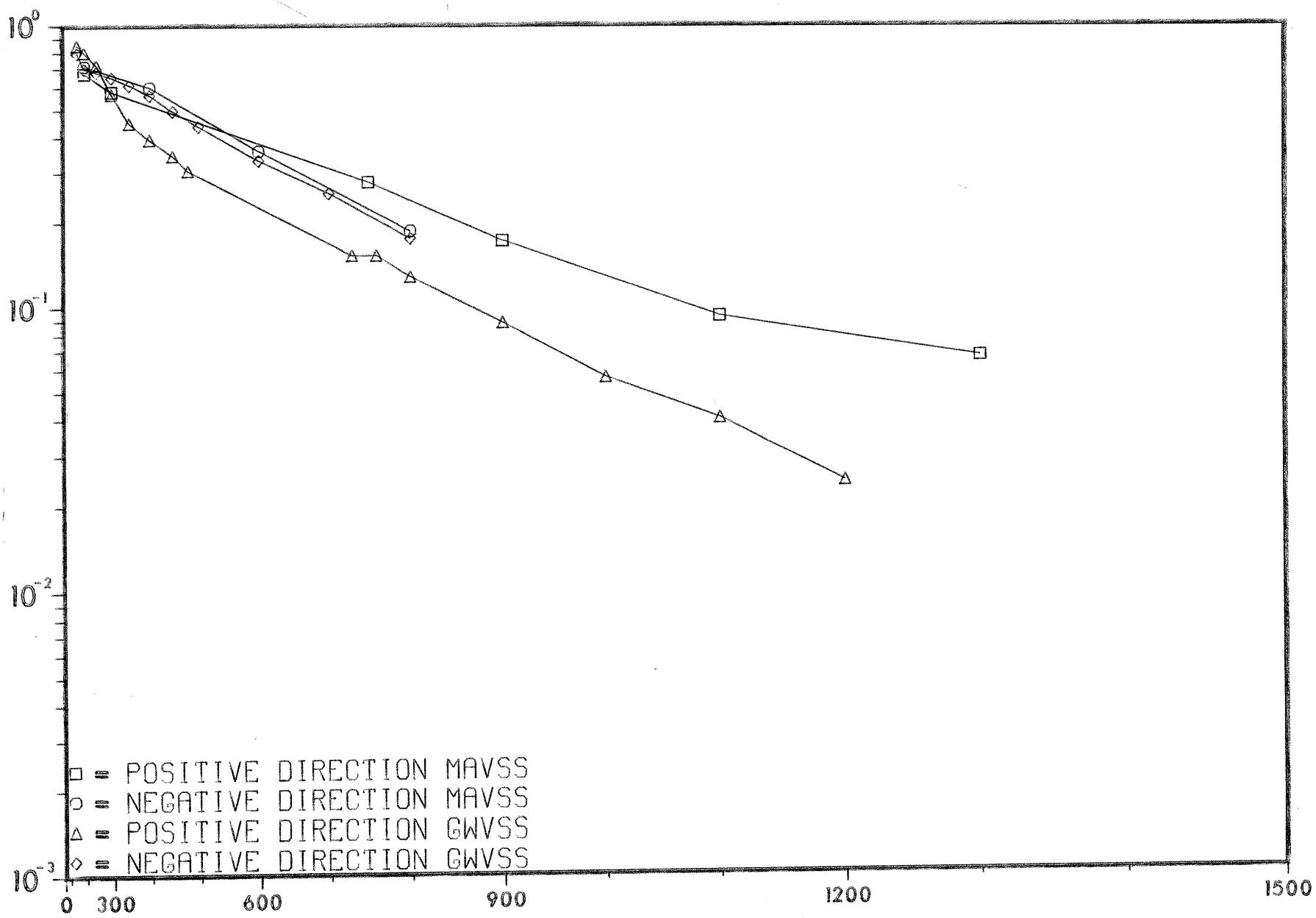

FIGURE C-4. PROBABILITY OF DETECTING A VORTEX AS A FUNCTION OF DISTANCE FROM THE RUNWAY CENTERLINE: AIRCRAFT TYPE = B-747

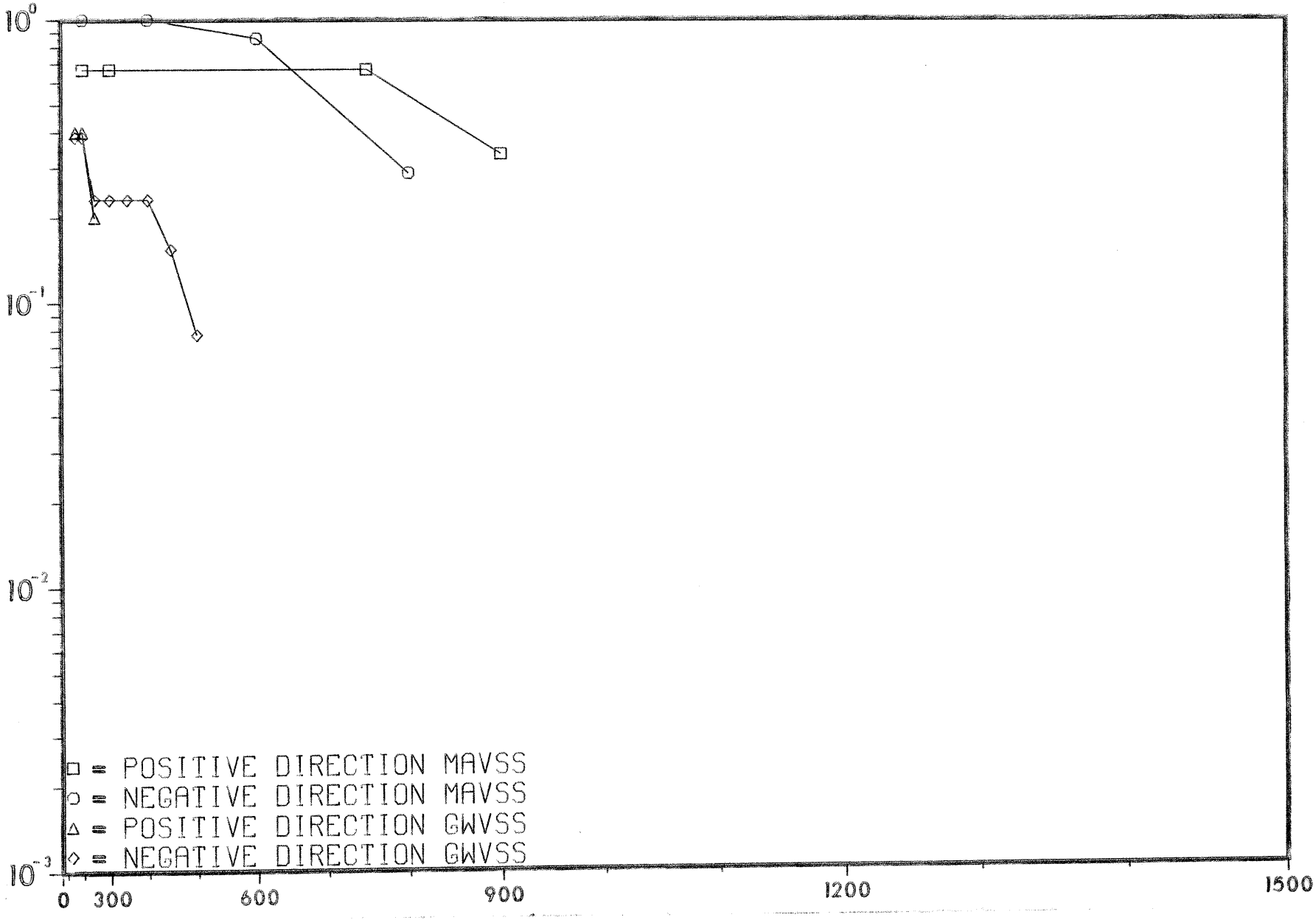

FIGURE C-5. PROBABILITY OF DETECTING A VORTEX AS A FUNCTION OF DISTANCE FROM THE RUNWAY CENTERLINE: AIRCRAFT TYPE = DC-8

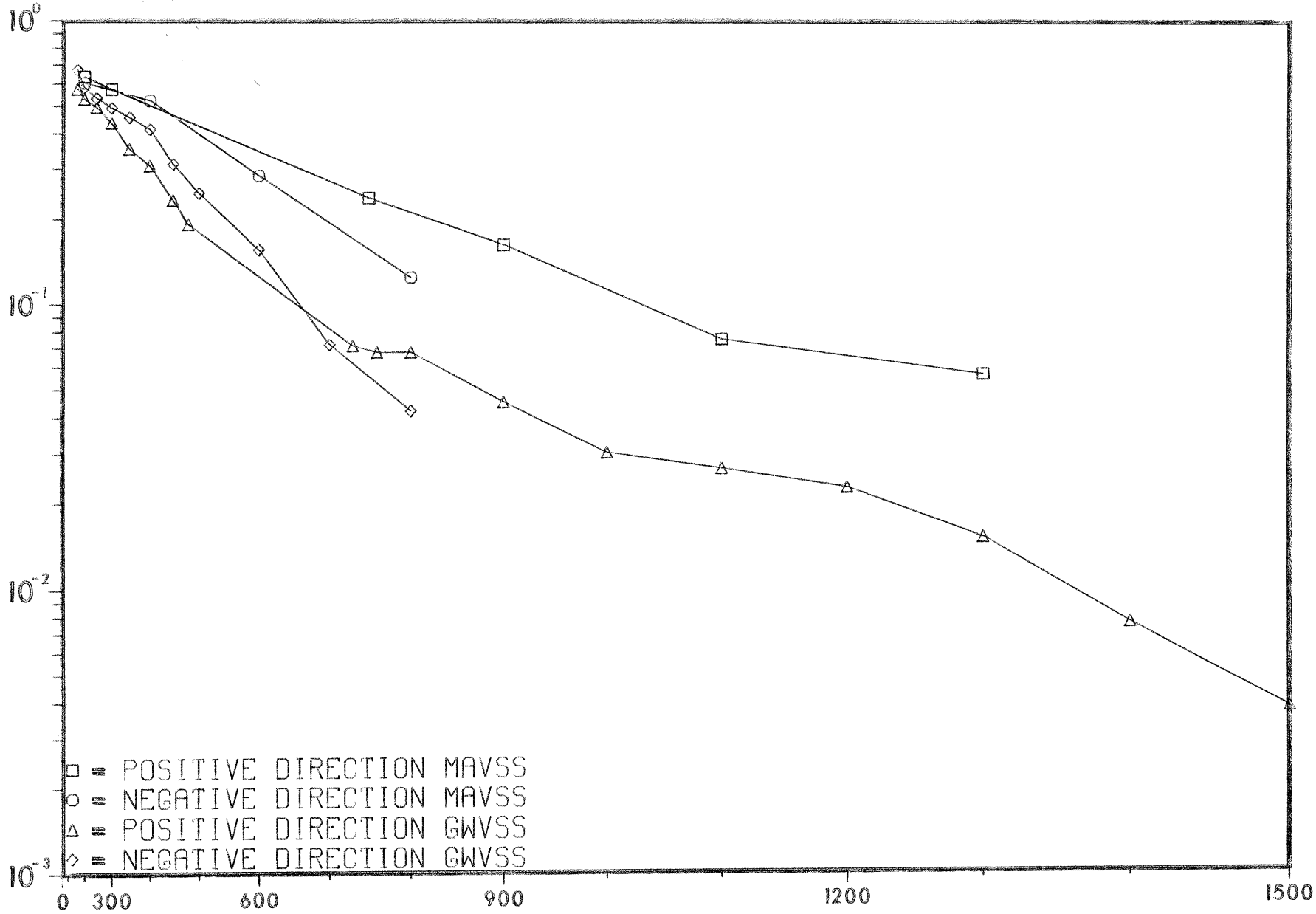

FIGURE C-6. PROBABILITY OF DETECTING A VORTEX AS A FUNCTION OF DISTANCE FROM THE RUNWAY CENTERLINE: AIRCRAFT TYPE = DC-8H

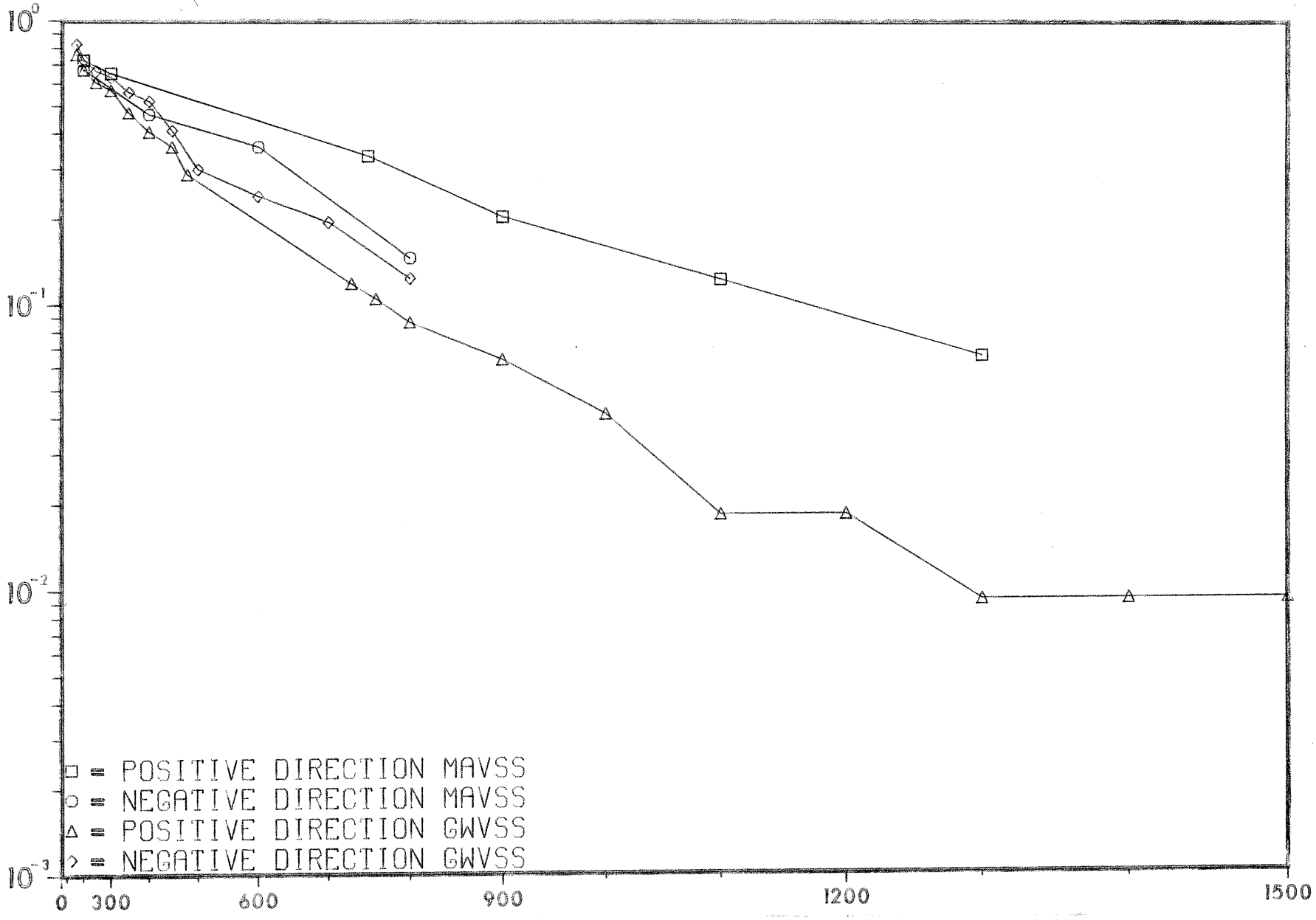

FIGURE C-7. PROBABILITY OF DETECTING A VORTEX AS A FUNCTION OF DISTANCE FROM THE RUNWAY CENTERLINE: AIRCRAFT TYPE = L1011

REFERENCES

1. Burnham, D.C., *Chicago Monostatic Acoustic Vortex Sensing System, Volume I: Data Collection and Reduction,* FAA-RD-79-103, I, Oct. 1979, DOT/Volpe National Transportation Systems Center, Cambridge, MA.

2. Burnham, D.C., and J.N. Hallock, *Chicago Monostatic Acoustic Vortex Sensing System, Volume II: Decay of B-707 and DC-8 Vortices,* FAA-RD-79-103,II, Sept. 1981, DOT/Volpe National Transportation Systems Center, Cambridge, MA.

3. Burnham, D.C., and J.N. Hallock, *Chicago Monostatic Acoustic Vortex Sensing System, Volume III: Executive Summary: Decay of B-707 and DC-8 Vortices,* FAA-RD-79-103,III, Jan. 1982, DOT/Volpe National Transportation Systems Center, Cambridge, MA.

4. Franke, J., V. Schilling, and G. Tetzlaff, *Wake Vortex Propagation in the Atmospheric Boundary Layer,* pp. 47-1 to 47-19, Proceedings of the Aircraft Wake Vortex Conference, DOT-FAA-SD-92/101, June 1992, DOT/Volpe National Transportation Systems Center, Cambridge, MA.

5. Hallock, J.N. and W.R. Eberle, Ed., *Aircraft Wake Vortices: A State-of the Art Review of the United States R&D Program,* FAA-RD-77-23, Feb. 1977, DOT/Volpe National Transportation Systems Center, Cambridge, MA.

6. Burnham, D.C., and J.N. Hallock, *Chicago Monostatic Acoustic Vortex Sensing System, Volume IV: Wake Vortex Decay,* FAA-RD-79-103, IV, July 1982, DOT/Volpe National Transportation Systems Center, Cambridge, MA.

7. Critchley, J.B., and P.B. Foot, *United Kingdom Civil Aviation Authority Wake Vortex Database: Analysis of Incidents Reported Between 1972 and 1990,* pp. 8-1 to 8-18, Proceedings of the Aircraft Wake Vortex Conference, June 1992, DOT-FAA-SD-92/1.1, June 1992, DOT/Volpe National Transportation Systems Center, Cambridge, MA.

8. Hallock, J.N., et al. *Joint US/UK Vortex Tracking Program at Heathrow International Airport, Vol. II: Data Analysis,* FAA-RD-76-58, II, Sept. 1976, DOT/Volpe National Transportation Systems Center, Cambridge, MA.

9. Sullivan, T.E., J.N. Hallock and B.P. Winston, *Analysis of Ground-Wind Vortex Sensing System Data from O'Hare International Airport,* FAA-RD-80-133, Sept. 1980, DOT/Volpe National Transportation Systems Center, Cambridge, MA.

10. Sullivan, T.E., et al. *Aircraft Wake Vortex Takeoff Tests at Toronto International Airport,* FAA-RD-78-143, Feb. 1979, DOT/Volpe National Transportation Systems Center, Cambridge, MA.